ESCRT function at stress-induced ER-Golgi contact sites in *Saccharomyces cerevisiae*

DISSERTATION

Oliver Pajonk

Heidelberg

2024

Inaugural dissertation

for

obtaining the doctoral degree

of the

Combined Faculty of Mathematics, Engineering and Natural Sciences of the

Ruprecht - Karls - University

Heidelberg

Presented by

M.Sc. Oliver Pajonk

Born in: Heidelberg/ Germany

Oral examination: 13.12.2024

ESCRT function at stress-induced ER-Golgi contact sites in *Saccharomyces cerevisiae*

Referees: PD Dr. Axel Mogk
Prof. Dr. Sebastian Schuck

For my dad. I wish you were here.

Table of content

1 ABBREVIATIONS 1

2 SUMMARY 2

3 ZUSAMMENFASSUNG 3

4 CONTRIBUTIONS BY CO-WORKERS 4

5 INTRODUCTION 5

5.1 The endoplasmic reticulum 5

5.2 Endoplasmic reticulum stress 5

5.2.1 Physiological relevance 5

5.2.2 Chemical and biological means to induce ER stress 6

5.2.3 Morphological changes of the ER upon ER stress 6

5.3 ER export 7

5.3.1 Canonical vesicular export from the ER 7

5.3.2 Special modes of ER export 8

5.3.3 Transport of lipids from the ER to the Golgi 9

5.3.4 ER export during ER stress 9

5.4 The ESCRT machinery 10

5.5 Previous work 11

5.6 Aims of this thesis 13

6 MATERIAL & METHODS 14

6.1 Materials 14

6.1.1 Buffers and solutions 14

Table 1: Buffers and solutions used in this study. 14

6.1.2 Growth media and plates 17

Table 5: Media plates for growth of yeast and bacteria 17

Table 6: Media plates containing antibiotics for growth of yeast and bacteria 18

Table 7: Media plates used for the preparation of screening libraries by synthetic genetic array 18

6.1.3 Enzymes, standards and kits 20

6.1.4 Antibodies 20

6.2 Molecular biology methods 20

6.2.1 Plasmids 20

6.2.2 Oligonucleotides 21

6.2.3 Molecular cloning 21

6.3 Yeast methods 22

6.3.1 Yeast strains 22

6.3.2 Library generation for genetic screens using the synthetic genetic array method 25

6.3.3 Growth conditions and ER stress induction 25

6.3.4 Yeast transformation 26

6.3.5 Colony PCR 26

6.3.6 Flow cytometry 26

6.3.7 Light microscopy 27

6.3.8 Image processing 27
6.4 Biochemistry methods 28
6.4.1 Cell lysis 28
6.4.2 Protein determination 28
6.4.3 SDS-PAGE 28
6.4.4 Western blot 29
7 RESULTS 30
7.1 Characterization of ESCRT recruitment to ER clusters upon stress 30
7.1.1 Bro1 co-localizes with Snf7 at ER clusters upon ER stress 30
7.2 Genetic screens for the identification of genes involved in Snf7 recruitment to ER clusters 30
7.2.1 Generation of the query strain 30
7.2.2 Genetic screen with the ER deletion collection 32
7.2.3 Genetic screen with the ts allele collection of essential genes 33
7.3 Validation of screen hits 34
7.3.1 GPI-anchor remodeling proteins are required for the formation of ER clusters 34
7.3.2 p24 proteins and their interaction with COPII components are required for ER cluster formation 35
7.3.3 Depletion of essential genes with the auxin-inducible degron system 39
7.3.4 General ER export machinery is required for the formation of ER clusters 40
7.3.5 The Dsl1-tethering complex localizes to ER clusters and is required for ER cluster formation 42
7.4 Spatial arrangement of ER export machinery at ER clusters 44
7.5 ER-Golgi tethering proteins re-localize to ER clusters upon ER stress 48
7.5.1 Nvj2p re-localizes to ER clusters upon ER stress 48
7.5.2 Tcb3p co-localizes with Snf7 at ER clusters after stress in a Bro1p-dependent manner 50
7.6 Sites of Snf7-positive ER clusters are putative ER-Golgi contacts marked by Tcb3p and Cop1p 54
8 DISCUSSION 56
8.1 ER contact sites 57
8.2 ER export of proteins at ER clusters 59
8.3 Physiological relevance of ESCRT recruitment to ER clusters 60
8.4 Limitations of this study 62
8.5 Conservation of ESCRT recruitment to ER clusters 63
9 OUTLOOK 64
10 REFERENCES 66
11 ACKNOWLEDGEMENTS 74

1 ABBREVIATIONS

Abbreviation	Full name
DTT	dithiothreitol
ER	endoplasmic reticulum
ERES	ER-exit sites
GPI	glycosylphosphatidylinositol
GPI-AP	glycosylphosphatidylinositol-anchored protein
HTL	HaloTag ligand
ILV	intraluminal vesicle
MVB	multivesicular body
PFA	paraformaldehyde
PH	Pleckstrin-Homology
PTM	post-translational modification
SMP	Synaptotagmin-like mitochondrial-lipid-binding
Tm	tunicamycin
TMP	transmembrane protein
ts	temperature-sensitive
UPR	unfolded protein response

2 SUMMARY

The endoplasmic reticulum (ER) is the major site of protein folding and lipid synthesis in eukaryotic cells. All secretory proteins are translocated into the ER, folded and modified, packed into vesicles and eventually exported towards the Golgi apparatus. These essential processes are menaced by changing environmental conditions or cellular needs. When the folding capacity in the ER lumen is overwhelmed or when lipid bilayer composition and stiffness deviate from the functional steady state, cells experience ER stress. Cells have mechanisms in place to cope with ER stress and restore homeostasis, one of which is the unfolded protein response (UPR). In this pathway, a transcriptional cascade is triggered that alleviates stress by the upregulation of chaperones and lipid synthesis genes. In the yeast *Saccharomyces cerevisiae*, ER stress also triggers the UPR-independent recruitment of ESCRT-III component Snf7p to specific ER domains termed ER clusters. The biological role of ESCRT recruitment to ER clusters and its contribution to ER stress relief are not known.

In this thesis, I characterized the phenotype of Snf7 recruitment to ER clusters in yeast. I showed that the ESCRT-associated protein Bro1 is essential for the recruitment of fluorescently labelled Snf7 to ER clusters and provided evidence that this recruitment reflects a physiological process. I performed genetic screens to identify genes involved in the formation of ER clusters upon ER stress and genes involved in recruiting Snf7 to these sites. I determined that glycosylphosphatidylinositol (GPI)-anchor remodeling proteins, the p24 adaptor complex for ER-to-Golgi transport and its interaction with COPII proteins, the COPII ER export machinery and the Dsl1 tethering complex are required for the formation of ER clusters. I dissected the spatial arrangement of COPI component Cop1p and COPII components at ER clusters in live cell imaging and determined that Cop1p frequently co-localizes with Snf7 puncta at ER clusters whereas COPII proteins surround Snf7 puncta in a flower-like assembly. Furthermore, I observed that the ER tethering proteins Nvj2p and Tcb3p co-localize with Snf7 puncta at ER clusters and that re-localization of Tcb3p to ER clusters depends on successful ESCRT recruitment. Both Nvj2p and Tcb3p were shown to be involved in non-vesicular ceramide transport as ER-Golgi tethers during ER stress. Given the co-localization of Tcb3p and Nvj2p with Snf7 and Cop1p at ER clusters, it is conceivable that ER clusters represent ER-Golgi contact sites that might facilitate non-vesicular transport of ceramide during ER stress and thereby increase ceramide transport efficiency.

In conclusion, I characterized ESCRT recruitment to ER clusters upon ER stress and assigned a potential physiological role to this process. This study adds to our understanding of ER stress responses in yeast. A better understanding of how different stress responses contribute to stress relief in yeast will improve our understanding of homologous processes in mammalian systems.

3 ZUSAMMENFASSUNG

Das endoplasmatische Retikulum (ER) ist der wichtigste Ort der Proteinfaltung und Lipidsynthese in eukaryontischen Zellen. Alle sekretorischen Proteine werden in das ER transloziert, gefaltet und modifiziert, in Vesikel verpackt und anschließend in den Golgi-Apparat exportiert. Diese essenziellen Prozesse werden durch sich ändernde Umweltbedingungen oder zelluläre Bedürfnisse beeinflusst. Wenn die Faltungskapazität im ER-Lumen überlastet ist oder wenn die Zusammensetzung und Steifheit der Lipiddoppelschicht vom funktionalen Zustand abweicht, erfahren die Zellen sogenannten ER-Stress. Die Zellen verfügen über Mechanismen, um ER-Stress zu verringern und die Homöostase wiederherzustellen. Einer dieser Mechanismen ist die ungefaltete Proteinantwort (UPR). In diesem Signalweg wird eine Transkriptionskaskade ausgelöst, die den Stress durch die Hochregulierung von Chaperonen und Lipidsynthesegenen mildert. In der Hefe *Saccharomyces cerevisiae* löst ER-Stress auch die UPR-unabhängige Rekrutierung der ESCRT-III-Komponente Snf7 zu spezifischen ER-Domänen, den sogenannten ER-Clustern, aus. Die biologische Rolle der ESCRT-Rekrutierung zu ER-Clustern und ihr Beitrag zur Minderung von ER-Stress sind bisher nicht bekannt.

In dieser Arbeit habe ich den Phänotyp der Snf7-Rekrutierung zu ER-Clustern in Hefe charakterisiert. Ich habe gezeigt, dass das ESCRT-assoziierte Protein Bro1 für die Rekrutierung von fluoreszenzmarkiertem Snf7 zu ER-Clustern essenziell ist, und konnte nachweisen, dass diese Rekrutierung einen physiologischen Prozess darstellt. Ich habe genetische Screens durchgeführt, um Gene zu identifizieren, die an der Bildung von ER-Clustern bei ER-Stress beteiligt sind, sowie Gene, die für die Rekrutierung von Snf7 zu diesen Stellen benötigt werden. Ich stellte fest, dass Proteine zum Umbau des Glycosylphosphatidylinositol (GPI)-Ankers, der p24-Komplex für den ER-zu-Golgi-Transport und seine Interaktion mit COPII-Proteinen, die COPII ER-Exportmaschinerie und der Dsl1-Tethering-Komplex für die Bildung von ER-Clustern erforderlich sind. Ich konnte die räumliche Anordnung der COPI-Komponente Cop1p und den COPII-Komponenten an ER-Clustern in lebenden Zellen mikroskopisch untersuchen und feststellen, dass Cop1p häufig mit Snf7-Signal an ER-Clustern kolokalisiert, während COPII Proteine das Snf7-Signal in einer blütenartigen Anordnung umgeben.

Darüber hinaus habe ich beobachtet, dass die ER-Tethering-Proteine Nvj2p und Tcb3p mit Snf7-Signal an ER-Clustern kolokalisieren und dass die Re-Lokalisierung von Tcb3p zu ER-Clustern von der erfolgreichen ESCRT-Rekrutierung abhängt. Es ist bekannt, dass Nvj2p und Tcb3p als ER-Golgi-Tether am nichtvesikulären Ceramid-Transport während ER-Stress beteiligt sind. Angesichts der Kolokalisierung von Tcb3p und Nvj2p mit Snf7 und Cop1p an ER-Clustern ist es denkbar, dass ER-Cluster bei ER-Stress ER-Golgi-Kontaktstellen darstellen, die den nichtvesikulären Transport von Ceramid erleichtern und dadurch die Effizienz des Ceramid-Transports erhöhen könnten.

Zusammenfassend lässt sich sagen, dass ich die Rekrutierung von ESCRT zu ER-Clustern bei ER-Stress charakterisiert und diesem Prozess eine potenzielle physiologische Rolle zugewiesen habe. Diese Studie trägt zu unserem Verständnis der ER-Stressreaktionen in Hefe bei. Ein besseres Verständnis wie verschiedene Stressreaktionen zum Stressabbau in Hefe beitragen wird unser Verständnis homologer Prozesse in Säugetiersystemen verbessern.

4 CONTRIBUTIONS BY CO-WORKERS

I undertook this project together with Lis Albert, another PhD student from the research group of Sebastian Schuck at the Biochemistry Center of Heidelberg University. While the goals of both PhD theses were to identify the role of ESCRT proteins at stress-induced ER clusters, we took complementary approaches to identify new proteins that are involved in ESCRT recruitment to these sites. This enabled a broader approach to our scientific question and raised confidence in the acquired results, which largely overlapped. Lis Albert and Sebastian Schuck contributed to the conceptualization of this project to great extent. The experiments in this study were conceptualized and performed by me unless stated otherwise in this section, the results section and in figure legends.

The phenotype of Snf7 recruitment to ER clusters upon ER stress was first observed by Jasmin Schäfer. She determined that whereas Bro1p is essential for Snf7 recruitment, no upstream ESCRT proteins are required. She generated the strain expressing an ER marker and tagged Snf7 alongside the endogenous Snf7p that was used as a reference for quantifications in Figure 3, Figure 7, Figure 8A and B, Figure15 B and Figure 16C.

The *BRO1* deletion strain used in Figure 3 was generated by Jasmin Schäfer. Acquisition of microscopy images and Snf7 puncta quantifications for Figure 3B were performed by Lis Albert.

Images in Figure 4B were acquired by Lis Albert.

The query strain used for both the ER deletion (Figure 5) and the ts screen (Figure 6) was generated by Carlos Martin de Hijas. Strains for the ER deletion collection were picked by Peter Bircham from the deletion collection of essential genes. The MATLAB script for the semi-automated image analysis of both screens was originally written by Peter Bircham and modified by Dimitris Papagiannidis. The ER deletion screen was imaged by Dimitris Papagiannidis and hits were manually assigned by Dimitris Papagiannidis, Jasmin Schäfer, Sebastian Schuck, and me.

Control strains for the depletion of Sec63p-miniIAA7-mCherry and Vph1-miniIAA7-mCherry included strains generated by Dorottya Polos and Sebastian Schuck.

The Western blot of Lst1p-miniIAA7-FLAG levels (Figure 10C) and the imaging of Dsl1p-miniIAA7 depletion (Figure 11A) were performed by Natalie Friemel under my supervision.

The *BRO1* deletion strain used in Figure 11C was generated by Lis Albert.

Chrysafenia Papavissarion tested the tagging of three yeast proteins with HaloTag7 and performed the four-color live cell imaging in Figure 13 under my supervision.

One of the replicates quantifying cytosolic Tcb3 puncta upon ER stress in Figure 15C was acquired by Lis Albert.

The pie chart in Figure 16B was conceptualized and generated by Lis Albert.

5 INTRODUCTION

5.1 The endoplasmic reticulum

All chemical reactions require specific conditions to take place efficiently. Since optimal reaction conditions vary drastically between different reactions occurring in cells, a compartmentalization is indispensable. Cells achieve this compartmentalization by segregating various chemical reactions in membrane-bound organelles. One organelle of particular importance is the endoplasmic reticulum (ER), which is formed by one continuous lipid bilayer. The ER makes up the nuclear envelope that encapsulates the nucleus and its DNA, the hereditary information of the cell. In the cell periphery, the ER additionally forms an interconnected network of sheets and tubules, responsible for synthesis of certain proteins and lipids.

5.2 Endoplasmic reticulum stress

5.2.1 Physiological relevance

Almost all secretory proteins, which make up a third of all proteins, are translocated into the ER as an unfolded polypeptide chain by the translocon (Rapoport *et al*, 2017). As it enters the ER lumen, the translated and translocating polypeptide starts folding (Mingarro *et al*, 2000). At this step, signal sequences that directed the proteins to the ER in the first place are removed (Milstein *et al*, 1972) and many proteins are modified by N-linked glycosylation (Bulleid *et al*, 1992; Chen *et al*, 2001). The partially folded polypeptide is then received by chaperones to assure the correct folding of the polypeptide into a functional protein (Gaut & Hendershot, 1993). ER luminal chaperones can already engage with the translocating polypeptide chain and thereby assist in ER protein import (Matlack *et al, 1999*). If the load of polypeptides that requires folding exceeds a critical level that cannot be met by the ER-resident folding machinery, cells experience ER stress. In yeast and metazoa, this accumulation of misfolded proteins is sensed by the serine-threonine kinase and endoribonuclease Ire1p and triggers the unfolded protein response (UPR) (Nikawa & Yamashita, 1992; Mori *et al*, 1993; Okamura *et al*, 2000; Walter & Ron, 2011). In unstressed conditions, inactive Ire1p is bound by the major luminal Hsp70 chaperone of the ER (Kar2p in yeast, BiP in metazoa). Upon ER stress, Kar2p becomes increasingly occupied by unfolded polypeptides and no longer binds Ire1p, which leads to its activation (Bertolotti *et al*, 2000; Okamura *et al*, 2000). Then, Ire1p phosphorylates itself and other Ire1p molecules, which results in the formation of Ire1p oligomers that cluster in the ER membrane (Shamu & Walter, 1996; Welihinda & Kaufman, 1996; Aragón *et al*, 2009). At Ire1p clusters, *HAC1* mRNA is spliced by active Ire1p and the tRNA ligase Trl1 (Mori et al., 1996; Cox & Walter, 1996; Sidrauski *et al*, 1996; Sidrauski & Walter, 1997). This splicing reaction removes an intron that interacts with the 5'-UTR of *HAC1* mRNA and hinders the initiation of translation in unstressed conditions (Cox & Walter, 1996). Spliced *HAC1* mRNA is readily translated and Hac1p shuttles into the nucleus. There it acts as transcription factor that specifically binds

and activates transcription of genes that contain an Unfolded Protein Response Element (UPRE; Mori *et al*, 1996). The resulting induction of genes involved in lipid synthesis and ER protein folding restores homeostasis (Cox *et al*, 1993; Mori *et al,* 1996).

More recently, lipid bilayer stress has emerged as another trigger of the UPR. A mutated version of Ire1p lacking the ER luminal domain and therefore incapable of sensing misfolded/unfolded proteins can still perform UPR signaling (Promlek *et al*, 2011; Ho *et al*, 2020). It is proposed that the stiffness of the membrane is a major characteristic that can be sensed by Ire1p (Radanović & Ernst, 2021). A higher degree of membrane stiffness could be caused by an increase of saturated lipids in the ER membrane (Pineau *et al*, 2009) or by the accumulation of late secretory proteins in the ER membrane, which results in an altered protein:lipid ratio (Covino *et al*, 2018).

5.2.2 Chemical and biological means to induce ER stress

ER stress is a natural condition that cells are challenged with during their development and in certain environments. It was demonstrated that ER stress management is of particular importance during embryonic development in mice, since absence of UPR components resulted in embryonic lethality (Kratochvílová *et al*, 2016). Also, nutritional alterations like high concentrations of saturated fatty acids and sterols were shown to induce ER stress in yeast (Pineau *et al*, 2009). Under laboratory conditions, there are a handful of ways to artificially induce ER stress in yeast cells, of which many interfere with protein folding. Two examples and classic compounds to induce ER stress are tunicamycin (Tm) and dithiothreitol (DTT). Tunicamycin is synthesized by Streptomyces lysosuperificus and other bacteria and acts as an antibiotic nucleoside analogue that binds to the UDP-N-acetyl-glucosamine-1-P transferase (Alg7p in yeast) (Yoo *et al*, 2018). At steady state, this enzyme catalyzes the transfer of Glc-Nac-P from UDP-GlcNac to Dol-P at the ER (Burda & Aebi, 1999). This reaction is the first committed step of the dolichol pathway of protein N-linked glycosylation (Kukuruzinska & Lennon, 1995), which is a post-translational modification (PTM) that many secretory proteins undergo (Breitling & Aebi, 2013).If N-linked glycosylation is halted, proteins that would usually acquire this PTM cannot fold properly and therefore accumulate in the ER lumen resulting in ER stress. DTT is a strong reducing agent and also interferes with protein folding (Braakman *et al*, 1992). Unlike the cytosol, which is a reducing environment, the ER lumen is an oxidizing compartment, which allows the formation of intramolecular disulfide bonds between cysteine residues of newly synthesized polypeptides. For many proteins this process is essential for successful folding. Given the oxidizing nature of the ER lumen, ER is most affected by DTT. However, DTT also interferes with oxidative protein folding in mitochondria (Zarges & Riemer, 2024).

5.2.3 Morphological changes of the ER upon ER stress

Activation of the UPR in response to accumulation of misfolded proteins in the ER lumen is accompanied by morphological changes of the ER. In yeast, the upregulation of lipid synthesis by the UPR leads to

ER expansion. The total coverage of the cytosolic face of the plasma membrane by ER increases from about 50% in untreated cells to over 80% after DTT treatment (Papagiannidis *et al*, 2021). ER expansion is mainly based on the generation of more ER sheets as the proportion of tubular ER remains similar to steady state levels (Schuck *et al*, 2009; Papagiannidis *et al,* 2021). Moreover, cytoplasmic extensions of the peripheral ER, which correspond to large ER sheets, can be observed (Schuck *et al*, 2009). While we understand that morphological changes of the ER upon ER stress, in particular a higher abundance of ER sheets, facilitate protein folding (Schuck *et al,* 2009), it is understudied how other central ER functions, such as ER export, are affected by the stress-induced changes of ER morphology.

5.3 ER export

5.3.1 Canonical vesicular export from the ER

After translocation into the endoplasmic reticulum (ER) and proper folding, proteins leave the ER in vesicles with the help of the COPII machinery and are transported to the Golgi, where they are further modified and sorted to be sent towards their final destination (Boncompain & Weigel, 2018). ER export by COPII-coated vesicles is a well-studied process, but recent findings have challenged the established model of vesicle-mediated ER-to-Golgi transport by proposing the existence of tubular extensions from the ER to the Golgi as alternative protein carriers (Weigel *et al*, 2021; Malis *et al*, 2022).

As for the long established model of vesicle-mediated transport, cargo export from the ER is initiated by the activation of the small GTPase Sar1p (Figure 1; D'Arcangelo *et al*, 2013; Nakano & Muramatsu, 1989; Barlowe *et al*, 1993) by the ER-localized guanine nucleotide exchange factor Sec12p (Nakano & Brada, 1988; d'Enfert et al. 1991). GTP loading leads to membrane association of Sar1p and allows it to induce membrane curvature (Lee *et al*, 2005). Membrane association of Sar1p additionally recruits the heterodimeric complex of the COPII coat proteins Sec23p and Sec24p (Matsuoka *et al*, 1998).This is known as the prebudding complex, which in turn recruits the heterotetrameric complex of the additional COPII coat components Sec13p and Sec31p (Matsuoka *et al,* 1998). While the inner coat made up of Sar1p, Sec23p and Sec24p oversees cargo loading, the outer layer consisting of Sec13p and Sec31p acts as scaffold for the bending of the membrane (Fath *et al*, 2007; Čopič *et al*, 2012). Besides this minimal set of COPII components, other proteins contribute to efficient ER export. The soluble protein Sec16p binds to the other COPII components at the cytoplasmic site of ER-exit sites (ERES; Espenshade *et al*, 1995; Connerly *et al*, 2005) and organizes the whole assembly at discrete domains (Shindiapina & Barlowe, 2010).

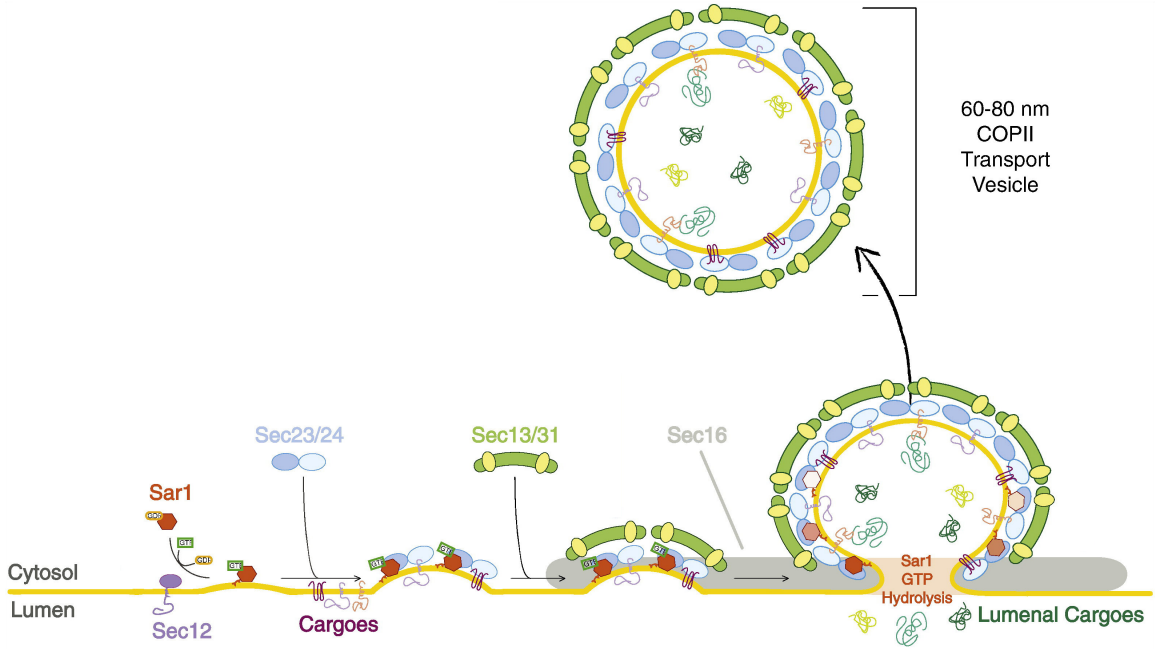

Figure 1. Canonical ER export mediated by the COPII machinery.
The schematic was conceptualized and created by D'Arcangelo *et al,* 2013. I modified the schematic and used it with permission of Elsevier B.V.

5.3.2 Special modes of ER export

The general COPII machinery can be adapted for the export of selected cargo proteins in specialized transport carriers. For instance, Lst1p is a Sec24 homologue that preferentially forms the heterodimer with Sec23 in the ER export of GPI-anchored proteins (GPI-APs) and other bulky cargo (Roberg *et al*, 1999;Muñiz *et al*, 2001; Miller *et al*, 2003). The ER export of GPI-APs is thought to be particularly challenging. The asymmetric topology of GPI-anchored proteins, including a small GPI-anchor attached to a larger protein, is thought to counteract membrane bending towards the cytosol achieved by the COPII coat (Miller & Schekman, 2013). Moreover, GPI-APs are only anchored within the inner leaflet of the ER membrane and can thus not be recognised from the cytosol. Therefore, selective transport and recognition by the COPII machinery requires prior binding to specific export receptors (Muñiz & Riezman, 2016). Prior to ER export, the GPI-anchor is heavily remodelled. Only GPI-APs with a fully remodelled GPI-anchor concentrate at ERES (Castillon *et al*, 2009), where they bind to their ER export receptor, the p24 complex. This heteromeric complex is formed by the p24 protein family members Emp24p and Erv25p, which in turn specifically recruits Lst1p (Lopez *et al*, 2019).

According to the canonical model of ER export, COPII vesicles bud off from the ER membrane, but alternative ER transport carriers have been described in mammalian cells (Malis *et al*, 2022). In this scenario, the ER forms long, tubular structures that move along microtubules towards the Golgi while still being connected to the ER (Weigel *et al,* 2021). Here, the COPII machinery acts as a scaffold stabilizing these structures at their ER-associated neck instead of forming protein coats of vesicles that bud off from the ER membrane. Also, the COPI machinery, which was classically described to direct

Golgi-to-ER trafficking (Barlowe & Miller, 2013), was recently reported to stabilize these tubular ER-to-Golgi transport carriers, albeit more distally from the ER than COPII. Hence, ER export appears to be more complex than previously appreciated and may be carried out by unusual membrane structures. The effect of classic components of ER-to-Golgi transport on membrane shape is well-characterized in vitro and in vivo, thus it remains to be understood how more complex membrane structures can be assumed with the same components.

5.3.3 Transport of lipids from the ER to the Golgi

Not only proteins but also lipids are transported from the ER to the Golgi. Many lipids or their precursors are synthesized in the ER and subsequently transported to various cellular locations. One example for selective transport of lipids is ceramide, which is synthesized in the ER and then transported to the Golgi in order to be turned into complex sphingolipids. Ceramide synthesis in yeast is initiated by the serine palmitoyl transferases Lcb1 and Lcb2, which form 3-ketohydrosphingosine from palmitoyl-CoA and L-serine (Hanada, 2003; Lowther *et al*, 2012). Further processing by Tsc10 and Lag1/Lac1 yields ceramide, which serves as backbone for complex sphingolipids (Hannun & Obeid, 2018). Ceramide then clusters within the ER membrane (Silva *et al*, 2007). These clusters coincide with the sites where GPI-APs are concentrated before they both leave the ER together via COPII-dependent vesicular transport (Lopez *et al*, 2019). Even though the majority of ceramide is transported to the Golgi via the vesicular route at steady state, non-vesicular transport of ceramide exhibits an alternative route for ceramide transport (Hanada *et al*, 2003). In yeast, a fraction of ceramide is transported by Svf1 via non-vesicular transport at steady state (Limar *et al*, 2023).

5.3.4 ER export during ER stress

It is not understood how ER stress effects the rate of ER export, but it is plausible that different types of cargo are affected in different ways. In general, ER stress is characterized by high levels of unfolded proteins in the ER. The folding state of the cargo proteins could have an impact on binding to their specific export receptors and their successful export from the ER (Phillips *et al*, 2020). Members of the p24 complex might also play a role in confining misfolded proteins to the ER upon stress, since higher levels of misfolded proteins and ER residents leave the ER when p24 proteins are mutated (Elrod-Erickson & Kaiser, 1996; Wen & Greenwald, 1999). While some proteins are retained in the ER during ER stress, others are rapidly exported. Mammalian cells have a mechanism in place, called RESET pathway, which is triggered by ER stress and leads to the rapid ER export of misfolded GPI-anchored proteins (Satpute-Krishnan *et al*, 2014; Cheatham *et al*, 2023). Another example is the inner nuclear membrane protein Emerin. This protein is selectively exported from the ER upon stress in a COPII-dependent manner (Buchwalter *et al*, 2019).

Not only the export of proteins, but also ER export of certain lipids is affected upon ER stress. At steady state, the majority of ceramide in yeast is transported in vesicles from the ER to the Golgi and only a

small fraction depends on non-vesicular transport mediated by Nvj2p (Liu *et al*, 2017). Upon ER stress, however, accumulation of ceramide in the ER is disproportionally higher in *nvj2Δ* cells, suggesting that non-vesicular transport of ceramide has an increased relevance during ER stress (Liu *et al*, 2017).
Another way how ER stress could affect ER export are the morphological changes of the ER that accompany ER stress. ER stress leads to ER expansion and particularly to an increase of ER sheets (Schuck *et al*, 2009; Papagiannidis *et al*, 2021), which are regions of low membrane curvature. ER-exit sites, however, are preferentially organized at high-curvature ER membrane (Okamoto *et al*, 2012). Thus, the lower percentage of high-curvature ER upon ER stress might inhibit vesicular ER export.

5.4 The ESCRT machinery

In addition to COPI and COPII proteins, ESCRT proteins constitute another membrane remodelling machinery involved in membrane trafficking. It consists of four soluble multi-subunit complexes, ESCRT-0 to ESCRT-III, and the AAA ATPase Vps4 (Henne *et al*, 2011). The first described and best understood role of the ESCRT machinery is the sorting of ubiquitinated transmembrane protein cargo into endosomes during multivesicular body (MVB) formation (Katzmann *et al*, 2001).

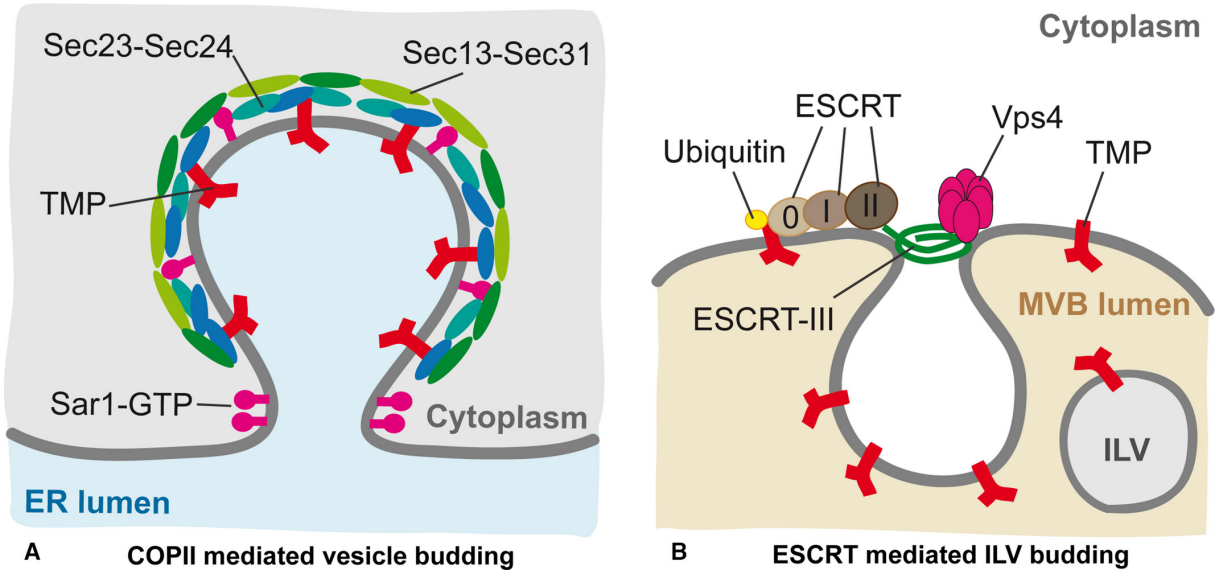

Figure 2. Two opposing topologies of membrane budding events in yeast.
(A) COPII mediated vesicle budding during ER export. COPII vesicle budding displays a normal topology (i.e. budding into the cytosol).
(B) ESCRT mediated budding of intraluminal vesicles (ILV) in multivesicular body (MVB) formation. ILV budding displays a reverse topology (i.e. budding away from the cytosol).
The schematic was conceptualized and created by (Alonso Y Adell *et al*, 2016). I used this schematic with permission of John Wiley and Sons.

In the case of MVB formation, ubiquitinated transmembrane proteins (TMPs) in the endosomal membrane is recognized by ESCRT-0, which leads to the hierarchical recruitment of ESCRT-I followed by ESCRT-II. Subsequently, ESCRT-III with its prominent member Snf7p is recruited. Snf7p has an outstanding role in this process, since it polymerizes to form spirals that generate force, bend the membrane, and eventually results in membrane scission. This process requires the activity of Vps4p (Figure 2B; Alonso Y Adell *et al*, 2016; McCullough *et al*, 2018). In this classic example, the membrane buds away from the cytosol, which is contrary to the direction of membrane budding events during ER export mediated by the COPII machinery (Figure 2; Alonso Y Adell *et al*, 2016). More recently, however, functions of the ESCRT machinery were described during which the membrane buds into the cytosol (McCullough *et al*, 2018). The ESCRT machinery is involved in a variety of cellular processes, ranging from cytokinesis, virus budding, nuclear envelope reformation (in mammals) and membrane repair to autophagy (Hurley, 2015). With the emerging new roles of the ESCRT machinery in a variety of cellular contexts, it has been found that the recruitment order of ESCRT components can vary from the hierarchy described in MVB formation. For example, the adaptor proteins ALIX/Bro1p and CHMP7/Chm7, which are involved in membrane repair in mammalian cells and yeast, directly recruit ESCRT-III subunits to membranes, independently of ESCRT-0/I/II (Jimenez *et al*, 2014; Thaller *et al*, 2019).

5.5 Previous work

Jasmin Schäfer, a former PhD student in the research group of Sebastian Schuck, made the initial observation that ER stress caused by tunicamycin treatment triggered the recruitment of the ESCRT-III protein Snf7 to ER regions that we later termed ER clusters (Figure 3A). For this, she introduced a construct into yeast cells containing a fusion protein of Snf7p with the green fluorophore mNeonGreen (referred to as mNeon in figure panels). This construct was expressed alongside the endogenous protein Snf7p at a low level using the weak *VPS24* promoter. The reason for this strain design was that multiple ESCRT-III subunits that form polymers cannot be functionally tagged. The presence of tagged Snf7 at a low level besides the functional endogenous Snf7p allows the tracking of ESCRT function and is commonly used in the ESCRT field (Teis *et al*, 2008). Whereas Snf7-mNeonGreen localized mainly to MVBs and the cytosol at steady state, treatment with tunicamycin for 3 h triggered a pronounced recruitment to ER clusters (Figure 3A). These Snf7 puncta were very bright, and we could not observe MVB staining of Snf7-mNeonGreen when untreated and Tm-treated images were presented with the same display range (Figure 3A). Lis Albert quantified the phenotype of Snf7 recruitment to ER clusters after tunicamycin treatment and could reliably observe typically one Snf7 punctum per cell in roughly 50% of all cells, which accounts to around 0.5 Snf7 puncta per cell (Figure 3B). This phenotype and the question of the underlying biological function were the incentive for the study discussed in this thesis. As ESCRT-III subunit Snf7 can be recruited in different ways in various cellular functions, Jasmin Schäfer determined in simple deletion strains that no members of upstream ESCRT-0/-I/-II complexes were required for the recruitment of Snf7 to ER clusters upon ER stress (data not shown).

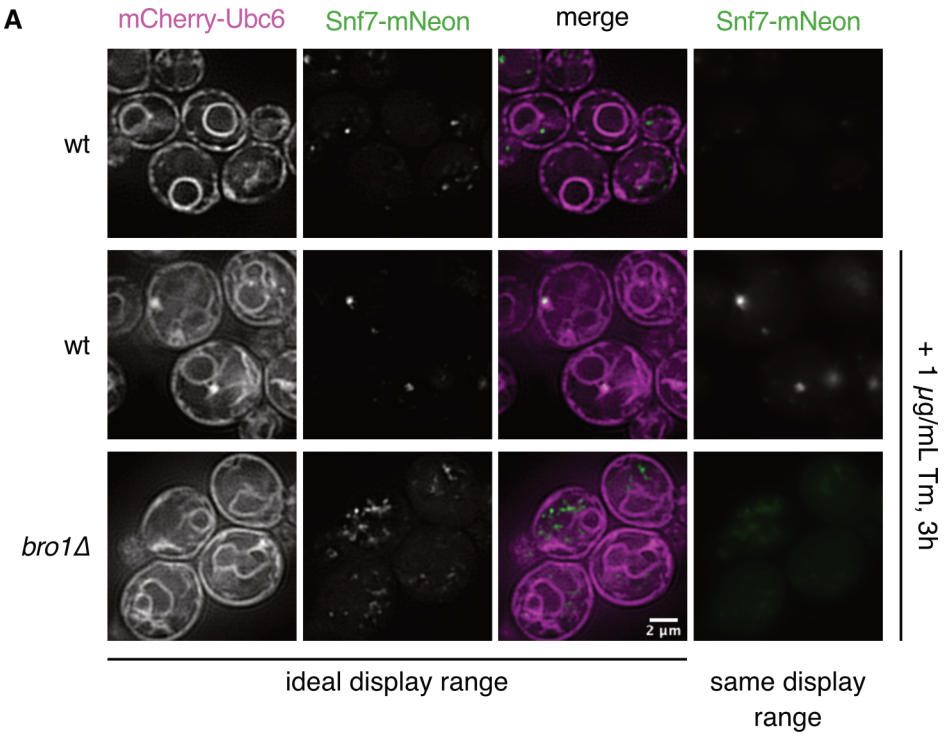

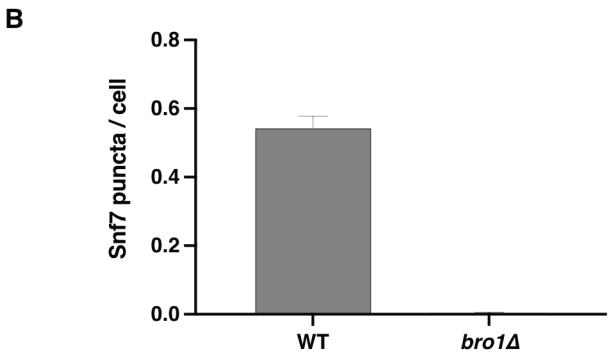

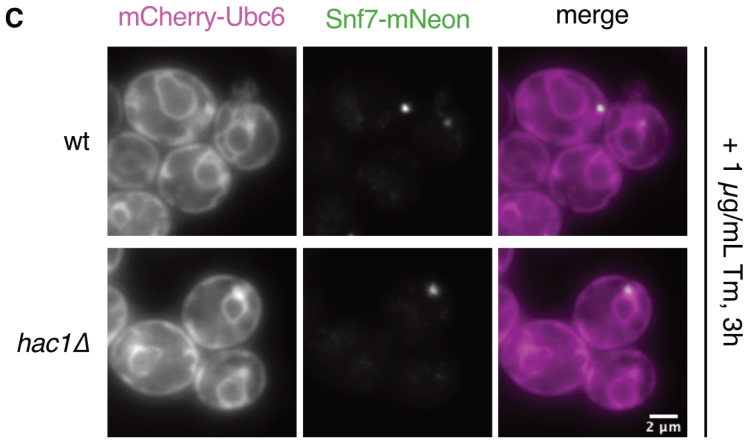

Figure 3. The ESCRT-III component Snf7 is recruited to ER clusters upon ER stress in a Bro1-dependent but UPRI-independent manner.

(A) Fluorescence microscopy images of the W303 yeast strain stably expressing mCherry-Ubc6 and Snf7-mNeonGreen. Exponentially growing cells were either treated with 1 µg/mL tunicamycin (Tm) for 3 h or left

untreated before imaging. Both strains were generated by Jasmin Schäfer. The first three columns (left to right) show deconvolved images and the last column "Snf7-mNeon" shows raw images to allow quantitative comparison of the fluorescence signal. Widefield microscopy images were deconvolved using the Richardson-Lucy algorithm with 30 iterations and an automatically determined noise level.

(B) Quantification of Snf7-mNeon puncta in wt and *bro1Δ* cells after treatment with 1 μg/mL tunicamycin for 3 h. Percentages of cells from all cells are plotted that show Snf7-mNeonGreen puncta. For all genotypes more than 200 cells were quantified after images were randomized to reduce bias. The experiment was performed in n = 3 replicates, error bars correspond to standard error of the mean (SEM). All replicates were acquired and quantified by Lis Albert.

(C) Fluorescence microscopy images of the W303 yeast strain stably expressing mCherry-Ubc6 and Snf7-mNeonGreen in wt and *hac1Δ*. Exponentially growing cells were treated with 1 μg/mL tunicamycin (Tm) for 3 h before imaging.

Only the ESCRT-associated Bro1 domain protein Bro1p was essential for the recruitment of Snf7-mNeonGreen to ER clusters since Snf7-mNeonGreen remained in the cytosol and at MVBs upon ER stress (Figure 3A). Also, Snf7-mNeonGreen recruitment to ER clusters was still functional in *hac1Δ* cells, which means that this process does not require the UPR (Figure 3C).

5.6 Aims of this thesis

In recent years, a growing number of biological roles have been ascribed to the action of the ESCRT machinery. To this day, no stress-induced function of the ESCRT proteins at specific ER sites is known. My work focused on two specific goals: I set out to

a) identify the machinery that is required for ESCRT recruitment to the ER and

b) assign a biological function to this process.

This approach would help to determine the contribution of this ESCRT-mediated process to the cellular response to ER stress. My work in yeast may allow to ask whether stress-induced ESCRT recruitment to the ER also happens in mammals.

6 MATERIAL & METHODS

6.1 Materials

6.1.1 Buffers and solutions

Table 1: Buffers and solutions used in this study.

Buffer/solution	Composition
Acrylamide mix (30%, 37.5:1)	29.2% (w/v) acrylamide 0.8% (w/v) N,N'-myethylen-bisacrylamide
Amino acid mix	2% in water, autoclaved
Ammonium persulfate (APS)	10% (w/v) in water
Betaine	5 M in water containing 0.5% (w/v) Orange G
Blotting buffer	25 mM Tris 192 mM glycine 20% (v/v) techn. EtOH
Colony PCR buffer (10x)	200 mM Tris-HCl, pH 8.8 100 mM (NH4)2SO4 100 mM KCl 25 mM MgCl2
cOmplete protease inhibitors (25x)	1 tablet in 2 mL water
dNTPs	10 mM each of dATP, dGTP, dCTP and dTTP
Glucose (10x)	20% (w/v) in water, autoclaved
Lithium acetate	1 M in water, sterile-filtered
Loading dye (5x)	50% (v/v) glycerol 10% (v/v) 10x TAE buffer 0.05% (w/v) Orange G
Lysis buffer	50 mM HEPES, pH 7.5 0.5 mM EDTA
Polyethylene glycol (PEG) 3350	50% (w/v) in water, sterile-filtered

Ponceau S	0.1% Ponceau S 5% (v/v) acetic acid
Salmon sperm DNA	10 mg/mL in water
SDS-PAGE running buffer	25 mM Tris 0.1% (w/v) SDS 192 mM glycine
SDS-PAGE sample buffer (4x)	278 mM Tris, pH 6.8 44.4% (v/v) glycerol 4.4% (w/v) Lithium dodecyl sulfate (LDS) 0.02% (w/v) bromophenol blue 0.1 volume β-mercaptoethanol, freshly added before use
Separating gel buffer	2 M Tris, pH 8.8
Sodium dodecyl sulfate (SDS)	15% (w/v) in water
Stacking gel buffer	0.5 M Tris, pH 6.8
TAE buffer (50x)	2 M Tris 1 M acetic acid 50 mM EDTA
TBS/Tween (TBST)	10 mM Tris, pH 7.4 150 mM NaCl 0.1% (v/v) Tween
Transformation mix	33% (w/v) Polyethylene glycol (PEG) 3350 100 mM Lithium acetate 0.28 µg/mL salmon sperm DNA, freshly boiled before use
Tunicamycin (Tm)	1 mg/mL in DMSO
Yeast nitrogen base (YNB)	6.9% (w/v) in water, autoclaved

Table 2: Composition of the synthetic complete amino acid mix.

For drop out plates (SC -His/-Leu/-Trp/-Ura), the respective amino acid was excluded from the amino acid mix.

Component	Amount
Adenine	0.5 g
Alanine	2 g
Arginine	2 g
Asparagine	2 g
Aspartic acid	2 g
Cysteine	2 g
Glutamic acid	2 g
Glutamine	2 g
Glycine	2 g
Histidine	2 g
Inositol	2 g
Isoleucine	2 g
Leucine	4 g
Lysine	2 g
Methionine	2 g
Para-aminobenzoic acid	0.2 g
Phenylalanine	2 g
Proline	2 g
Serine	2 g
Threonine	2 g
Tyrosine	2 g
Tryptophan	2 g
Uracil	2 g
Valine	2 g

Table 3: Amino acid supplement used for sporulation plates in library generation.

Component	Amount
Histidine	2 g
Leucine	4 g
Lysine	2 g
Uracil	2 g

6.1.2 Growth media and plates

Table 4: Growth media for liquid culture of yeast or bacteria.

Medium	Composition
SCD	2% (w/v) glucose 0.69% (w/v) YNB 0.2% (w/v) amino acid mix
YPD	1% (w/v) yeast extract 2% (w/v) peptone 2% (w/v) glucose
LB	1% (w/v) tryptone 0.5 % (w/v) yeast extract 1% (w/v) NaCl
LB + ampicillin	1% (w/v) tryptone 0.5 % (w/v) yeast extract 1% (w/v) NaCl 100 μg/mL ampicillin

Table 5: Media plates for growth of yeast and bacteria

Plates	Composition
SCD plates	0.69% (w/v) YNB 0.2% (w/v) amino acid mix 2% (w/v) glucose 2% (w/v) agar
YPD plates	1% (w/v) yeast extract 2% (w/v) peptone 2% (w/v) glucose 2% (w/v) agar

Table 6: Media plates containing antibiotics for growth of yeast and bacteria

Plates	Composition
YPD G418 plates	1% (w/v) yeast extract 2% (w/v) peptone 2% (w/v) glucose 1% (w/v) agarose 20 μg/mL Geneticin (G418)
YPD hph plates	1% (w/v) yeast extract 2% (w/v) peptone 2% (w/v) glucose 1% (w/v) agarose 100 μg/mL Hygromycin B
YPD nat plates	1% (w/v) yeast extract 2% (w/v) peptone 2% (w/v) glucose 1% (w/v) agarose 10 μg/mL Nourseothricin (ClonNat)
LB ampicillin plates	1% (w/v) tryptone 0.5 % (w/v) yeast extract 1% (w/v) NaCl 2% (w/v) agar 100 μg/mL ampicillin

Table 7: Media plates used for the preparation of screening libraries by synthetic genetic array.

Plates	Composition
Sporulation plates	0.1% (w/v) yeast extract 1% (w/v) potassium acetate 0.01% (w/v) amino acid supplement 0.05% (w/v) glucose 2% (w/v) agar 50 μg/mL Geneticin (G418)

SC -HIS/-ARG/-LYS/+can/+thia	0.17% (w/v) YNB 0.1% (w/v) monosodium glutamate 0.2% (w/v) amino acid mix -his, -arg and -lys 2% (w/v) glucose 2% (w/v) agar 50 µg/mL canavanine 50 µg/mL thialysine
SC -HIS/-ARG/-LYS/-URA/+can/+thia	0.17% (w/v) YNB 0.1% (w/v) monosodium glutamate 0.2% (w/v) amino acid mix -his, -arg , -lys, -ura 2% (w/v) glucose 2% (w/v) agar 50 µg/mL canavanine 50 µg/mL thialysine
SC -HIS/-ARG/-LYS/-URA/+can/+thia/+G418	0.17% (w/v) YNB 0.1% (w/v) monosodium glutamate 0.2% (w/v) amino acid mix -his, -arg , -lys, -ura 2% (w/v) glucose 2% (w/v) agar 50 µg/mL canavanine 50 µg/mL thialysine 200 µg/mL Geneticin (G418)
SC -HIS/-ARG/-LYS/-URA/+can/+thia/+G418/ +nat	0.17% (w/v) YNB 0.1% (w/v) monosodium glutamate 0.2% (w/v) amino acid mix -his, -arg , -lys, -ura 2% (w/v) glucose 2% (w/v) agar 50 µg/mL canavanine 50 µg/mL thialysine 200 µg/mL Geneticin (G418) 100 µg/mL Nourseothricin (ClonNat)

6.1.3 Enzymes, standards and kits

Table 8: Enzymes used in this study.

Enzyme	Supplier
OptiTaq DNA polymerase	Roboklon
Q5 High-fidelity DNA polymerase	New England Biolabs
Taq polymerase	Sigma-Aldrich
T4 DNA ligase	Thermofisher Scientific
Restriction enzymes	New England Biolabs

Table 9. DNA and protein standards used in this study.

Standard	Supplier
GeneRuler 1kb Plus DNA ladder	Thermofisher Scientific
PageRuler Plus Prestained Protein ladder	Thermofisher Scientific

Table 10. Kits used in this study.

Kit	Supplier
miniBio Column Plasmid MiniPrep	miniBio Life Science Products
miniBio Gel and PCR Cleanup	miniBio Life Science Products
Pierce Rapid Gold Protein Assay Kit	Thermofisher Scientific

6.1.4 Antibodies

Table 11. Antibodies used in this study.

Antibody	Supplier
mouse anti-FLAG (M2, F1804)	Sigma-Aldrich
goat anti-mouse-HRP (31432)	Pierce (Thermofisher Scientific)

6.2 Molecular biology methods

6.2.1 Plasmids

Table 14: Plasmids used in this study.

Plasmid	Alias	Source
pSH-EFIRES-B-AtAFB2-mCherry	pSS1063	Addgene 129718; (Li et al., 2019)
pSH-EFIRES-P-Seipin-miniIAA7-mCherry	pSS1064	Addgene 129720; (Li et al., 2019)
pSH-EFIRES-P-Seipin-miniIAA7-3xFLAG	pSS1065	Addgene 129722; (Li et al., 2019)

pFA6a-IAA7-3xFLAG-kanMX6	pSS1154	This study
pFA6a-IAA7-cherry-kanMX6	pSS1155	This study
pRS413-ADH-AFB2	pSS1163	This study
pRS305-ADH-AFB2-CYCterm	pSS1195	This study
pFA6a-GFP-kanMX6	pSS037	(Longtine et al., 1998)
pRS305-Padh-Sec66-FLAG-GFP-Tcyc	pSS196	Sebastian Schuck

Plasmids of the pFA6a series used for tagging and deletion of genes in *S. cerevisiae* (Longtine et al., 1998; Janke et al., 2004) are not listed in the table above.

6.2.2 Oligonucleotides

Table 15: Oligonucleotides used in this study.

Primers	Sequence
Pac-miniIA7	GGTTAATTAACGGCTTCTCTGAGACCGTG
FLAG-Asc	AAGGCGCGCCCTACTTGTCATCGTCATCCTTG
cherry-Asc	AAGGCGCGCCCTACTTGTACAGCTCGTCC
SpeI-AFB2	TTACTAGTATGAACTACTTTCCCGATGAG
AFB2-stop-Eco	ATAGAATTCTTACAGAATCCAGACAAAGGGG

Oligonucleotides for tagging and deletion of genes in *S. cerevisiae* were designed according to (Longtine et al., 1998) and (Janke et al., 2004) and are not listed in the table above.

6.2.3 Molecular cloning

Oligonucleotides listed in Table 15 were used to generate the plasmids listed in Table 14.
For the amplification of DNA sequence, polymerase chain reaction (PCR) was used. The reactions were performed using OptiTaq DNA polymerase or Q5 High-fidelity DNA polymerase with the standard reaction conditions recommended by the supplier of the polymerases. Restriction digests were performed following the guidelines provided by New England Biolabs. PCR products were either directly purified using the miniBio Gel and PCR Cleanup kit or first separated on 1% agarose gels, extracted and then purified using the miniBio Gel and PCR Cleanup kit. Ligations were carried out following the instructions of the T4 DNA ligase manufacturer. After ligation, products were used for the transformation of *E. coli* DH5alpha cells. Plasmids were then retrieved using the miniBio Column Plasmid MiniPrep according to the manual provided by the manufacturer.
Plasmid pFA6a-IAA7-3xFLAG-kanMX6 was generated by amplification of mini-IAA7-3xFLAG from pSH-EFIRES-P-Seipin-miniIAA7-3xFLAG using oligonucleotides Pac-miniIA7 and FLAG-Asc and cloned into the PacI/AscI site of pFA6a-GFP-kanMX6. Plasmid pFA6a-IAA7-cherry-kanMX6 was generated by amplification of mini-IAA7-mCherry from pSH-EFIRES-P-Seipin-miniIAA7-mCherry with oligonucleotides Pac-miniIA7 and cherry-Asc, and cloned into the PacI/AscI site of pFA6a-GFP-kanMX6. Plasmid pRS413-ADH-AFB2 was generated by amplification of AFB2 from pSH-EFIRES-B-

AtAFB2-mCherry with oligonucleotides SpeI-AFB2 and AFB2-stop-Eco, and cloned into the SpeI/EcoRI site of pRS413-ADH. For generation of plasmid pRS305-ADH-AFB2-CYCterm, pRS413-Padh-AFB2-Tcyc was digested with SpeI/EagI and inserted into SpeI/EagI digested pRS305-Padh-Sec66-FLAG-GFP-Tcyc.

6.3 Yeast methods

6.3.1 Yeast strains

Table 16: Yeast strains used in this study.

Strain genotype	Alias	Source
leu2-3,112 trp1-1 can1-100 ura3-1 his3-11,15	SSY122	(Szoradi et al., 2018)
ura3::P_{VPS24}-Snf7-mNeonGreen-URA3 trp1::P_{GPD}-mCherry-Ubc6-TRP1	SSY2544	This study (Jasmin Schäfer)
ura3::P_{VPS24}-Snf7-mNeonGreen-URA3 trp1::P_{GPD}-mCherry-Ubc6-TRP1 bro1Δ::nat	SSY2555	This study (Jasmin Schäfer)
ura3::P_{VPS24}-Snf7-Scarlet-i-URA3 trp1::P_{GPD}-BFP-Ubc6-TRP1 BRO1-mNeonGreen::nat	SSY2834	This study
ura3::P_{TEF}-mCherry-Ubc6-URA3 BRO1-mNeonGreen-HA::nat	SSY2693	This study (Jasmin Schäfer)
ura3::P_{VPS24}-Snf7-mNeonGreen-URA3 trp1::P_{GPD}-mCherry-Ubc6-TRP1 snf7Δ::nat	SSY3008	This study
Y8205 his3::P_{GPD}-TagBFP-PLCdelta-PH2-hph ura3::P_{VPS24}-Snf7-mNeonGreen-ura3::P_{TEF}-mCherry-Ubc6::nat vps27Δ::URA3	SSY2643	This study (Carlos Martin de Hijas)
ura3::P_{VPS24}-Snf7-mNeonGreen-URA3 trp1::P_{GPD}-mCherry-Ubc6-TRP1 bst1Δ::HIS3	SSY3359	This study
ura3::P_{VPS24}-Snf7-mNeonGreen-URA3 trp1::P_{GPD}-mCherry-Ubc6-TRP1 per1Δ::HIS3	SSY3360	This study
ura3::P_{VPS24}-Snf7-mNeonGreen-URA3 trp1::P_{GPD}-mCherry-Ubc6-TRP1 ted1Δ::HIS3	SSY3361	This study
ura3::P_{VPS24}-Snf7-mNeonGreen-URA3 trp1::P_{GPD}-mCherry-Ubc6-TRP1 erv25Δ::HIS3	SSY2832	This study
ura3::P_{VPS24}-Snf7-mNeonGreen-URA3 trp1::P_{GPD}-mCherry-Ubc6-TRP1 emp24Δ::HIS3	SSY2833	This study

ura3::P_{VPS24}-Snf7-Scarlet-i-URA3 trp1::P_{GPD}-BFP-Ubc6-TRP1 EMP24-mNeonGreen::HIS3	SSY2936	This study
ura3::P_{VPS24}-Snf7-Scarlet-i-URA3 trp1::P_{GPD}-BFP-Ubc6-TRP1 emp24-AA-mNeonGreen::HIS3	SSY3358	This study
SEC63-mCherry::TRP1	SSY1403	This study (Jasmin Schäfer)
SEC63-miniIAA7-mCherry::kan	SSY3029	This study (Sebastian Schuck)
SEC63-miniIAA7-mCherry::kan trp1::P_{ADH}-AtAFB2-TRP1	SSY3071	This study
VPH1-mCherry::HIS3	SSY939	This study (Dorottya Polos)
VPH1-miniIAA7-mCherry::kan	SSY3031	This study (Sebastian Schuck)
VPH1-miniIAA7-mCherry::kan trp1::P_{ADH}-AtAFB2-TRP1	SSY3072	This study
ura3::P_{VPS24}-Snf7-mNeonGreen-URA3 trp1::P_{GPD}-mCherry-Ubc6-TRP1 SEC16-miniIAA7-FLAG::kan leu2::P_{ADH}-AtAFB2-LEU2	SSY3260	This study
ura3::P_{VPS24}-Snf7-mNeonGreen-URA3 trp1::P_{GPD}-mCherry-Ubc6-TRP1 SEC24-miniIAA7-FLAG::kan leu2::P_{ADH}-AtAFB2-LEU2	SSY3261	This study
ura3::P_{VPS24}-Snf7-mNeonGreen-URA3 trp1::P_{GPD}-mCherry-Ubc6-TRP1 SEC31-miniIAA7-FLAG::kan leu2::P_{ADH}-AtAFB2-LEU2	SSY3262	This study
ura3::P_{VPS24}-Snf7-mNeonGreen-URA3 trp1::P_{GPD}-mCherry-Ubc6-TRP1 LST1-miniIAA7-FLAG::kan leu2::P_{ADH}-AtAFB2-LEU2	SSY3425	This study
ura3::P_{VPS24}-Snf7-mNeonGreen-URA3 trp1::P_{GPD}-mCherry-Ubc6-TRP1 DSL1-miniIAA7-FLAG::kan leu2::P_{ADH}-AtAFB2-LEU2	SSY3463	This study (Natalie Friemel)
ura3::P_{VPS24}-Snf7-Scarlet-i-URA3 trp1::P_{GPD}-BFP-Ubc6-TRP1 DSL1-mNeonGreen-HA::HIS3	SSY3496	This study
ura3::P_{VPS24}-Snf7-Scarlet-i-URA3 trp1::P_{GPD}-BFP-Ubc6-TRP1 DSL1-mNeonGreen-HA::HIS3 bro1Δ::nat	SSY4156	This study (Lis Albert)
ura3::P_{VPS24}-Snf7-Scarlet-i-URA3 trp1::P_{GPD}-BFP-Ubc6-TRP1 SEC24-mNeonGreen-HA::HIS3	SSY3380	This study

ura3::P_{VPS24}-Snf7-Scarlet-i-URA3 trp1::P_{GPD}-BFP-Ubc6-TRP1 SEC31-mNeonGreen-HA::HIS3	SSY3381	This study
ura3::P_{VPS24}-Snf7-Scarlet-i-URA3 trp1::P_{GPD}-BFP-Ubc6-TRP1 LST1-mNeonGreen-HA::HIS3	SSY3351	This study
ura3::P_{VPS24}-Snf7-Scarlet-i-URA3 trp1::P_{GPD}-BFP-Ubc6-TRP1 LST1-mNeonGreen-HA::HIS3	SSY3493	This study
BRO1-Halo::HIS3	SSY3838	This study (Fay Papavissarion)
SEC63-Halo::HIS3	SSY3839	This study (Fay Papavissarion)
SEC31-Halo::HIS3	SSY3840	This study (Fay Papavissarion)
ura3::P_{VPS24}-Snf7-Scarlet-i-URA3 trp1::P_{GPD}-BFP-Ubc6-TRP1 COP1-mNeonGreen-HA::HIS3 SEC24-Halo::kan	SSY3897	This study (Fay Papavissarion)
ura3::P_{VPS24}-Snf7-Scarlet-i-URA3 trp1::P_{GPD}-BFP-Ubc6-TRP1 NVJ2-mNeonGreen::HIS3	SSY3896	This study
ura3::P_{VPS24}-Snf7-mNeonGreen-URA3 trp1::P_{GPD}-mCherry-Ubc6-TRP1 kan-GEM-P_{GAL}-NVJ2	SSY4147	This study
ura3::P_{VPS24}-Snf7-mNeonGreen-URA3 trp1::P_{GPD}-mCherry-Ubc6-TRP1 kan-GEM-P_{GAL}-LAG1	SSY4148	This study
ura3::P_{VPS24}-Snf7-scarlet-i-URA3 trp1::P_{GPD}-BFP-Ubc6-TRP1 TCB3-mNeonGreen::HIS3	SSY4153	This study
ura3::P_{VPS24}-Snf7-scarlet-i-URA3 trp1::P_{GPD}-BFP-Ubc6-TRP1 TCB3-mNeonGreen::HIS3 nvj2Δ::nat	SSY4193	This study
ura3::P_{VPS24}-Snf7-scarlet-i-URA3 trp1::P_{GPD}-BFP-Ubc6-TRP1 TCB3-mNeonGreen::HIS3 bro1Δ::nat	SSY4155	This study
bro1(Y320D) trp1::P_{TEF}-BFP-Ubc6-TRP1 ura3::P_{VPS24}-Snf7-scarlet-i-URA3 TCB3-mNeonGreen::HIS3	SSY4190	This study
ura3::P_{VPS24}-Snf7-mNeonGreen-URA3 trp1::P_{GPD}-mCherry-Ubc6-TRP1 nvj2Δ::nat	SSY3987	This study
ura3::P_{VPS24}-Snf7-mNeonGreen-URA3 trp1::P_{GPD}-mCherry-Ubc6-TRP1 tcb3Δ::hph tcb2Δ::nat tcb1Δ::LEU2	SSY4200	This study

ura3::P_{VPS24}-Snf7-Scarlet-i-URA3 trp1::P_{GPD}-BFP-Ubc6-TRP1 TCB3-mNeonGreen::HIS3 COP1-Halo::kan	SSY4376	This study
ura3::Pvps24-Snf7-neon-URA3 trp1::Pgpd-cherry-Ubc6-TRP1 dga1Δ::HIS3 lro1Δ::nat	SSY4189	This study

Yeast strains were generated using the PCR-based method originally described in (Longtine *et al*, 1999) and further modified by Janke and colleagues (Janke *et al*, 2004). Genomic integration of constructs for the expression of ectopic proteins relying on homologous recombination was performed according to (Sikorski & Hieter, 1989).

6.3.2 Library generation for genetic screens using the synthetic genetic array method

The query strain used for both screens and the corresponding collection was crossed using the synthetic genetic array methodology described in (Tong & Boone, 200). This was achieved by automatic arraying with a Singer ROTOR HDA colony manipulation robot (Singer Instruments) that was kindly provided by the lab of Michael Knop at the Zentrum für Molekularbiologie (ZMBH) of Heidelberg University.
First, collections were pinned on YPD + G418 plates and grown at 30°C (25°C for the ts collection) overnight. At the same time, query strain was grown in SC -URA +hph +nat medium before pinning on YPD +nat +hph plates. Query strain and libraries were mated on YPD plates at room temperature for 24 h. Diploid selection was achieved by pinning on YPD + G418 plates and strains were grown at 30°C (25°C for ts collection) for 30 h (48 h for ts collection). Sporulation was achieved by growth on sporulation plates + ¼ G418 at 23°C for 7 days. Then, Mat-a haploids were selected on SC-His/-Arg/-Lys/+can/+thial plates at 30°C (25°C for ts collection) for 2 days before final selection was achieved by spotting on SC-His/-Arg/-Lys/+can/+thial/ -URA/+nat/+hph/+G418 plates.

6.3.3 Growth conditions and ER stress induction

Yeast cells were grown at 30°C in glass tubes in a shaking incubator for all experiments (except screening libraries and deepwell plates for flow cytometry experiments). Only cells in early log-phase, i.e. logarithmic growth phase (OD_{600nm} 0.1 – 1) were used for experiments. Cells were grown in liquid SCD medium except for yeast transformation. For this cells were grown in the richer YPD medium.
For induction of stress, exponentially growing cells at OD_{600nm} 0.3 were treated with 1 μg/mL tunicamycin for 3 h.

6.3.4 Yeast transformation

Yeast strains were transformed using the LiAc method (Ito *et al*, 1983). A yeast culture was grown in YPD medium overnight into saturation. The next morning, cells were back-diluted in 5 mL YPD in order to reach an OD of 1 within the next four hours. After four hours growth, cells were spun down in 15 mL falcon tubes at 5,000 x g, washed with one volume of water, transferred into 1.5 mL microcentrifuge tubes and centrifuged again, this time at 10,000 x g using a table microcentrifuge. After the supernatant was discarded, transforming DNA was added to the pellet (10 % of the PCR volume of transforming DNA). Subsequently, cells were resuspended in 360 µl tansformation mix (Table 1) and subjected to heat shock at 42°C for 40 min. After heat shock, cells were spun down and resuspended in 1 mL YPD medium. If cells acquired transforming DNA that contained an antibiotic resistance gene, cells were recovered at 30°C for three to six hours. From the 1 mL culture in YPD, 100 µL cells were plated on selective plates using glass beads. After 2 days at 30°C, colonies were restreaked on selective plates and subjected to colony PCR to check for successful genetic modification.

6.3.5 Colony PCR

Colony PCR was performed to check the successful genetic modification of yeast strains. Single colonies were picked from restreaked single colonies. In 0.5 mL PCR strips, a sample from the single colonies was resuspended using the colony PCR mix (Table 1). PCR was performed with standardized conditions supplied by the manufacturer of the Taq polymerase (Sigma-Aldrich). Next, 8 µL of the finished PCR was loaded on a 2x TAE + 1% agarose gel. Stain G was included in the hot agarose solution before the gel was poured into a running chamber. The PCR product was visualized with an illumination table (BL star 16 from Biometra) and GeneRuler 1kb Plus DNA ladder (Thermofisher Scientific) acted as size reference.

6.3.6 Flow cytometry

The auxin-inducible degradation of Sec63p-miniIAA7-mCherry and Vph1p-miniIAA7-mCherry was analyzed by flow cytometry. For this, cells were grown in 96 deep-well plates in two sets. Once cells reached exponential growth phase, one set of samples was treated with 750 µM auxin. Right after the addition of auxin, the first time point was measured at a FACS Canto flow cytometer (BD) using a custom-made high throughput sample (HTS) loader. The signal of mCherry was measured using the 561 nm laser. Recorded signals were normalized to cell size using the forward scatter. A wt strain was included to subtract background autofluorescence. In between time points, cultures on deep-well plates were returned to the shaking incubator at 30°C.

6.3.7 Light microscopy

All microscopic images were acquired using widefield microscopy. For this, two widefield microscopes were used. The first one was the Olympus IX81 CellSens microscope with a PLAPO 100x/1.45 Oil DIC objective (Olympus) and an Orca R2 camera (Hamamatsu). This microscope was part of the ZMBH Imaging facility on campus. The other widefield system used for this study was the Nikon Ti2 microscope with a PLAN APO 100x/1.45 objective (Nikon) and an Orca Fusion-BT camera (Hamamatsu) from the lab of Sebastian Schuck at Biochemistry Center (BZH) of Heidelberg University. Prior to imaging, yeast cells were spun down, resuspended in 20 μL remaining medium and 3 μL were spotted on cover slips. Cell suspensions were then covered by an agarose pad (1% agarose dissolved in SCD, melted, and poured on objective slides).

The yeast screen was performed using a Nikon Ti-E widefield microscope equipped with a motorized stage, the Nikon perfect focus system (PFS), a Flash4 sCMOS camera (Hamamatsu), a 60x/1.49 oil immersion lens (Nikon) and a custom-built oil pump for continuous oil supply during imaging from the lab of Michael Knop at Zentrum für Molekularbiologie (ZMBH) of Heidelberg University. Imaging was performed in 96 deep well glass bottom plates (MatriPlate MGB096-1-2-LG-L). Before cells were added, plates were Concanavalin A (ConA) coated. For this, 100 μL Bioconnex (1:1000 in ethanol) was added and incubated for 20 min. After washes with ethanol and destilled water, 100 μL ConA (0.1 mg/mL in water) was added for 30 min. Just before the addition of cells to the plates, wells were washed with water. For the screening, cells were inoculated in SCD and grown overnight at 30°C (25°C for the ts collection). Then, 100 μL of cells normalized to an OD of around 0.2 were added to the ConA coated 96 deep well glass bottom plates. After 2 h, medium was removed and 1 mL fresh SCD containing 5 μg/mL tunicamycin was added. Cells were imaged after 3 h of Tm treatment using the screening microscope.

For the ts screen, cells were fixed after 3 h of Tm treatment. For this, the supernatant of all wells was removed and 200 μl of 4% para-formaldehyde (PFA) in PBS were added. After 10 min, the PFA solution was removed and wells were washed 3x with PBS. Cells were then imaged using the screening microscope.

6.3.8 Image processing

Hyperstacks and montages of images were created in Fiji. Before quantification of Snf7 puncta in different genotypes, Fiji plugin “Blind Analysis Tools” was used to assign random names to files and therefore avoid bias. For selected images acquired at the Olympus IX81 CellSens microscope, in-built deconvolution algorithm “Wiener filter” was used to reduce out of focus light. For this, Z stacks were acquired with a step size of 200 nm. For selected images acquired at the Nikon Ti2 microscope, batch deconvolution by NIS Elements was used to deconvolve images. The “Richardsson-Lucy” algorithm was used with 30 iterations and the noise level was set to “automatic”. Images that were subjected to deconvolution with the NIS software were acquired as Z stacks with a 200 nm step size in the nd file format. Images acquired from the screening microscope were analyzed using a MATLAB script written by Peter Bircham and later modified by Dimitris Papagiannidis.

6.4 Biochemistry methods

6.4.1 Cell lysis

Cell lysis was performed using the bead beating method. For this, exponentially growing cells were harvested by centrifugation at 1000 x g for 5 min, washed in one volume of cold water and either snap-frozen in liquid nitrogen for short-term storage or immediately processed in cell lysis. Cell pellets were resuspended on ice in cold lysis buffer (Table 1) containing 1x complete protease inhibitors (Table 1). Then, cell suspensions were transferred into 2 mL screw cap tubes containing 0.7 g 1 mm glass beads. Cells were lysed using a FastPrep24 (MP Biomedical) by vortexing at 6 m/s for 40 seconds. Afterwards, 200 μL of 15 % SDS were added, and cell lysates were transferred to a new set of pre-cooled 1.5 mL microfuge tubes. Samples were then incubated at 65°C for 5 min before samples were returned to ice. Then, lysates were cleared by centrifugation in a tabletop centrifuge at maximum speed at 4°C. Supernatants of the clearing spin were transferred into fresh 1.5 mL microcentrifuge tubes.

6.4.2 Protein determination

Protein concentrations of cell lysates were determined using the Pierce Rapid Gold Protein Assay Kit (Thermo Fisher Scientific). For this, 1 μL cell lysate and 9 μL water were combined in a 96 flat bottom plate in duplicates. Also, 10 μL of BSA standard solution ranging from 0 to 2 mg/mL were prepared in duplicates along with the cell lysates to act as reference. After BCA reagents A and B were mixed at a ratio of 50:1, 200 μL were added to each sample or standard well. Plates were incubated at room temperature for 5 min before absorbance was measured at 480 nm using a plate reader (Tecan infinite50). Using the standard curve generated from the measured absorbance of BSA reference samples, protein concentrations were determined.

6.4.3 SDS-PAGE

Cell lysates were diluted with water to generate a set of samples with the same protein amount. After addition of 0.1 volume of β-mercaptoethanol to 4x SDS-PAGE sample buffer, SDS-PAGE sample buffer was added to diluted cell lysates. Cell lysates were then boiled at 65°C for 5 min. An amount of 20 μg total protein was loaded per sample on a 7.5% SDS-PAGE gel. The gel was run at 200 V at room temperature until the running front was exiting the separating gel.

6.4.4 Western blot

Gels from SDS-PAGE were rinsed once in blotting buffer before the Western blot sandwich was assembled. Proteins were blotted on nitrocellulose membranes (GE Healthcare) at 4°C and 100 V for 1 h. After blotting, membranes were washed once with TBST and then placed in 5% (w/v) skimmed milk powder in TBST for 1 h for blocking. After blocking, primary antibodies were diluted in 5% (w/v) skimmed milk powder in TBST and membranes were incubated at 4°C overnight. This incubation was followed by three washes with TBST for 5 min each. Secondary antibodies were diluted in 5% (w/v) skimmed milk powder in TBST and membranes were incubated at room temperature for 1 h. Subsequently, membranes were washed three times with TBST. For visualization, ECL solution A and B (West Pico Plus from Pierce) were mixed 1:1 and added to the membrane. Membranes were incubated with resulting mix for 5 min at room temperature and scanned at a chemiluminescence imager (Amersham Imager 600).

Table 17: SDS-PAGE recipe for the separating gel.

7.5% separating gel	
H_2O	3.2 ml
separating gel buffer	1.2 ml
30% acrylamide mix	1.5 ml
15% SDS	40 µl
10% APS	60 µl
TEMED	6 µl

Table 18: SDS-PAGE recipe for the stacking gel.

4% stacking gel	
H_2O	1.2 ml
stacking gel buffer	0.5 ml
30% acrylamide mix	0.27 ml
15% SDS	13 µl
10% APS	20 µl
TEMED	2 µl

7 RESULTS

7.1 Characterization of ESCRT recruitment to ER clusters upon stress

7.1.1 Bro1 co-localizes with Snf7 at ER clusters upon ER stress

Previous work identified Bro1 as an essential factor for the recruitment of the ESCRT-III component Snf7 to ER clusters after ER stress. Consequently, I tagged *BRO1* endogenously with an mNeonGreen tag to study its localization in relation to ER clusters and Snf7-Scarlet-i. Non-functional Snf7-Scarlet-i was expressed at a low level besides the functional endogenous Snf7p to track ESCRT activity without interfering with ESCRT function. After ER stress treatment for 3 h, all Snf7-Scarlet-i puncta at ER clusters contained a strong Bro1p-mNeonGreen signal (Figure 4A). Therefore, Bro1 is not only essential for the recruitment of Snf7 to ER clusters but also co-localizes with Snf7 at these sites. This raised the question whether the re-localization of Bro1 to ER clusters can also be observed in the absence of tagged Snf7. For this experiment, I used a strain that only expressed Bro1p-mNeonGreen and an ER marker. After 3 h of ER stress, I only observed a small number of Bro1p-mNeonGreen puncta at ER clusters (roughly 2% of cells), which still formed in the absence of tagged Snf7 (Figure 4B; this field of view was acquired by Lis Albert). These Bro1 puncta at ER clusters were also less bright than Bro1 puncta that co-localize with tagged Snf7 (Figure 4A). The discrepancy of abundance of Bro1 puncta between the presence and absence of tagged Snf7 could mean that tagged Snf7 did not only act as a tracer of ESCRT activity in my experiments. A possible explanation for this is that the expression of tagged Snf7 besides the endogenous Snf7 leads to a stabilization of ESCRT structures. To rule out that the ESCRT structures at ER clusters after stress were an artifact of tagged Snf7 and did not represent biologically relevant sites of ESCRT activity, I tested the recruitment of Snf7-mNeonGreen to ER clusters in the absence of endogenous Snf7p. However, I detected no recruitment of Snf7-mNeonGreen to ER clusters when the functional, endogenous *SNF7* was deleted (Figure 4C). This supports the idea that ESCRT recruitment to ER clusters is a physiological process and not an artifact caused by the expression of a non-functional protein. In conclusion, Bro1p and endogenous Snf7p are required for the recruitment of Snf7-mNeonGreen to ER clusters after ER stress and Bro1p co-localizes with tagged Snf7 at these sites. It remained unclear which factors at the ER can be recognized and bound by Bro1 or Snf7. In order to identify these factors, I performed two genetic screens.

7.2 Genetic screens for the identification of genes involved in Snf7 recruitment to ER clusters

7.2.1 Generation of the query strain

To be able to study the recruitment of Snf7 to ER clusters upon ER stress, I set out to perform yeast library screens.

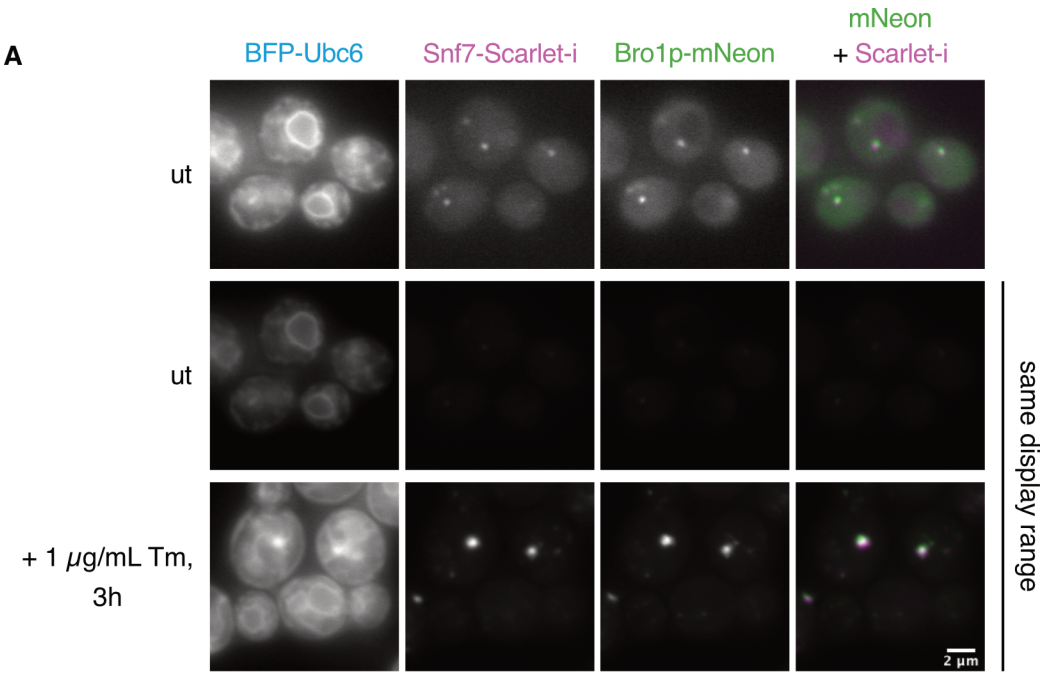
A
BFP-Ubc6
Snf7-Scarlet-i
Bro1p-mNeon
mNeon
+ Scarlet-i
ut
ut
+ 1 µg/mL Tm, 3h
same display range
2 µm

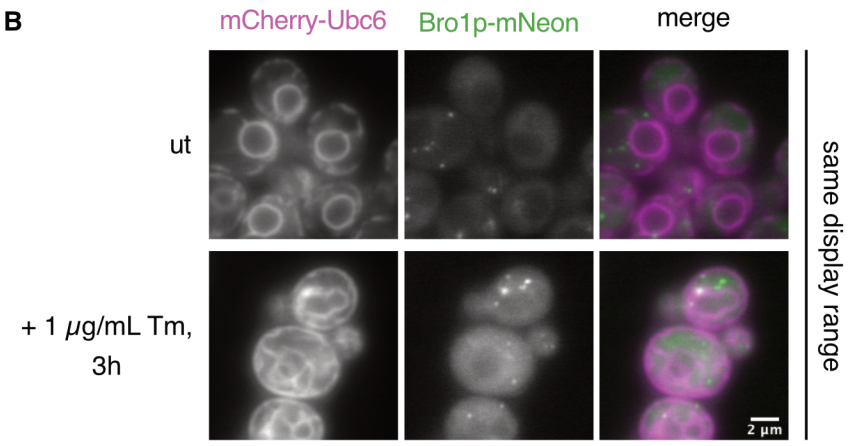
B
mCherry-Ubc6
Bro1p-mNeon
merge
ut
+ 1 µg/mL Tm, 3h
same display range
2 µm

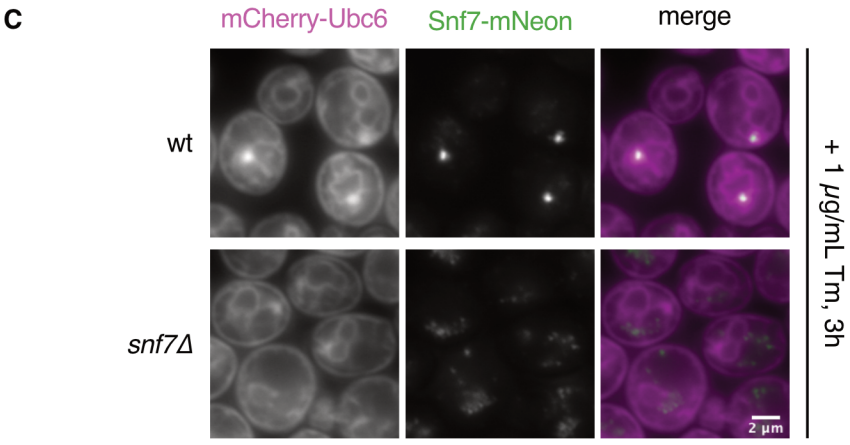
C
mCherry-Ubc6
Snf7-mNeon
merge
wt
snf7Δ
+ 1 µg/mL Tm, 3h
2 µm

Figure 4. Bro1p-mNeon co-localizes with Snf7-Scarlet-i at ER clusters in the presence of functional, endogenous Snf7.

(D) Fluorescence microscopy images of the W303 yeast strain stably expressing BFP-Ubc6, Snf7-Scarlet-i and Bro1p-mNeon. Exponentially growing cells were either treated with 1 μg/mL tunicamycin (Tm) for 3 h or left untreated before imaging. Untreated cells are shown in two display ranges so that the signal can be appreciated but also compared to the strong signal in treated cells.

(E) Fluorescence microscopy images of W303 yeast strain stably expressing mCherry-Ubc6 and Bro1p-mNeon. This strain was generated by Jasmin Schäfer. Exponentially growing cells were either treated with 1 μg/mL tunicamycin (Tm) for 3 h or left untreated before imaging. Images are presented with the same display range and signals can be compared quantitatively. This field of view was acquired by Lis Albert.

(F) Fluorescence microscopy images of W303 yeast strains stably expressing mCherry-Ubc6 and Snf7-mNeon in wt or *snf7Δ* background. Images show both strains treated with 1 μg/mL tunicamycin (Tm) for 3 h. Images are presented with the same display range and signals can be compared quantitatively.

The synthetic genetic array (SGA) technology enables the crossing of marker proteins into the yeast strain libraries (Tong & Boone, 2006). For this, a query strain of the opposite mating type than the library and carrying all required genetic modifications was generated first. Carlos Martin de Hijas, a former rotation student in the lab, introduced an ER marker and tagged Snf7 expressed at a low level into the yeast Y8205 synthetic genetic array starting strain. He also introduced a deletion of *VPS27* to free Snf7 from endosomes and thereby increase the cytosolic pool of the protein. He also added a plasma membrane marker to facilitate the semi-automated imaging of the libraries.

7.2.2 Genetic screen with the ER deletion collection

Since Bro1 and Snf7 are both soluble proteins, it is possible that a factor at the ER exists that binds either or both proteins upon ER stress. A genetic yeast screen could reveal genes that are involved in this process. Therefore, Peter Bircham selected a subcollection of the deletion collection of non-essential genes in yeast containing genes encoding ER and ER-associated proteins. This would reduce the complexity of the screen and target the outcome towards ER factors important for the formation of ER clusters and the recruitment of Snf7 or Bro1 to ER clusters. After the query strain was crossed with the ER deletion collection, cells were grown in 96 well glass bottom plates, treated with tunicamycin to induce the recruitment of Snf7 to ER clusters and then imaged using an automated screening microscope (Figure 5A). The images were analyzed in a semi-automated manner using a MATLAB script generated by Peter Bircham and modified by Dimitris Papagiannidis. After imaging, I assigned screen hits together with Dimitris Papagiannidis, Jasmin Schäfer and Sebastian Schuck. A hit was defined by an obvious reduction of Snf7 puncta in the cells present on the crops of images provided by the image analysis tool. From 713 genes in the ER deletion collection, we assigned 25 genes as hits. I assigned hits to the following categories: ER export, GPI-anchor remodeling, GET machinery, ER structure, lipid metabolism, ribosomal proteins and other (Figure 5B). Sei1p and Mdm12p are proteins involved in the formation of ER contact sites with lipid droplets (LDs) (Hugenroth & Bohnert, 2020) and with mitochondria (Jeong *et al*, 2016), respectively. Therefore, I included both in the “ER structure” category.

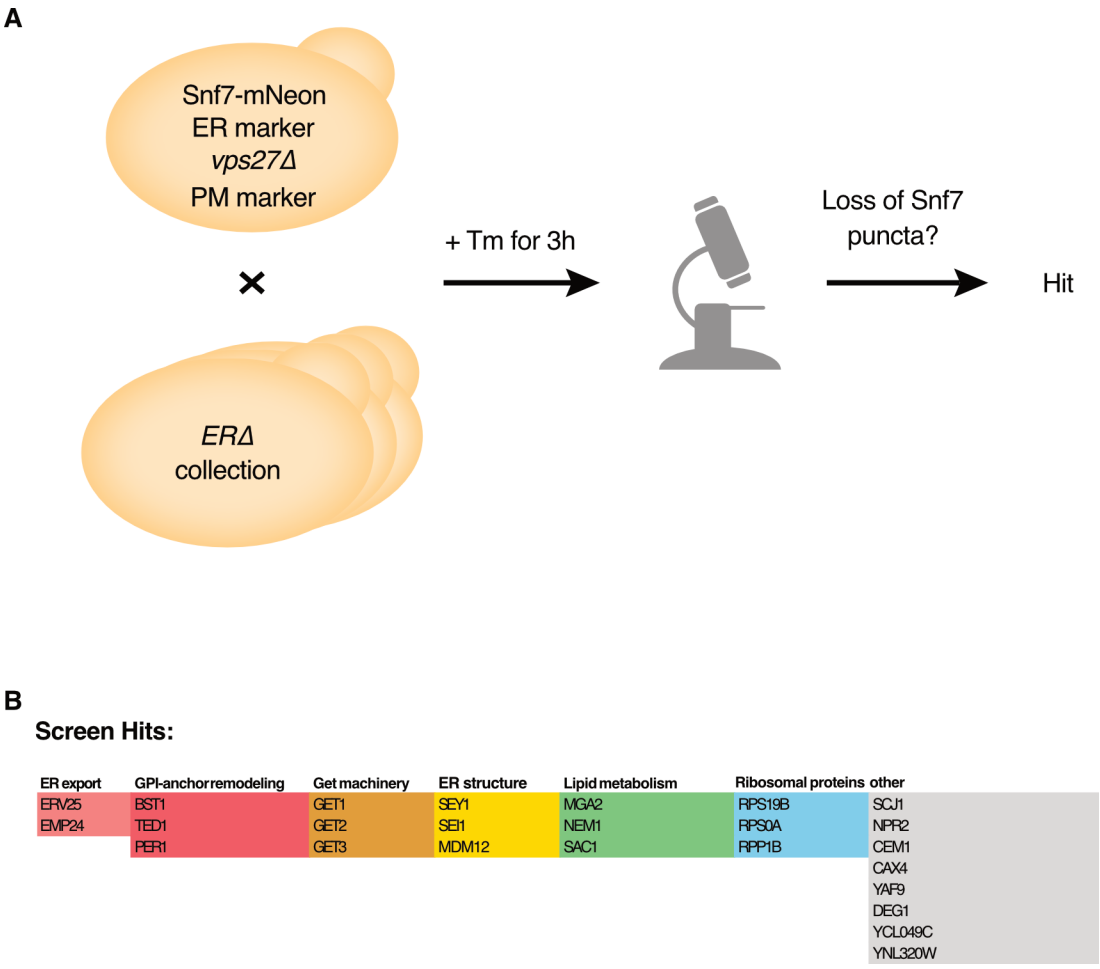

Figure 5. A screen with the ER deletion collection of non-essential genes to identify factors involved in Snf7 recruitment to ER clusters upon ER stress.

(A) Schematic of the screening procedure. A Y8205 query strain that stably expressed Snf7-mNeonGreen, an ER marker, and a plasma membrane (PM) marker in the vps27Δ background was crossed with the ER deletion collection of non-essential genes. The resulting strains were grown in multi well plates, treated with 1 μg/mL tunicamycin for 3 h, automatically imaged at a screening microscope and semi-automatically analyzed using a custom MATLAB script.

(B) Hits were manually assigned by Dimitris Papagiannidis, Jasmin Schäfer, Sebastian Schuck and me based on the loss of Snf7 puncta formation at ER clusters. Hits were summarized in functionally related categories.

7.2.3 Genetic screen with the ts allele collection of essential genes

A quarter of all genes in yeast cannot be studied by deletion because their function is essential for the survival of the cell. One possibility to overcome this restriction is the concept of temperature-sensitive (ts) alleles of essential genes. Temperature-sensitive alleles have a functional gene product at permissive temperature in a physiological temperature range. As soon as the temperature is increased or drops below a certain value and thereby reaches the restrictive temperature, the gene product is non-functional, which results in a conditional knock-out situation of this essential gene.

This is a concept that has been used in the past for studying the function of many essential genes. One example is the famous screen performed in the Schekman lab that identified many essential components of the secretory pathway (Novick *et al*, 1980). The ts allele collection of essential genes is a collection of 787 ts alleles that cover 497 of the 1101 essential genes in yeast (Li *et al*, 2011). This collection was created in the lab of Charles Boone at the Donnelly Centre of the University of Toronto and kindly provided to us by the lab of Michael Knop at the Zentrum für Molekulare Biologie (ZMBH) of Heidelberg University. After I crossed the ts allele collection of essential genes with the query strain, I grew cells up in 96 well glass bottom plates at 23°C, which I chose as permissive temperature. Subsequently, I treated cells with tunicamycin and at the same time shifted the temperature to 37°C. Each ts allele has its own restrictive temperature. I chose 37°C to affect the vast majority of all ts alleles. Only a handful of alleles contained higher restrictive temperatures, but this was no concern, as other alleles targeting the same gene had lower temperatures (< 37°C) in most cases (Li *et al*, 2011). After treatment and temperature shift for 3 h, I fixed cells and imaged the plates at the automated screening microscope (Figure 6A). I analyzed the acquired images in a semi-automated manner using a MATLAB script generated by Peter Bircham and modified by Dimitris Papagiannidis. After imaging, I assigned screen hits based on the same criterion as for the screen with the ER deletion collection. From 787 genes in the ts allele collection of essential genes, I assigned 156 genes as hits. I assigned the following categories to the hits: ER-Golgi trafficking, GPI-anchor remodeling, lipid metabolism and proteasome and related (Figure 6B).

7.3 Validation of screen hits

7.3.1 GPI-anchor remodeling proteins are required for the formation of ER clusters

The screens with the ER deletion and ts allele collection revealed that remodeling of the GPI-anchor is required for Snf7 puncta formation at ER clusters upon stress. It was remarkable that we identified four out of six genes that are involved in the remodeling of the GPI-anchor, namely *BST1*, *PER1*, *TED1* and *CDC1* (ts screen). As a next step, I introduced the single deletions of *BST1*, *PER1* and *TED1* into the W303 strain and tested if the recruitment of Snf7-mNeonGreen upon stress is affected in this strain background as well. W303 is the standard strain background that I have previously used for co-localization experiments of Bro1p and will use for all experiments except for the genetic screens. All single deletions showed a reduction of Snf7-mNeonGreen recruitment to the ER and the defect was most pronounced in *bst1Δ* and *Δted1* cells (Figure 7A and B). The deletion of *BST1* and *TED1* not only drastically reduced the frequency of Snf7 puncta, but also abolished ER cluster formation to a large extent (Figure 7B). The fact that remaining ER clusters often still had Snf7 puncta associated with them suggests that GPI-anchor remodeling genes are particularly important for the formation of ER clusters. Since ER clusters also exist in *bro1Δ* cells that are devoid of any Snf7 puncta after stress (Figure 3), ER cluster formation likely happens upstream of Snf7 recruitment by Bro1.

A

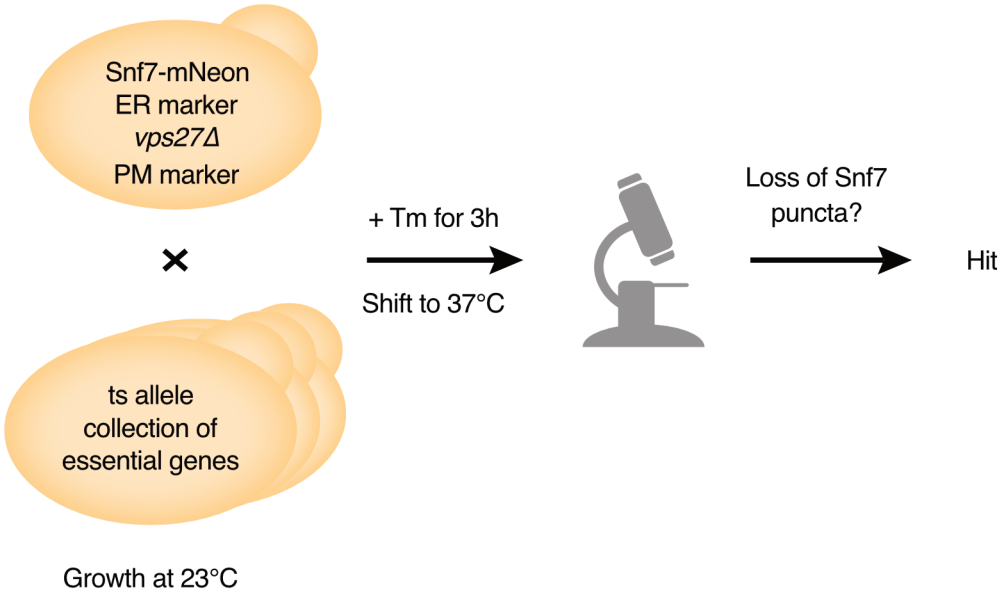

B

Screen Hits (selection):

ER-Golgi trafficking	Lipid metabolism	Proteasome and related	GPI-anchor remodeling
COP1	CDS1	PRE2	CDC1
SEC12	ERG3	PUP1	
SEC13	LCB1	RPT2	
SEC16	LCB2	SCL1	
SEC18	TSC3	CIC1	
SEC22		CDC48	
SEC23			
SEC31			
SEC39			
SLY1			
TIP20			
USO1			
YIP1			

Figure 6. A screen with the ts allele collection of essential genes to identify factors involved in Snf7 recruitment to ER clusters upon ER stress.

(A) Schematic of the screening procedure. A Y8205 query strain that stably expressed Snf7-mNeonGreen, an ER marker, and a plasma membrane (PM) marker in the vps27Δ background was crossed with the ER deletion collection of non-essential genes. The resulting strains were grown in multi well plates at 23°C, treated with 1 μg/mL tunicamycin and shifted to 37°C for 3 h, fixed, automatically imaged at a screening microscope and semi-automatically analyzed using a custom MATLAB script generated by Peter Bircham and Dimitris Papagiannidis.

(B) Hits were manually assigned based on the loss of Snf7 puncta formation at ER clusters. Hits were summarized in functionally related categories. This table shows an excerpt of all annotated hits.

7.3.2 p24 proteins and their interaction with COPII components are required for ER cluster formation

After GPI-anchor remodeling is completed in the ER, GPI-anchored proteins interact with the p24 complex, which is their specific ER export receptor (Muñiz *et al*, 2000).

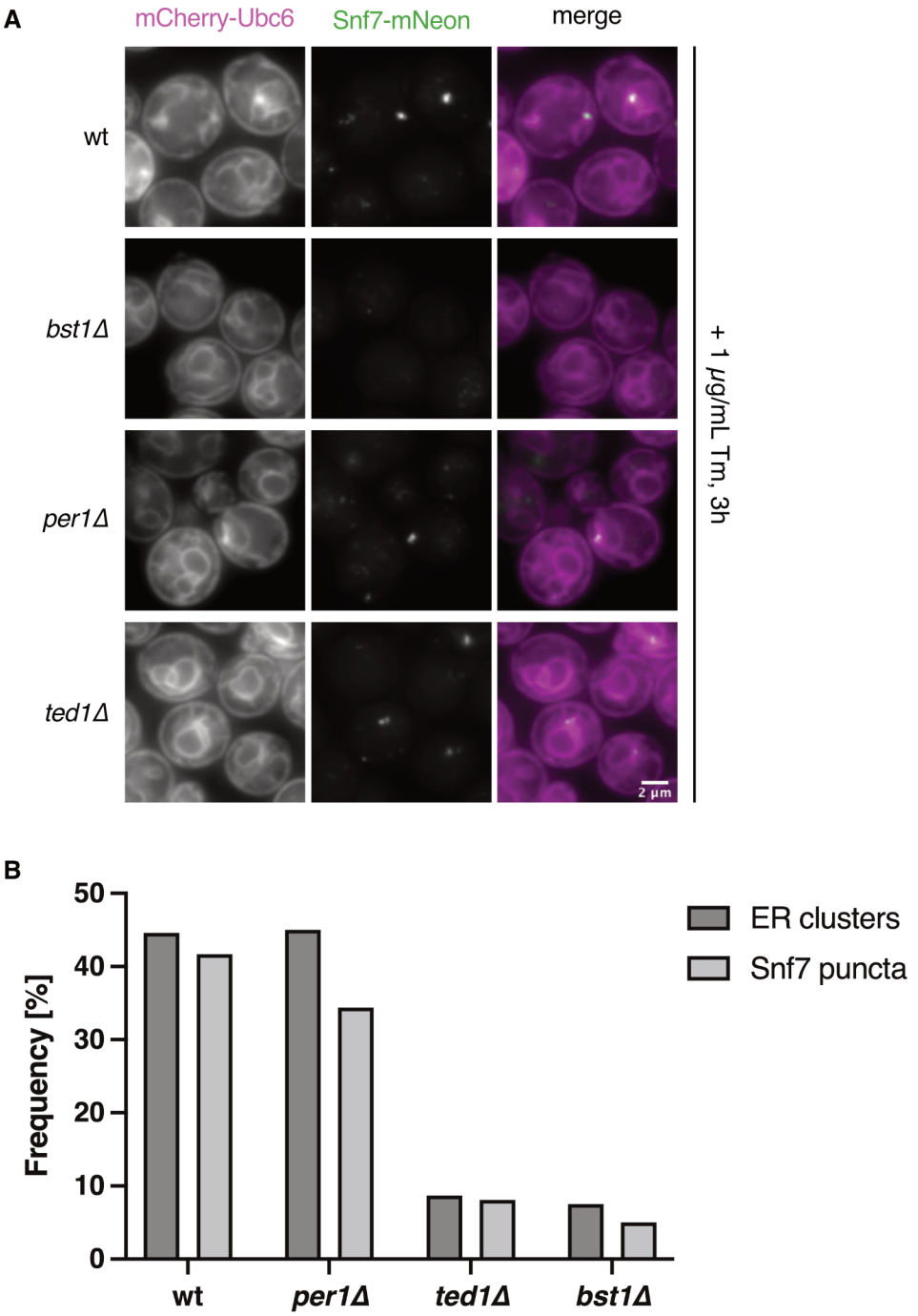

Figure 7. GPI-anchor remodeling is required for the formation of ER clusters upon ER stress.

(A) Fluorescence microscopy images of W303 yeast strains stably expressing mCherry-Ubc6 and Snf7-mNeonGreen in wt, *bst1Δ*, *per1Δ* and *ted1Δ* backgrounds. Exponentially growing cells were treated with 1 µg/mL tunicamycin (Tm) for 3 h before imaging. Images are presented with the same display range and signals can be compared quantitatively.

(B) Quantification of Snf7-mNeon puncta and ER clusters in different genetic backgrounds after treatment with 1 µg/mL tunicamycin for 3 h. Percentages of cells from all cells that show Snf7-mNeon puncta and/or ER clusters are plotted. For all genotypes more than 200 cells were quantified after images were randomized to reduce bias.

The ER deletion screen identified two prominent members of the p24 complex in yeast, Emp24p and Erv25p. Yeast has eight p24 proteins, but Emp24p and Erv25p are the only members of their specific subfamilies. Deletion of either of them is thought to destabilize the whole p24 complex (Hirata *et al*, 2013). I introduced both single deletions into the yeast W303 strain and tested their requirement for recruiting Snf7-mNeonGreen to ER clusters upon ER stress. Both deletions showed a strong reduction of Snf7 recruitment to ER clusters (Figure 8A). Additionally, both deletions decreased the abundance of ER clusters considerably, like the deletions of GPI-anchor remodeling genes that I tested previously (Figure 8A and B). Hence, both the GPI-anchor remodeling proteins and the p24 complex are important for the formation of ER clusters upstream of Snf7 recruitment to these sites. All p24 proteins are single-spanning transmembrane proteins that have a short cytosolic C-terminal tail, which contains a diaromatic motif that is important for the interaction with COPII components (Belden & Barlowe, 2001). To test if the interaction of Emp24p and the general ER export machinery COPII is relevant for the recruitment of Snf7 to ER clusters, I mutated the two aromatic residues of Emp24p to alanine and tagged the protein with mNeonGreen (Figure 8C, see (D'Arcangelo *et al*, 2015)). At steady state, Emp24p-mNeonGreen showed a weak ER staining and some punctate structures in the cytosol (not shown) that likely corresponded to Golgi cisternae, since Emp24p is known to shuttle between the ER and the Golgi (Sohn *et al*, 1996).

I observed a similar staining pattern when cells expressed emp24-AA-mNeonGreen (not shown). Upon ER stress, Emp24p-mNeonGreen staining was mostly restricted to the ER and concentrated in ER clusters (Figure 8C). It remained unclear if the concentration of Emp24p-mNeonGreen in ER clusters exceeded the concentration of a general ER marker at these sites. Additionally, some Emp24p-mNeonGreen localized to smaller cytosolic puncta that likely resembled transport vesicles. These puncta were smaller than the Golgi puncta that were stained at steady state. Whereas the expression of Emp24p-mNeonGreen resulted in a normal frequency of Snf7 puncta formation upon ER stress, emp24-AA-mNeonGreen expression resulted in almost complete absence of Snf7 puncta (Figure 8C). The exclusive ER staining of emp24-AA-mNeonGreen was also devoid of any ER clusters, similar to the phenotype that was observed in *emp24Δ* cells (Figure 8A). This observation suggested that the interaction of Emp24p with the general ER export machinery COPII is required for the formation of ER clusters and the subsequent recruitment of Snf7 to these sites. The remodelling of GPI-APs may be needed to cluster p24 proteins, which in turn are needed to recruit COPII. This could be necessary to generate the ER clusters.

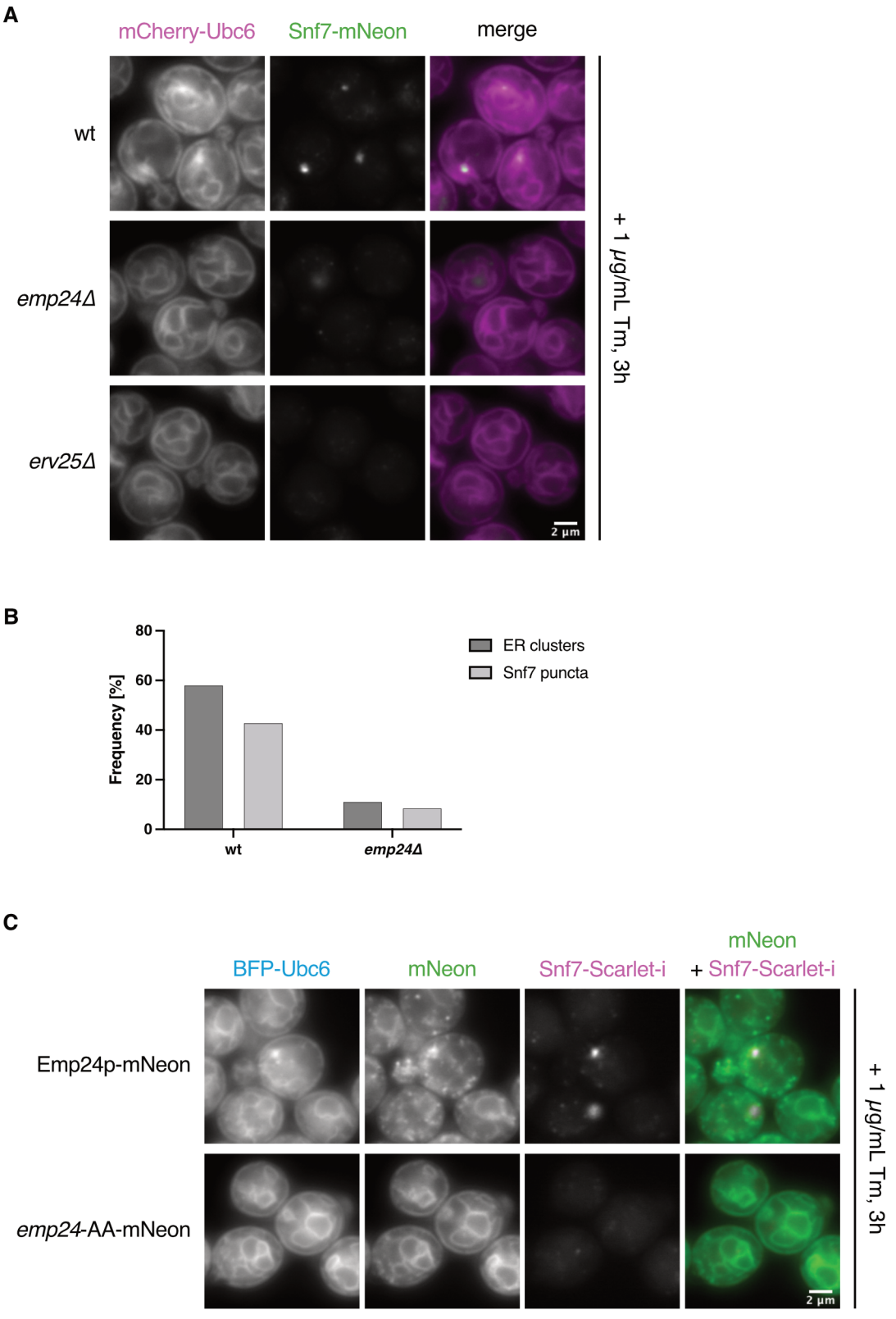

Figure 8. The p24 complex and its interaction with the general ER export machinery is required for the formation of ER clusters upon ER stress.

(A) Fluorescence microscopy images of W303 yeast strains stably expressing mCherry-Ubc6 and Snf7-mNeonGreen in wt, *emp24Δ* and *erv25Δ* backgrounds. Exponentially growing cells were treated with 1 µg/mL tunicamycin (Tm) for 3 h before imaging. Images are presented with the same display range and signals can be compared quantitatively.

(B) Quantification of Snf7-mNeonGreen puncta and ER clusters in wt and *emp24Δ* cells after treatment with 1 μg/mL tunicamycin for 3 h. Percentages of cells that show Snf7-mNeonGreen puncta and/or ER clusters are plotted. For all genotypes more than 200 cells were quantified after images were randomized to reduce bias.

(C) Fluorescence microscopy images of the W303 yeast strains stably expressing BFP-Ubc6, Snf7-Scarlet-i and Emp24p-mNeonGreen or *emp24*-AA-mNeonGreen. Exponentially growing cells were treated with 1 μg/mL tunicamycin (Tm) for 3 h before imaging. Images are presented with the same display range and signals can be compared quantitatively.

7.3.3 Depletion of essential genes with the auxin-inducible degron system

In order to test the requirement of essential genes for the recruitment of Snf7 to ER clusters, I adapted a tool that was originally developed in the lab of Masato Kanemaki and further improved in the lab of Elina Ikonen: the auxin-inducible degron system. Here, a degron derived from plants is attached to a protein of interest. At the same time, an F-box protein from plants is expressed that can be incorporated into yeast E3 ligases. Both, the degron and the F-box protein bind auxin, a plant hormone. As soon as auxin or a chemically modified analogue are supplied to cells expressing the F-box protein, auxin will bridge the degron and the F-box protein that is part of an E3 ligase. As a result, the protein of interest will be polyubiquitinated and subsequently degraded by the proteasome (Figure 9A). This approach allows the conditional depletion of essential proteins if the tagging does not interfere with the function of the corresponding protein. This tool would allow me to validate the hits derived from my ts screen.

First, to test the efficiency of the auxin-inducible degron system in our setup, I characterized the degradation of two unrelated target proteins. I focused on Sec63p, an essential and well-established ER protein of medium abundance (~9500 copies per cell), and Vph1p, which is a non-essential but abundant protein (~20500 copies per cell) and localizes to the vacuolar membrane. I tagged both proteins at the C-terminus with an mCherry fluorophore followed by the auxin degron miniIAA7. Introducing a fluorophore to the target proteins allowed me to follow the degradation of the proteins by flow cytometry. Indeed, both proteins were readily degraded in samples that received auxin treatment. Already after 60 min, levels of Sec63p-mCherry-miniIAA7 and Vph1p-mCherry-miniIAA7 dropped to 10% and 40%, respectively (Figure 9B).

Importantly, this degradation only took place when auxin was added and the F-box protein AtAFB2 was expressed. Hence, auxin-inducible degradation is a useful tool to study the conditional depletion of essential and non-essential proteins in yeast.

I set out to use this technique to confirm the hits of my ts screen, where multiple COPII components and genes involved in ER-Golgi trafficking were identified as relevant for the recruitment of Snf7 to ER clusters upon ER stress.

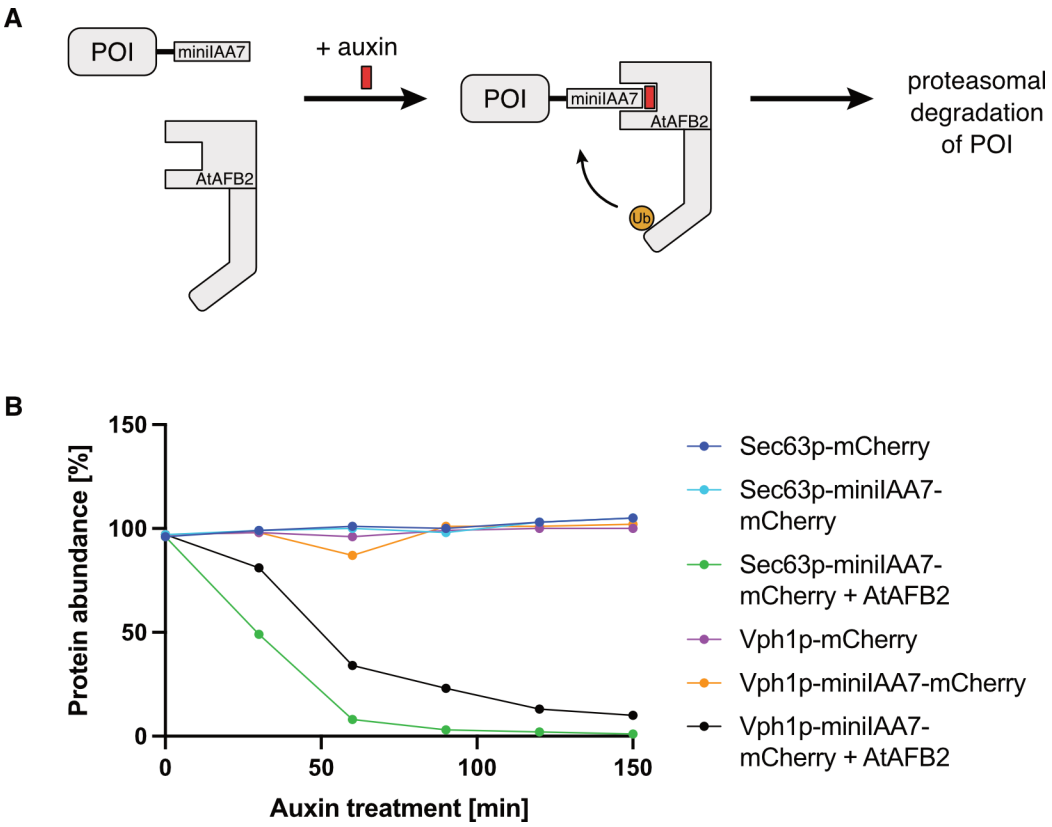

Figure 9. The auxin-inducible degron system is suitable for the rapid degradation of abundant proteins in yeast.

(A) Schematic of the auxin-inducible degron system. First, the protein of interest (POI) is tagged with the auxin degron miniIAA7 and the F-box protein AtAFB2 is stably expressed. This will result in the integration of AtAFB2 into yeast E3 ligases. Upon addition of auxin (IAA), auxin will bind to the auxin degron of the POI and the F-box protein AtAFB2 simultaneously. Consequently, the POI will be rapidly ubiquitinated by the E3 ligase and undergo proteasomal degradation.

(B) Auxin-induced degradation of Sec63p-miniIAA7-mCherry and Vph1p-miniIAA7-mCherry measured by flow cytometry. Two set of all strains were grown up in 96 well deep well plates. In exponential growth phase, 750 μM auxin was added to one of the sets to induce the degradation of Sec63p-miniIAA7-mCherry and Vph1p-miniIAA7-mCherry. Cells also expressed cytosolic BFP to normalize protein levels (mCherry signal) to translational capacity. Normalized protein levels are plotted in percentages of the corresponding non-treated set of strains.

7.3.4 General ER export machinery is required for the formation of ER clusters

Given that the interaction of COPII machinery with the p24 complex component Emp24p is required for the formation of ER clusters and subsequent recruitment of Snf7, I set out to validate the hits from the ts screens, in which I identified seven genes involved in COPII vesicle ER-to-Golgi trafficking. I tagged the ER-exit site marker Sec16p, the inner COPII coat component Sec24p and the outer COPII coat component Sec31p at the carboxy-terminus with the miniIAA7 tag and stably expressed the AtAFB2 F-box protein. While Snf7 puncta formation was still functional in these strains when I treated cells with tunicamycin, hardly any Snf7 puncta were present when cells were simultaneously treated with tunicamycin and auxin (Figure 10A and B).

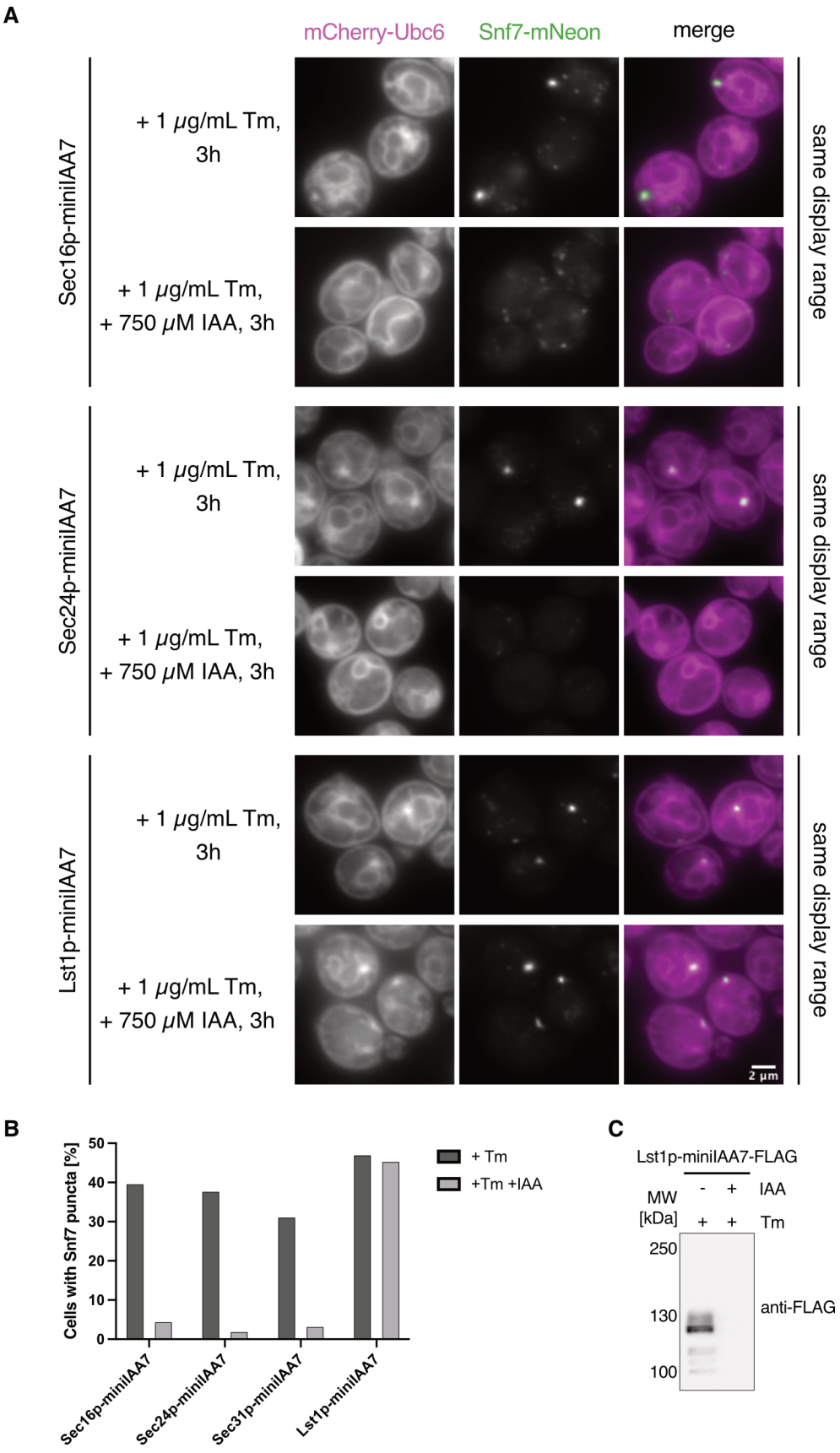
A
mCherry-Ubc6
Snf7-mNeon
merge
Sec16p-miniIAA7
+ 1 µg/mL Tm, 3h
+ 1 µg/mL Tm, + 750 µM IAA, 3h
Sec24p-miniIAA7
+ 1 µg/mL Tm, 3h
+ 1 µg/mL Tm, + 750 µM IAA, 3h
Lst1p-miniIAA7
+ 1 µg/mL Tm, 3h
+ 1 µg/mL Tm, + 750 µM IAA, 3h
same display range
same display range
same display range
2 µm
B
Cells with Snf7 puncta [%]
50
40
30
20
10
0
+ Tm
+Tm +IAA
Sec16p-miniIAA7
Sec24p-miniIAA7
Sec31p-miniIAA7
Lst1p-miniIAA7
C
Lst1p-miniIAA7-FLAG
MW [kDa]
- + IAA
+ + Tm
250
130
100
anti-FLAG

Figure 10. General ER export machinery is required for the efficient recruitment of Snf7-mNeon to ER clusters upon ER stress.

(A) Fluorescence microscopy images of W303 yeast strains stably expressing Sec16p-miniIAA7, Sec24p-miniIAA7 or Lst1p-miniIAA7 and Snf7-mNeonGreen together with the ER marker mCherry-Ubc6 after treatment with 1 μg/mL tunicamycin for 3 h or after 3 h of simultaneous treatment with 1 μg/mL Tm and 750 μM auxin (IAA). Images are presented with the same display range and signals can be compared quantitatively.

(B) Quantification of Snf7-mNeonGreen puncta in cells expressing Sec16p-miniIAA7, Sec24p-miniIAA7, Sec31p-miniIAA7 and Lst1-miniIAA7 after treatment with 1 μg/mL tunicamycin for 3 h or after 3 h of simultaneous treatment with 1 μg/mL Tm and 750 μM auxin (IAA). Percentages of cells that show Snf7-mNeonGreen puncta are plotted. For all genotypes more than 200 cells were quantified after images were randomized to reduce bias.

(C) Western Blot of auxin-inducible depletion of Lst1p-miniIAA7-FLAG in Tm-treated cells. Exponentially growing cells were harvested either after 3 h of 1 μg/mL Tm treatment or after 3 h of simultaneous treatment with 1 μg/mL Tm and 750 μM auxin (IAA). Equal protein amounts were loaded and visualized with a primary anti-FLAG antibody and a secondary antibody coupled to HRP. This experiment was performed by Natalie Friemel under my supervision.

It was difficult to assess if only Snf7 recruitment or both, Snf7 recruitment and ER cluster formation was impaired in this scenario, since the depletion of Sec16, Sec24 and Sec31 led to a distorted ER morphology. Overall, this experiment confirmed the ts screen outcome and suggested that COPII components are required for the recruitment of Snf7 to ER clusters and possibly also the formation of ER clusters.

The depletion of COPII components and the deletions of GPI-anchor remodeling proteins together with the specific ER export receptor for GPI-anchor proteins strongly reduced the recruitment of Snf7 to ER clusters or the formation of ER clusters. Lst1p is a homologue of Sec24p that is specifically required for the ER export of GPI-anchored proteins and other difficult cargo like oligomeric Pma1p assemblies (Roberg *et al*, 1999; Lee *et al*, 2002). Therefore, I set out to test the requirement of Lst1p for the recruitment of Snf7 to ER clusters. However, the depletion of Lst1p did not affect the recruitment of Snf7 to ER clusters or ER cluster formation (Figure 10A and B). This was not due to inefficient degradation of Lst1p-miniIAA7. A Western Blot that was performed by Natalie Friemel, a former rotation student in the lab, under my supervision confirmed that the depletion of Lst1p-miniIAA7 was successful, since no Lst1p-miniIAA7 was detected after combined treatment of tunicamycin and auxin (Figure 10C). It could not be ruled out that Lst1p is required for downstream processes at ER clusters.

7.3.5 The Dsl1-tethering complex localizes to ER clusters and is required for ER cluster formation

In the ts screen, Tip20 and Sec39 were identified as hits (Figure 6B). Both proteins are part of the Dsl1 tethering complex that is involved in the tethering of COPI vesicles in retrograde Golgi-to-ER trafficking. Dsl1 itself could not have been identified because the library strain carrying the *DSL1* ts allele did not grow in the experimental setup of the screen. Therefore, Nathalie Friemel generated a strain under my supervision that carried Dsl1p tagged with the auxin degron miniIAA7 and stably expressed AtAFB2.

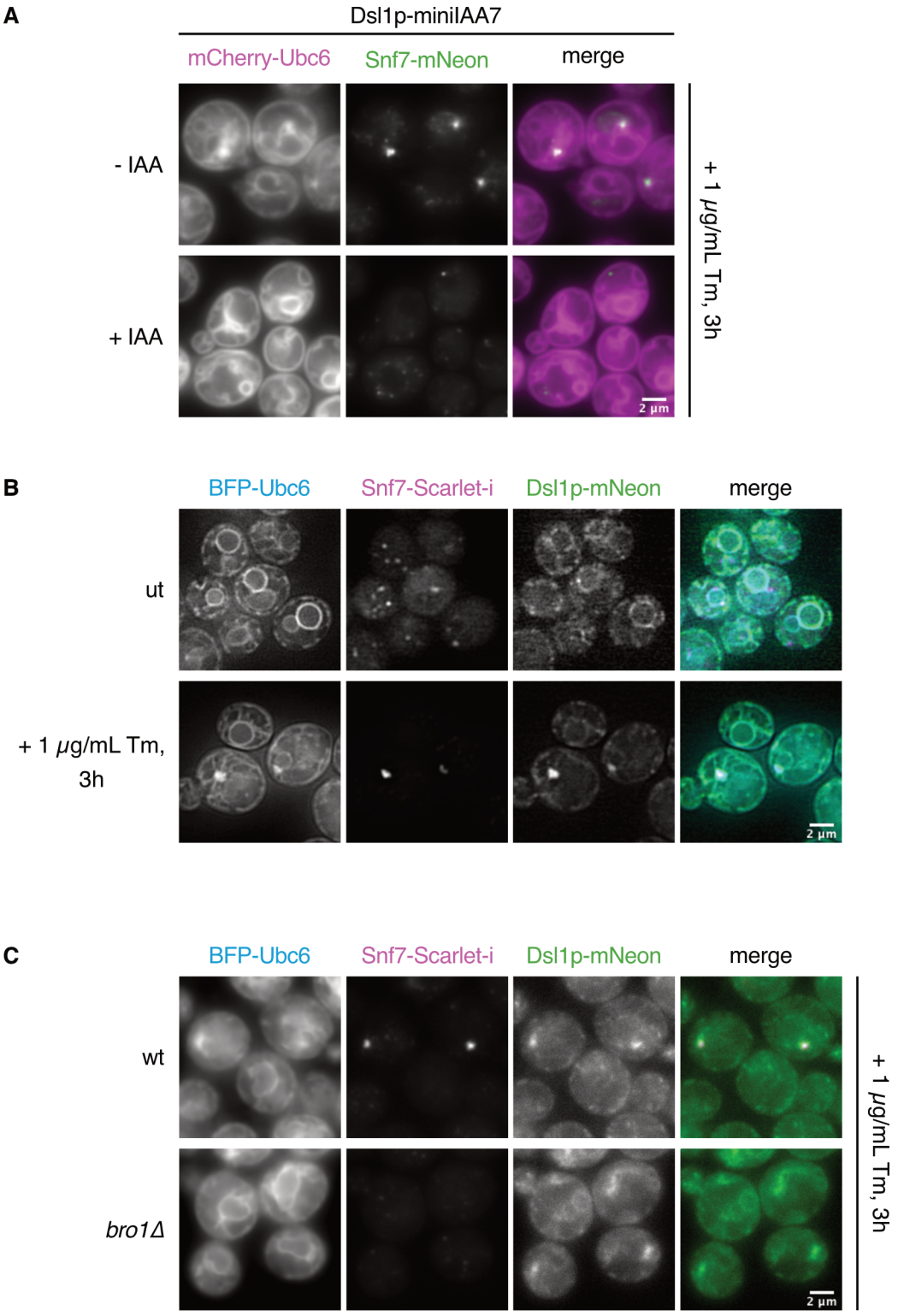

Figure 11. Dsl1 is required for the formation of ER clusters and is suitable as a marker for ER clusters.

(A) Fluorescence microscopy images of W303 yeast strains stably expressing Dsl1-miniIAA7, Snf7-mNeonGreen and mCherry-Ubc6 after treatment with 1 µg/mL tunicamycin for 3 h or after 3 h of simultaneous treatment with 1 µg/mL Tm and 750 µM auxin (IAA). This yeast strain was generated by Natalie Friemel under my supervision. Images are presented with the same display range and signals can be compared quantitatively. Images were acquired by Natalie Friemel under my supervision.

(B) Fluorescence microscopy images of the W303 yeast strain stably expressing BFP-Ubc6, Snf7-Scarlet-i and Dsl1p-mNeonGreen. Exponentially growing cells were either treated with 1 µg/mL tunicamycin (Tm) for 3 h or left untreated before imaging. Widefield microscopy images were deconvolved using the Richardson-Lucy algorithm with 30 iterations and an automatically determined noise level. Due to deconvolution, signal intensities are not quantitatively comparable between images.

(C) Fluorescence microscopy images of the W303 yeast strains stably expressing BFP-Ubc6, Snf7-Scarlet-i and Dsl1p-mNeonGreen in a wt or *bro1Δ* background. This strain was generated by Lis Albert. Exponentially growing cells were treated with 1 µg/mL tunicamycin (Tm) for 3 h before imaging. Images are presented with the same display range and the signals can be compared quantitatively.

She could confirm that simultaneous treatment of cells with tunicamycin and auxin results in complete absence of Snf7 puncta (Figure 11A). Also, ER morphology was strongly distorted in this condition (Figure 11A).

Subsequently, I set out to test if Dsl1p-mNeonGreen is also localizing to ER clusters, since the Dsl1 tethering complex resides at the ER membrane. While Dsl1p-mNeonGreen showed a punctate ER staining in untreated cells, Dsl1p-mNeonGreen was strongly enriched at ER clusters upon ER stress (Figure 11B). It even appeared to be enriched over the abundance of the general ER marker. This would suggest that the Dsl1-tethering complex is a marker for ER clusters as ER subdomains, possibly acting upstream of Snf7 recruitment. To test this idea, Lis Albert deleted *BRO1* in this strain and I checked if ER clusters can still be recognized after ER stress even though no Snf7 recruitment was possible anymore. Indeed, cells still showed accumulation of Dsl1p-mNeon at ER clusters, albeit clusters were less defined (Figure 11C). This suggests that Dsl1p-mNeon acts upstream of Snf7 recruitment and could be used as an ER cluster marker.

7.4 Spatial arrangement of ER export machinery at ER clusters

The requirement of the general ER export machinery for the recruitment of Snf7 to ER clusters raised the question whether this effect was direct or indirect. It can be expected that the depletion of general essential ER factors like the ER export machinery leads to general defects of ER function. The disability to recruit ESCRT proteins to ER clusters might then be a consequence of this general loss of ER functionality, rather than a specific effect where the COPII components are directly involved in ESCRT recruitment to ER clusters. I therefore tagged the COPII components Sec24p, Sec31p and Lst1p with a mNeonGreen tag and studied how their localization relates to the Snf7-Scarlet-i puncta at ER clusters. In untreated cells, all three COPII components localized to small puncta in the cytosol that hardly showed any overlap with Snf7-Scarlet-i that mainly resided on endosomes as small puncta (Figure 12A). After 3 h of tunicamycin treatment, Snf7-Scarlet-i massively re-localized to ER clusters as previously observed. Sec24p-mNeonGreen, Sec31p-mNeonGreen and Lst1p-mNeonGreen did not co-localize with Snf7-Scarlet-i puncta at ER clusters directly. However, they showed a punctate staining surrounding Snf7 puncta reminiscent of flower petals (Figure 12B). This arrangement appeared to be specific since almost all Snf7 puncta were surrounded by COPII puncta. The exact number of COPII puncta surrounding Snf7 puncta varied but the analyzed structures showed between two and six COPII puncta.

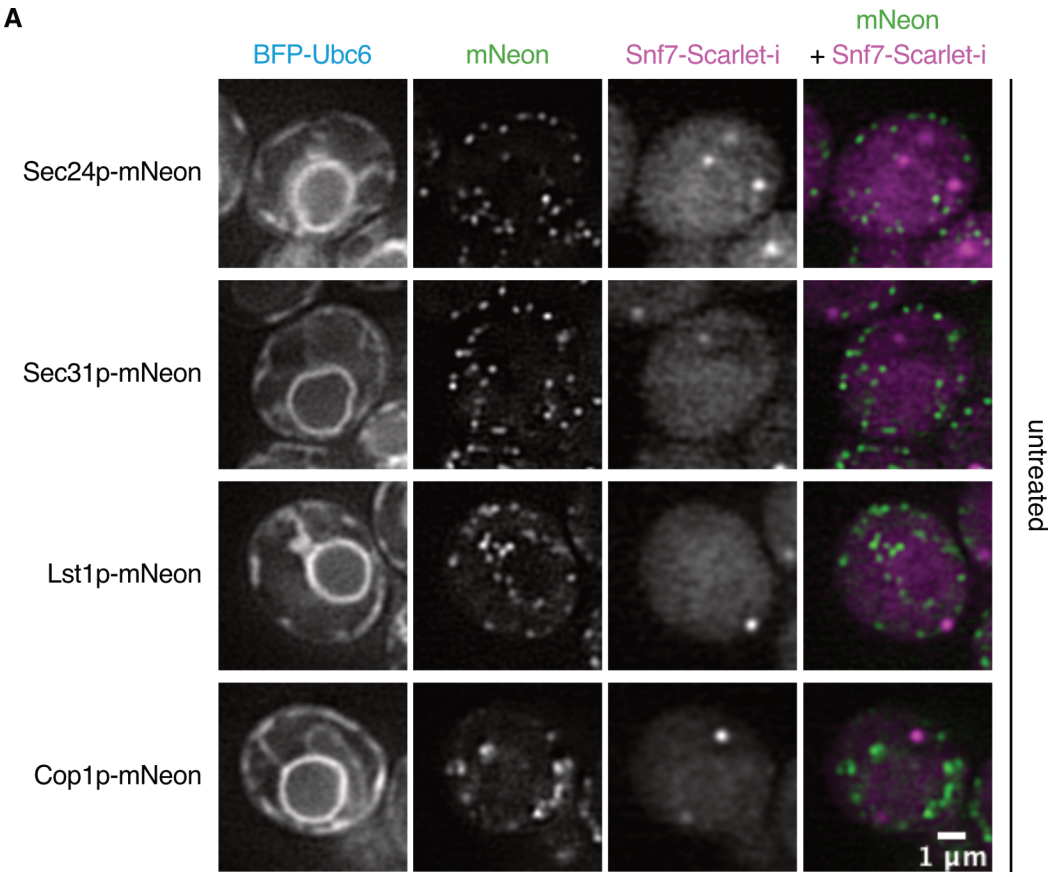
A
BFP-Ubc6
mNeon
Snf7-Scarlet-i
mNeon
+ Snf7-Scarlet-i
Sec24p-mNeon
Sec31p-mNeon
Lst1p-mNeon
Cop1p-mNeon
untreated
1 µm

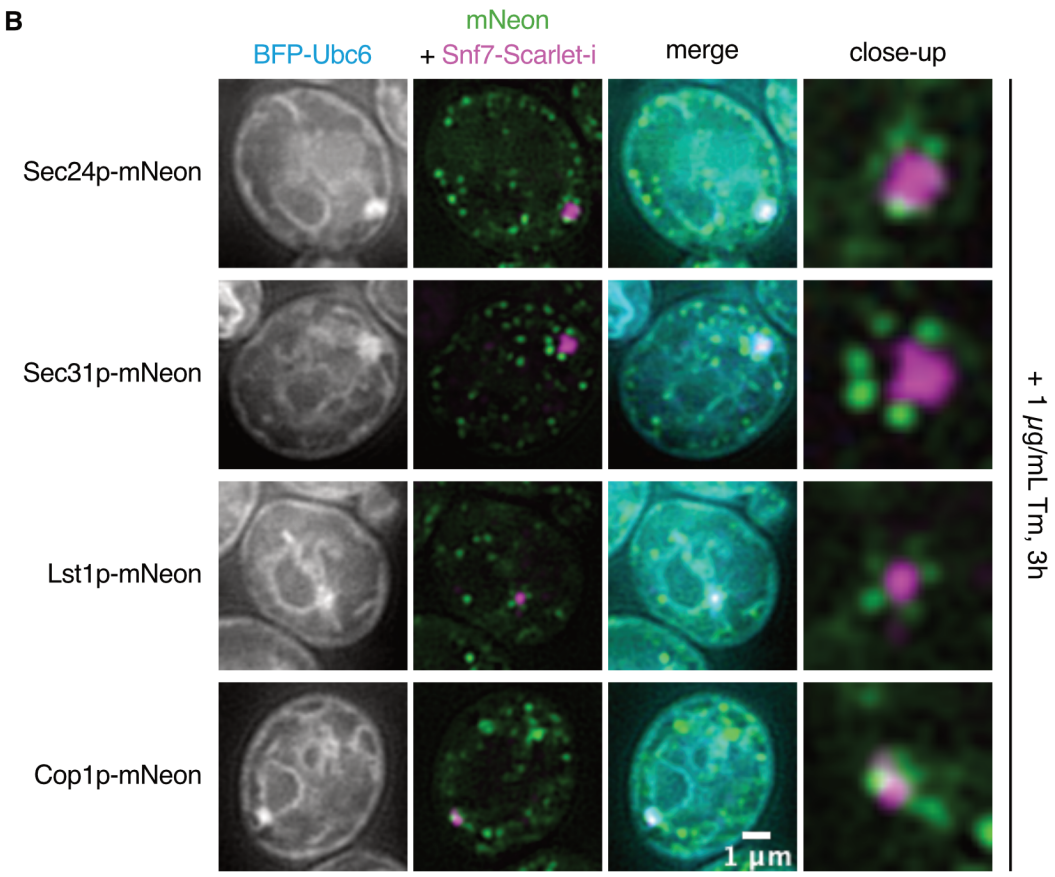
B
BFP-Ubc6
mNeon
+ Snf7-Scarlet-i
merge
close-up
Sec24p-mNeon
Sec31p-mNeon
Lst1p-mNeon
Cop1p-mNeon
+ 1 µg/mL Tm, 3h
1 µm

Figure 12. COPII components form flower-like arrangements around Snf7 puncta at ER clusters.

(A) Fluorescence microscopy images of W303 yeast strains stably expressing BFP-Ubc6, Snf7-Scarlet-i and Sec24p-mNeonGreen, Sec31p-mNeonGreen or Lst1p-mNeonGreen in exponentially growing cells. Widefield images were deconvolved using the Wiener filter plug-in from the Olympus cellSens software. Due to deconvolution, signal intensities are not quantitatively comparable between images, but are shown in the ideal display range for each image.

(B) Fluorescence microscopy images of W303 yeast strains stably expressing BFP-Ubc6, Snf7-Scarlet-i and Sec24p-mNeonGreen, Sec31p-mNeonGreen or Lst1p-mNeonGreen in exponentially growing cells after treatment with 1 μg/mL tunicamycin for 3 h. Widefield images were deconvolved using the Wiener filter plug-in from the Olympus cellSens software. Due to deconvolution, signal intensities are not quantitatively comparable between images, but are shown in the ideal display range for each image.

I also identified the COPI component Cop1p as a hit in the ts screen (Figure 6B) and therefore set out to study its localization in relation to Snf7 puncta and ER clusters.

Cop1p is usually involved in Golgi-to-ER retrograde trafficking. At steady state, Cop1p-mNeon localized to cytosolic puncta that partially appeared larger and patchier than the staining that was previously observed for COPII components (Figure 12A). It is likely that a fraction of the Cop1p staining marked Golgi structures while the rest of the staining corresponded to COPI vesicles. Upon ER stress, Cop1p-mNeon staining showed a punctate staining in proximity of Snf7 puncta and additional longer stretches that often directly overlapped with Snf7-Scarlet-i signal (Figure 12B). The observations that the COPII signal surrounded Snf7 whereas the COPI signal showed substantial co-localization with Snf7 raised the question how the localization of Cop1p and COPII components relate to each other at ER clusters.

We typically used only three fluorescent tags at once for yeast live cell imaging in our lab but an experiment studying Cop1p, COPII and Snf7 at ER clusters would require four fluorescent tags. Therefore, we collaborated with the lab of Kai Johnsson at the Max Planck Institute for Biomedical Research in Heidelberg to find a useful HaloTag-HaloTag ligand combination that would allow imaging of a protein of interest in the far-red emission spectrum. Most HaloTag ligands (HTLs) are only poorly taken up into yeast cells. After initial testing, Julian Kompa and Yin-Hsi Lin from the Johnsson lab determined that the combination of the HaloTag7 protein with the homemade and not commercially available SiR HaloTag Ligand (HTL) was usable in *S. cerevisiae*, which extended the spectrum of live cell imaging in yeast. Subsequently, Chrysafenia Papavissarion, a former rotation student in the lab, tagged three proteins of different abundance with the HaloTag7 tag (hereafter referred to as Halo) in the W303 wildtype strain under my supervision and stained these proteins with the SiR-HTL. Bro1p-Halo, Sec63p-Halo and Sec31p-Halo showed a useful staining (Figure 13A). The copy numbers of these three proteins corresponds to the top 5%, 10% and 25% in yeast. This confirmed that the combination of Halo and SiR-HTL can be used for a range of proteins of different abundance. It is conceivable that proteins, which are less abundant than Bro1p can still be detected with this HaloTag-HaloTag Ligand combination.

Next, Chrysafenia Papavissarion generated a strain under my supervision that contained all four proteins of interest fused to different fluorophores or the HaloTag: BFP-Ubc6 as general ER marker, Snf7-Scarlet-i, Cop1p-mNeon and Sec24p-Halo. She observed that whereas Cop1p-mNeon and

Sec24p-Halo did not share a great overlap of signal in untreated cells (not shown), both proteins showed proximity particularly at sites of Snf7 recruitment to ER clusters in Tm-treated cells (Figure 13B). This induced proximity of COPII and COPI components at ER clusters suggested that both trafficking machineries play a shared biological role at these sites. Since COPI machinery is usually involved in Golgi-to-ER trafficking, it is plausible that ER and Golgi converge at ER clusters upon stress and that this phenotype requires ESCRT proteins. This would imply that Cop1p signal corresponded indeed to Golgi structures and not to Golgi-derived vesicles, which could not be ruled out at this step. From this experiment, it also remained unclear if ER and putative Golgi structures only came into proximity or even formed a contact site at ER clusters.

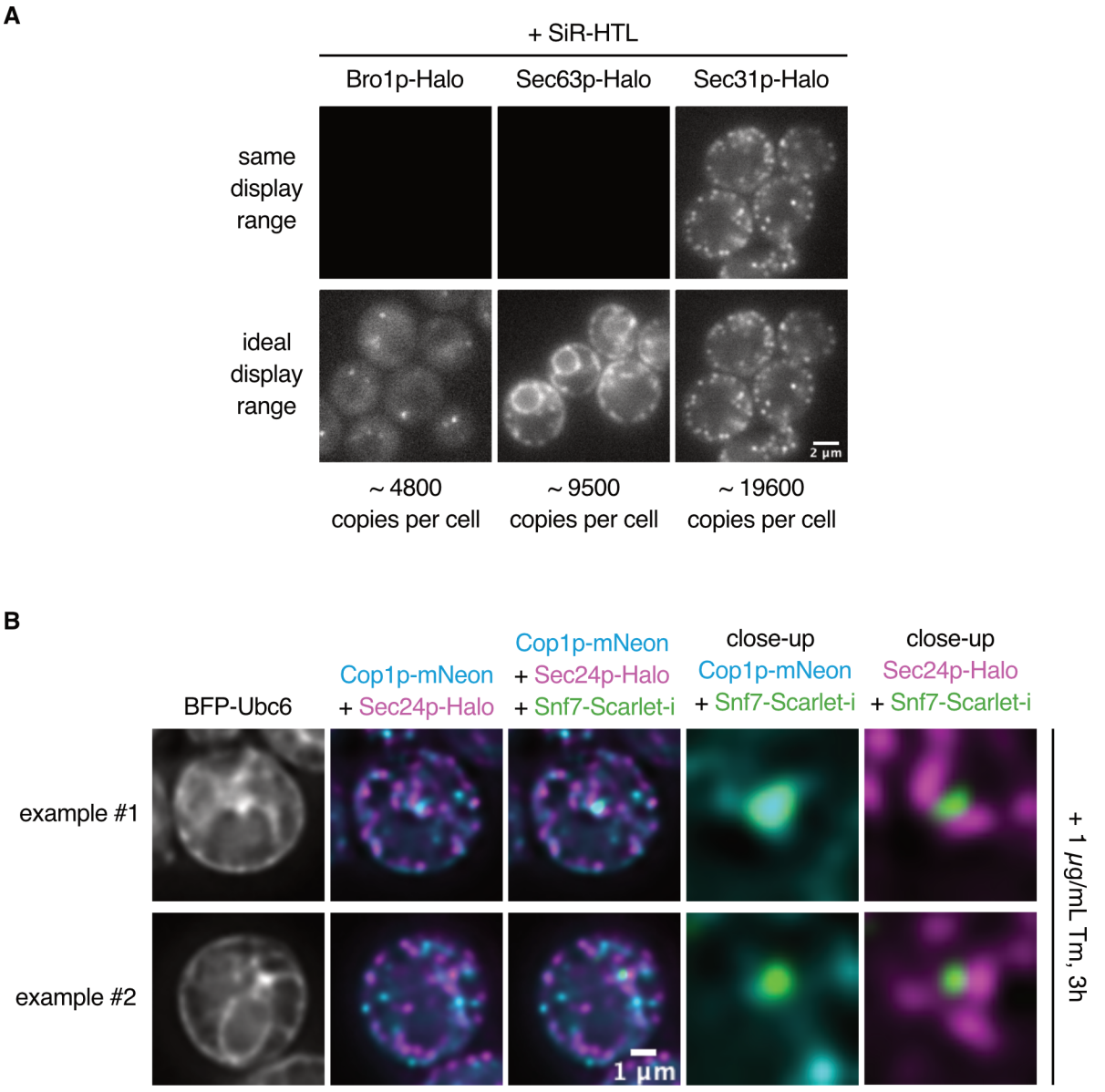

Figure 13. Spatial arrangement of Cop1p, Sec24p and Snf7 at ER clusters using four color live cell imaging.
(A) Fluorescence microscopy images of W303 yeast strains stably expressing Bro1p-Halo, Sec63p-Halo or Sec31p-Halo in exponentially growing cells after addition of the SiR-HaloTagLigand. Strains were generated and imaged by Chrysafenia Papavissarion under my supervision.

(B) Fluorescence microscopy images of W303 yeast strains stably expressing BFP-Ubc6, Snf7-Scarlet-I, Cop1p-mNeonGreen and Sec24p-Halo + SiR-HTL in exponentially growing cells after treatment with 1 μg/mL tunicamycin for 3 h. Widefield images were deconvolved using the Richardson-Lucy algorithm with 30 iterations and an automatically determined noise level. Strains were generated and imaged by Chrysafenia Papavissarion under my supervision.

7.5 ER-Golgi tethering proteins re-localize to ER clusters upon ER stress

7.5.1 Nvj2p re-localizes to ER clusters upon ER stress

In yeast, stress-induced ER-Golgi contacts have been reported before. Nvj2p localizes to the nucleus vacuole junction (NVJ) at steady state ((Toulmay & Prinz, 2012); Figure 14A). The NVJ is a contact site of the nuclear envelope and the vacuole, which is established by the proteins Nvj1p at the ER site and Vac8 at the vacuolar membrane (Pan *et al*, 2000). However, it has been shown that ER stress induced with DTT triggers the re-localization of Nvj2 from NVJs to ER-Golgi contact sites (Liu *et al*, 2017). Since Nvj2p appears to be a stress-inducible ER-Golgi tether, I tested whether Nvj2p co-localizes with ER clusters marked by Snf7. Therefore, I tagged Nvj2p with mNeonGreen in a strain that expressed Snf7-Scarlet-i and the ER marker BFP-Ubc6. At steady state, Nvj2p-mNeonGreen showed a punctate staining coinciding with the ER along the cell periphery and a stronger signal at the contact of the nuclear envelope with the vacuole, which likely corresponded to NVJ staining (Figure 14A). Upon ER stress, the punctate staining of Nvj2p-mNeonGreen at the peripheral ER remained, but additionally Nvj2p-mNeonGreen showed a pronounced co-localization with Snf7-Scarlet-i puncta at ER clusters (Figure 14A). It was difficult to determine whether the NVJ staining of Nvj2p-mNeon was lost after ER stress, since the vacuole tends to fragment when cells are facing ER stress. Also, ER stress treatment could lead to the disassembly of NVJs, which was suggested as an effect of DTT treatment (Liu *et al*, 2017). It is not clear if this effect would be also observed after tunicamycin treatment. The co-localization of the inducible ER-Golgi tether Nvj2p and Snf7 at ER clusters added to our hypothesis that ESCRT proteins are recruited to ER clusters to either assist in the formation or stabilize ER-Golgi contact sites. This hypothesis would entail that the recruitment of Nvj2p is a later step in this assembly. Therefore, I deleted *NVJ2* in a strain that expressed the general ER marker mCherry-Ubc6 and Snf7-mNeonGreen and tested whether the supposedly earlier step of ESCRT recruitment to ER clusters is impaired in the absence of the inducible ER-Golgi tether Nvj2p. The deletion of *NVJ2* slightly reduced the recruitment of Snf7 to ER clusters but did not abolish it (Figure 15B). Therefore, Nvj2p is not an essential factor for Snf7 recruitment. This was in line with the hypothesis that the recruitment of Nvj2p occurs downstream of ESCRT recruitment to ER clusters. In the literature, the overexpression of Nvj2p has been reported to be sufficient to drive the re-localization of Nvj2p to ER-Golgi contact sites and promote their formation (Liu *et al*, 2017). For this reason, I generated a strain that allows the inducible overexpression of Nvj2p from the *GAL* promoter that is activated by the artificial transcription factor GEM when bound by estradiol. However, strong overexpression of *NVJ2* did not trigger Snf7-recruitment to ER clusters even though these cells showed an expanded ER (Figure 14B).

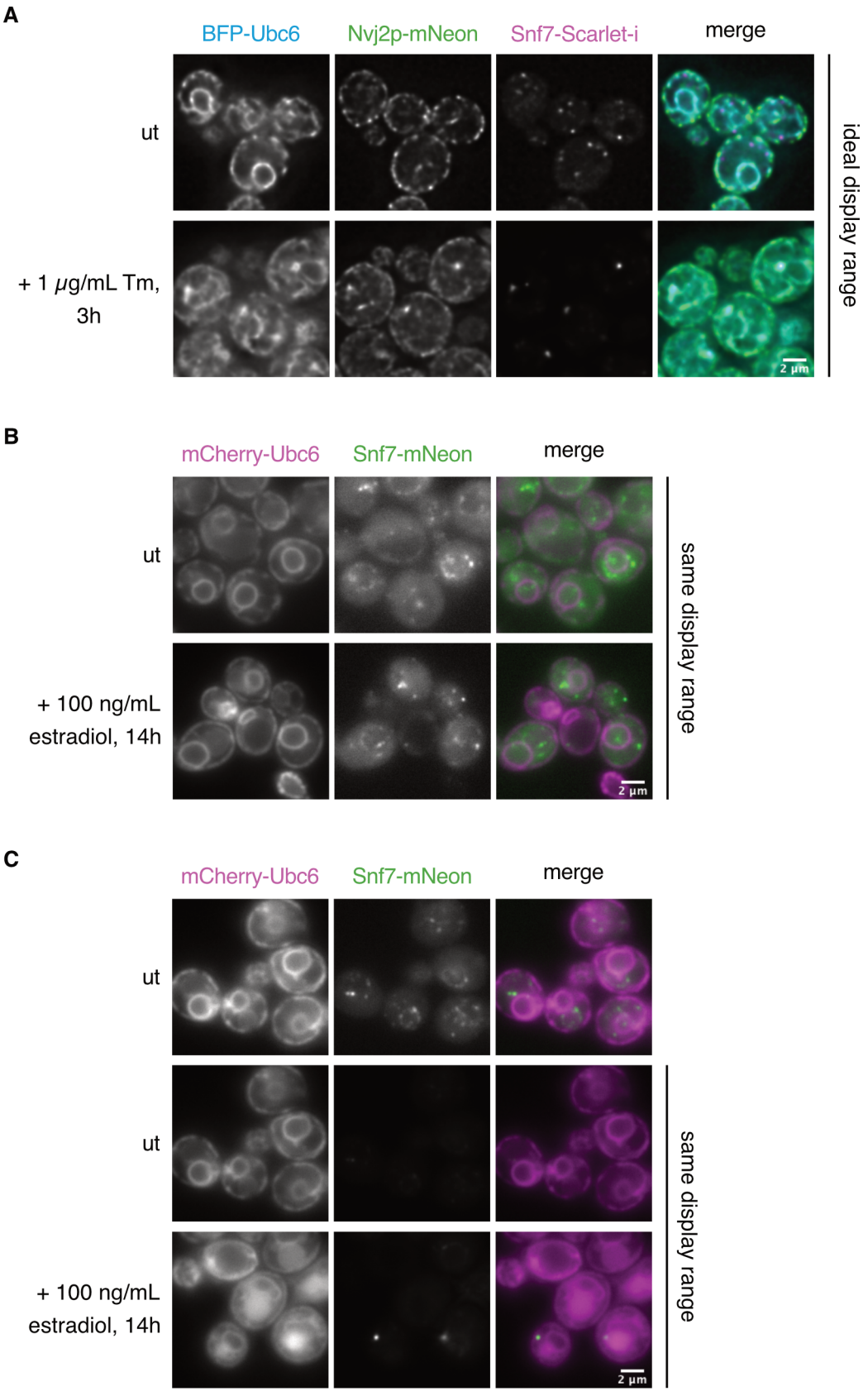

Figure 14. Inducible ER-Golgi tether Nvj2p re-localizes to ER clusters upon ER stress.

(A) Fluorescence microscopy images of the W303 yeast strain stably expressing BFP-Ubc6, Snf7-Scarlet-i and Nvj2p-mNeonGreen. Exponentially growing cells were either treated with 1 µg/mL tunicamycin (Tm) for 3 h or

left untreated before imaging. Widefield microscopy images were deconvolved using the Richardson-Lucy algorithm with 30 iterations and an automatically determined noise level. Due to deconvolution, signal intensities are not quantitatively comparable between images, but are shown in the ideal display range for each image.

(B) Fluorescence microscopy images of W303 yeast strains stably expressing mCherry-Ubc6 and Snf7-mNeonGreen. The endogenous promotor of *NVJ2* was replaced by the *GAL* promoter and the artificial transcription factor GEM was integrated. High expression of *NVJ2* was triggered by addition of 100 ng/mL estradiol for 14 h.

(C) Fluorescence microscopy images of W303 yeast strains stably expressing mCherry-Ubc6 and Snf7-mNeonGreen. The endogenous promotor of *LAG1* was replaced by the *GAL* promoter and the artificial transcription factor GEM was integrated. High expression of *LAG1* was triggered by addition of 100 ng/mL estradiol for 14 h.

The proposed biological function of Nvj2p puncta after ER stress in the literature is that formation of ER-Golgi contacts and recruitment to these sites facilitates the transport of ceramide, directly or indirectly, and that this is necessary during ER stress when vesicular transport is possibly compromised (Liu *et al*, 2017). Ceramide is produced in the ER and then transported to the Golgi, where it is used to generate complex sphingolipids. In the ts screen, Lcb1p, Lcb2p and Tsc3p were identified as hits (Figure 6B). Lcb1p and Lcb2p make up the serine palmytoyltransferase (SPT) in yeast (Nagiec *et al*, 1994) and Tsc3p is required for its optimal activity (Gable *et al*, 2000). This connection could provide a hint for the biological function of ESCRT recruitment to ER clusters: Vesicular transport of ceramide might be impaired upon ER stress; therefore, cells rely more on non-vesicular ceramide transport at ER-Golgi contact sites, which could be performed by the ER-Golgi tether Nvj2p.

In a situation in which no ceramide is produced by lack of a functional SPT, ESCRT recruitment and possible enhanced non-vesicular transport would become obsolete. Therefore, I tested if auxin-induced depletion of Lcb1p or Lcb2p would disrupt ER cluster formation and Snf7 recruitment. The results of this experiment were difficult to interpret, since Lcb1p/Lcb2p depletion greatly affected cell viability (data not shown). As an alternative, I tested whether overexpression of one of the ceramide synthase components Lag1p triggers Snf7 recruitment to ER clusters. Indeed, after long induction of Lag1p expression I observed occasional Snf7 puncta at ER positive sites but at a low frequency (Figure 14C). This could suggest that increased ceramide synthesis and possible accumulation of ceramide in the ER triggered the recruitment of Snf7 to the ER. However, many cells did not tolerate the long induction of Lag1p overexpression and showed a very distorted ER structure, which impeded the assessment of Snf7 recruitment and if the underlying ER structures were actual ER clusters.

7.5.2 Tcb3p co-localizes with Snf7 at ER clusters after stress in a Bro1p-dependent manner

Besides Nvj2p, two other proteins are known to be involved in non-vesicular transport of ceramide from the ER to the Golgi: Svf1p and Tcb3p (Limar *et al*, 2023; Ikeda *et al*, 2020). I tagged both proteins with mNeonGreen und tested their co-localization with Snf7-Scarlet-i at steady state and after induction of ER stress. At steady state Svf1p-mNeonGreen localized mainly to the cytosol and stained some larger,

punctate structures that could correspond to Golgi cisternae (data not shown). This was in line with the reported localization for Svf1p (Limar *et al*, 2023).

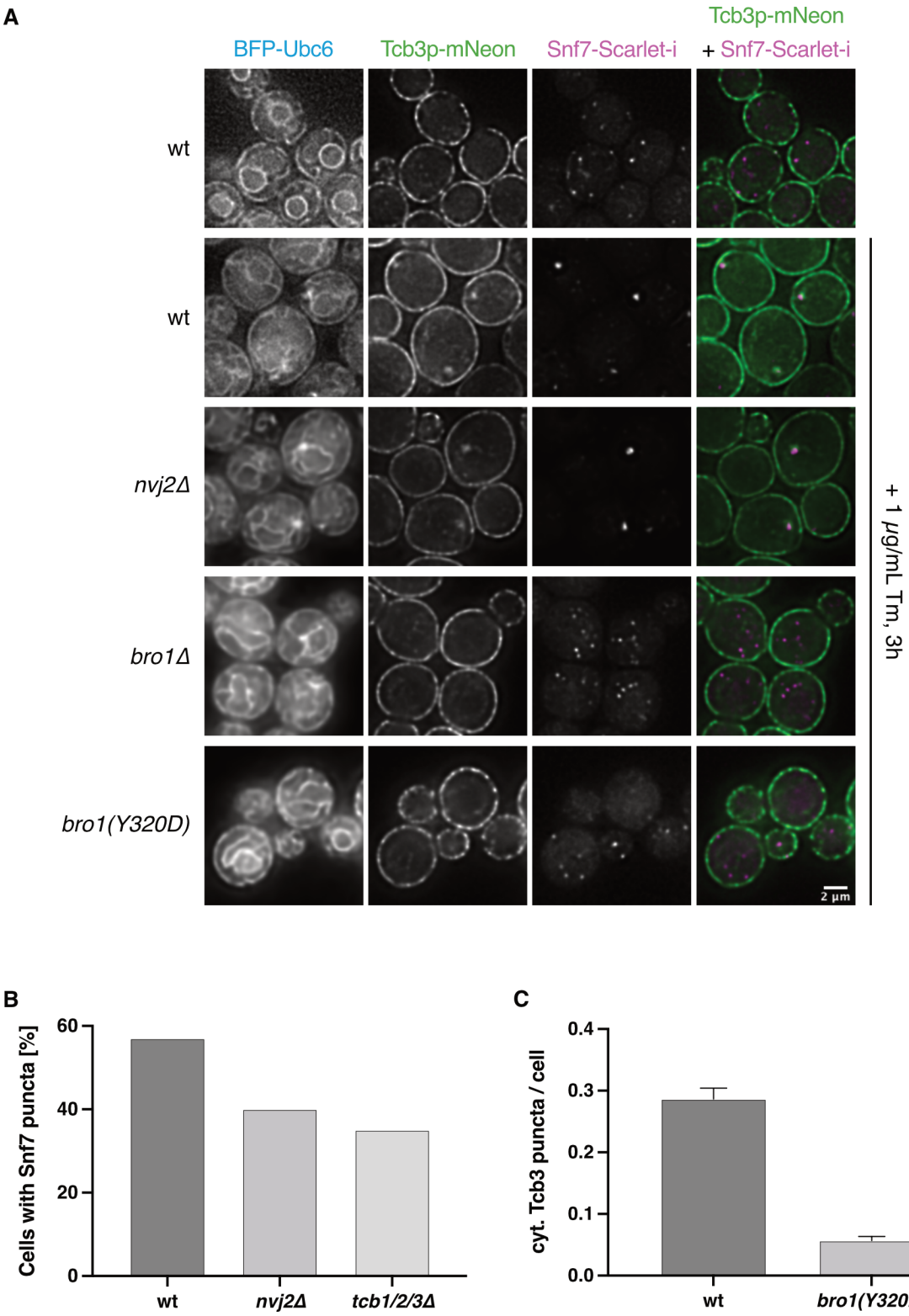

Figure 15. Yeast tricalbin Tcb3p re-localizes to ER clusters upon ER stress in a Bro1-dependent manner.

(A) Fluorescence microscopy images of the W303 yeast strains stably expressing BFP-Ubc6, Snf7-Scarlet-i and Tcb3p-mNeonGreen in wt cells and different deletion backgrounds. Exponentially growing cells were either treated with 1 µg/mL tunicamycin (Tm) for 3 h or left untreated before imaging. Widefield microscopy images

were deconvolved using the Richardson-Lucy algorithm with 30 iterations and an automatically determined noise level.

(B) Quantification of Snf7-mNeonGreen puncta in wt, *nvj2Δ* and *tcb1/2/3Δ* cells after treatment with 1 µg/mL tunicamycin for 3 h. Percentages of cells from all cells are plotted that show Snf7-mNeon puncta and/or ER clusters. For all genotypes more than 200 cells were quantified after images were randomized to reduce bias.

(C) Quantification of cytosolic Tcb3p-mNeon puncta in wt and *bro1Y320D* cells after treatment with 1 µg/mL tunicamycin for 3 h. Percentages of cells from all cells are plotted that show cytosolic Tcb3p-mNeon puncta at ER clusters. For all genotypes more than 200 cells were quantified after images were randomized to reduce bias. The experiment was performed in n = 3 replicates, error bars correspond to standard error of the mean (SEM). One of the three replicates was acquired by Lis Albert. All replicates were quantified by me.

After ER stress induction, Svf1p-mNeonGreen showed a less defined localization; whereas the cytosolic staining remained, putative Golgi structures were not observed. Importantly, Svf1p-mNeonGreen did not show any co-localization with Snf7-Scarlet-i at ER clusters (data not shown). Tcb3p is a yeast tricalbin and acts as one of six ER-PM tethering proteins (Manford *et al*, 2012). At steady state, Tcb3p-mNeon localized exclusively to the peripheral ER, which matched its role as ER-PM tether (Figure 15A). Upon ER stress, the peripheral staining of Tcb3p-mNeonGreen remained but I additionally observed cytosolic puncta of Tcb3 that overlapped with ER signal (Figure 15A). More specifically, Tcb3p-mNeonGreen localized to ER clusters and showed a strong co-localization with Snf7-Scarlet-i at these sites (Figure 15A). These cytosolic puncta were reminiscent of structures previously observed in cells overexpressing Tcb3p or treated with tunicamycin (Ikeda *et al*, 2020). Subsequently, I tested whether Tcb3p was required for the recruitment of Snf7 to ER clusters. Similar to the deletion of the ER-Golgi tether Nvj2p, deletion of all tricalbins (Tcb1p, Tcb2p and Tcb3p) reduced Snf7 recruitment slightly but tricalbins were not essential for the recruitment of Snf7 to ER clusters (Figure 15B). Also, deletion of *NVJ2* did not affect the co-localization of Tcb3p-mNeonGreen and Snf7-scarlet-i at ER clusters upon ER stress (Figure 15A).

These results suggested that both Tcb3p and Nvj2p recruitment to ER clusters occurs downstream of Snf7 recruitment. If the recruitment of Tcb3p to ER clusters was indeed a downstream event to the recruitment of Snf7, absence of ESCRT recruitment would also impact the formation of cytosolic Tcb3 puncta. To test this idea, I deleted *BRO1* and tested whether cytosolic Tcb3p-mNeonGreen puncta still form in these cells. After 3 h of tunicamycin treatment, I could hardly spot any cytosolic Tcb3p-mNeonGreen puncta (Figure 15A). This finding suggests that prior recruitment and possible remodeling of ER clusters by ESCRT-III protein Snf7 is essential for the later recruitment of Tcb3p.

To clarify whether the requirement of Bro1 for cytosolic Tcb3 puncta formation relies on its role at ER clusters with Snf7, the Bro1 variant *bro1Y320D was used.* This variant carries a mutation in the hydrophobic patch 2 of Bro1p (Kim *et al*, 2005). This mutant was initially characterized by Carlos Martin de Hijas regarding functionality of Snf7 recruitment. Lis Albert later established that Snf7 recruitment to ER clusters after ER stress is completely abolished in *bro1Y320D,* whereas sorting of MVB cargo, one of the classic readouts for ESCRT function at MVBs, is almost at the level of wt Bro1. The Bro1 variant *bro1Y320D* therefore uncouples the roles of Bro1 in MVB sorting and in the recruitment of Snf7 to ER clusters (Lis Albert, unpublished). Therefore, I tested whether the localization of Tcb3p to ER clusters was specifically affected in the strain background that expressed the Bro1 variant *bro1Y320D.* Indeed,

cytosolic Tcb3p-mNeonGreen puncta were also strongly reduced in *bro1Y320D* cells (Figure 15A and C). This result added to the hypothesis that ESCRT recruitment to ER clusters precedes the formation of cytosolic puncta by ER-Golgi tether Tcb3p. It is conceivable that ESCRT recruitment leads to the recruitment of Tcb3p and thereby enables or stabilizes ER-Golgi tethering.

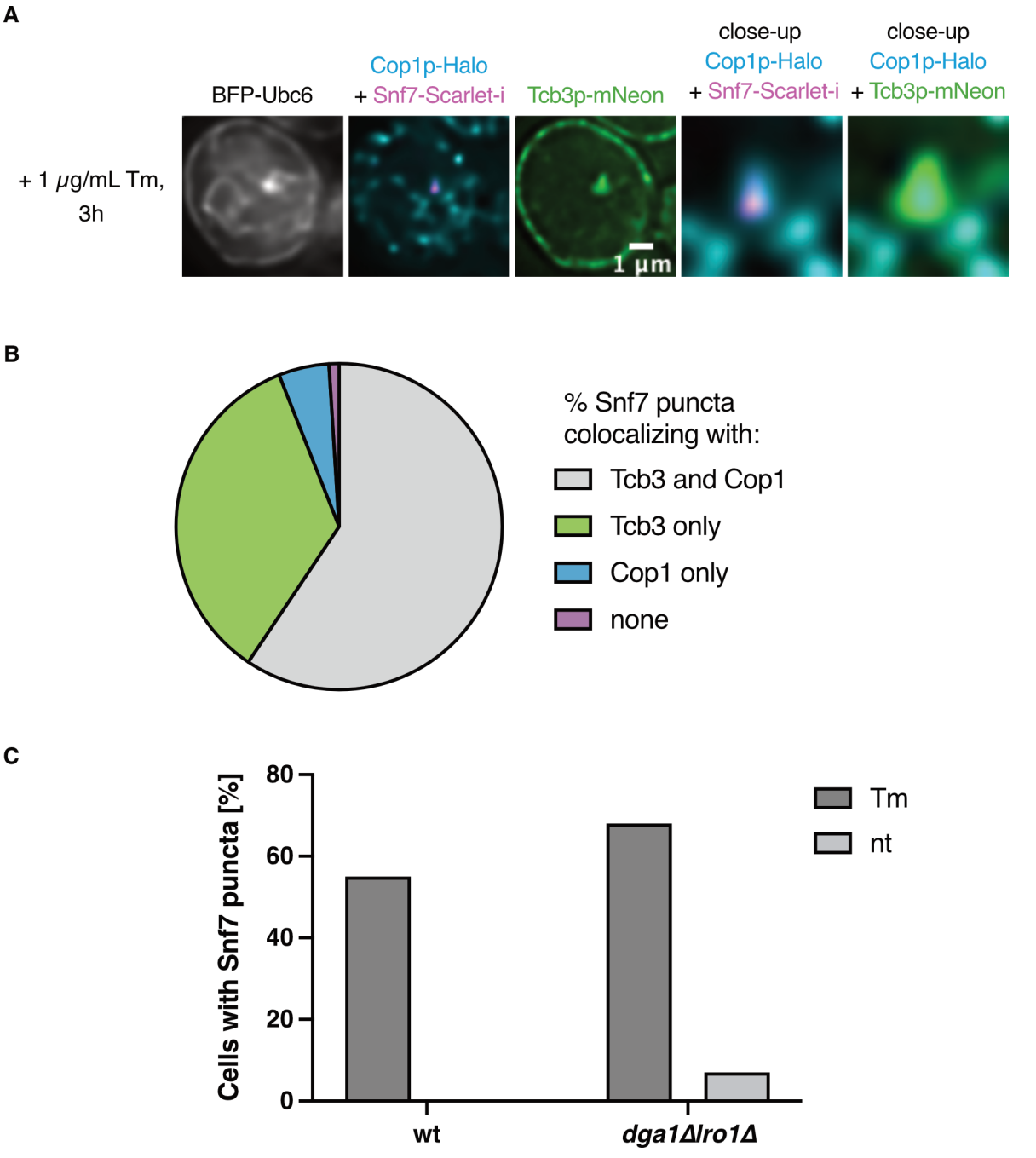

Figure 16. The majority of ER clusters simultaneously co-localize with the ER-Golgi tether Tcb3p and with the Golgi marker Cop1p.

(A) Fluorescence microscopy images of W303 yeast strains stably expressing BFP-Ubc6, Snf7-Scarlet-i, Tcb3p-mNeonGreen and Cop1p-Halo + SiR-HTL in exponentially growing cells after treatment with 1 µg/mL tunicamycin for 3 h. Widefield images were deconvolved using the Richardson-Lucy algorithm with 30 iterations and an automatically determined noise level.

(B) Proportions of Snf7-Scarlet-i puncta co-localizing with Cop1p-Halo, Cop1p-Halo and Tcb3p-mNeonGreen, Tcb3p-mNeonGreen or none of the above after treatment with 1 μg/mL tunicamycin for 3 h. The pie chart was conceptualized by Lis Albert.

(C) Quantification of Snf7-mNeonGreen puncta in wt and *dga1Δlro1Δ* cells. Before imaging, exponentially growing cells were either treated with 1 μg/mL tunicamycin for 3 h or left untreated. that showed Snf7-mNeonGreen puncta at ER clusters are plotted. For all genotypes more than 200 cells were quantified after images were randomized to reduce bias.

7.6 Sites of Snf7-positive ER clusters are putative ER-Golgi contacts marked by Tcb3p and Cop1p

I observed that ER clusters are sites where a variety of proteins of the ER-Golgi interface come together: COPII components of the general ER export machinery, the Dsl1 tethering complex involved in the reception of COPI vesicles in retrograde Golgi-to-ER trafficking, stress-induced ER-Golgi tethers Nvj2p and Tcb3p and Cop1p. The staining of Cop1p showed small puncta but also larger structures that often co-localized with Snf7 at ER clusters upon ER stress (Figure 12B and 13B). It is plausible that part of Cop1p staining corresponded to Golgi membranes. Cop1p might act as a more general Golgi marker and is thought to be involved in cisternal Golgi maturation by recycling of early Golgi proteins from later cisternae (Papanikou *et al*, 2015) in comparison to other marker proteins that are more restricted to specific parts of the Golgi (cis-, medial and trans-;(Tojima *et al*, 2024)). Hence, I studied the localization of Snf7, Tcb3p and Cop1p in another live cell imaging experiment to determine the frequency of putative Golgi structures marked by Cop1p overlapping with Snf7 and Tcb3p signal at ER clusters.

The majority of all Snf7-Scarlet-i puncta that I assessed in this experiment showed simultaneous co-localization with the ER-Golgi tether Tcb3p-mNeonGreen and the Golgi marker Cop1p-Halo (Figure 16A and B). The second largest category of Snf7-Scarlet-i puncta showed at least co-localization with the stress-inducible ER-Golgi tether Tcb3p (Figure 16B). Both categories together made up 95% of all analyzed Snf7 puncta. Since I could show previously that the localization of the ER-Golgi tether Tcb3p strongly depends on ESCRT recruitment to ER clusters (Figure 15C), these results suggest a role of ESCRT recruitment to ER clusters in the stabilization and/or formation of ER-Golgi contacts.

Why would ER-Golgi contacts be necessary upon ER stress? Experiments from the Prinz lab suggested that non-vesicular transport of ceramide was particularly important when vesicular transport of ceramide from the ER to the Golgi is compromised during ER stress (Liu *et al*, 2017). A reason for this could be the toxic accumulation of ceramide at the ER membrane. I could previously show that the overexpression of a ceramide synthase component Lag1p triggered the formation of Snf7 puncta at ER-positive structures (Figure 14C). Yeast cells have another way of alleviating stress from ceramide accumulation at the ER. Excess ceramide can be acylated and deposited in lipid droplets (Voynova *et al*, 2012). The diacylglycerol acyltransferases Dga1p and Lro1p are essential for this process. Therefore, I tested whether the absence of this ceramide detoxification pathway influences the recruitment of Snf7 to ER clusters. Indeed, I observed that *dga1Δlro1Δ* cells showed a stronger recruitment of Snf7-mNeonGreen to ER clusters upon ER stress (Figure 16C), which suggested that the demand for ESCRT

recruitment to ER clusters was higher in these cells. Even more so, *dga1Δlro1Δ* cells showed a low frequency of Snf7-mNeonGreen puncta at ER clusters in untreated cells. It is plausible that Snf7 recruitment to ER clusters becomes relevant in untreated cells based on elevated ceramide levels at the ER in the absence of Dga1p and Lro1p. Together, these results hint towards a role of ESCRT recruitment to ER clusters in the formation and/or stabilization of ER-Golgi contacts, where non-vesicular ceramide transport might occur.

8 DISCUSSION

In this work, I characterized the recruitment of ESCRT-III protein Snf7p to ER clusters upon ER stress in yeast and suggested a physiological role for this process. I performed genetic screens to discover genes involved in the process of stress-induced Snf7 recruitment to ER clusters and showed that GPI-anchor remodeling proteins, p24 complex proteins and their interaction with general ER export machinery is essential for the formation of ER clusters upon stress. I provided evidence that the general ER export machinery is not only essential for the recruitment of Snf7 to ER clusters but also forms specific assemblies at ER clusters. Using four-color live cell imaging, I could dissect the interplay of COPII and Cop1p at ER clusters. I also observed the localization of the ER-Golgi tethering proteins Nvj2p and Tcb3p to ER clusters, which for Tcb3p depends on Bro1. These tethers typically co-localized with Cop1p at ER clusters, which suggests that ER clusters are an interface between ER and Golgi compartments that show a compelling array of anterograde ER-to-Golgi and retrograde Golgi-to-ER trafficking proteins. It appears likely that ER clusters are stress-induced ER-Golgi contact sites that allow trafficking of e.g. accumulating ceramide from the ER to the Golgi, when vesicular transport is compromised during ER stress.

This conclusion assumes that ER stress indeed impairs vesicular trafficking mediated by COPII. However, this has not conclusively been shown. A study in mammalian Huh7 cells suggested that ER stress impairs the ER export of a model substrate and that a decreased number of COPII vesicle assembly on the ER could be the reason for this (Amodio *et al*, 2009). The folding state of the cargo proteins, which is clearly affected during ER stress, could have an impact on binding to their specific export receptors and their successful export from the ER (Phillips *et al*, 2020). It was also shown in yeast that ER export and ER-to-Golgi trafficking components are upregulated by the UPR (Travers *et al*, 2000). If ER export was indeed compromised by ER stress, upregulation of ER-to-Golgi trafficking proteins could help cells to restore normal levels of ER export. Another explanation would be that ER export components are produced to export cargo, which was initially stuck and accumulated in the ER during ER stress, as soon as ER stress is relieved. Yet another alternative would be that yeast actively increases ER export by upregulation of ER export components to clear proteins from the ER, even if they are misfolded, to restore homeostasis within the ER. However, this would come at the cost of misfolded proteins reaching other cellular compartments of the secretory pathway. Thus, it remains to be shown how ER stress impacts the net outcome of protein trafficking towards the Golgi. The effect of ER stress may also differ for the export of different classes of proteins, as well as in different organisms and cell types. Whereas GPI-APs are preferentially exported within minutes of ER stress in the RESET pathway in mammalian cells (Satpute-Krishnan *et al*, 2014; Cheatham *et al*, 2023), GPI-APs appear to be efficiently retained in the ER during ER stress in yeast (Anna Platzek, unpublished). A thorough study for the effect of ER stress on ER export in yeast and other model organisms remains to be performed in the future.

Based on the findings presented in this thesis, I propose the following speculative model of ESCRT function at ER clusters (Figure 17). ER stress triggered by tunicamycin treatment leads to elevated levels of ceramide in the ER membrane. The fact that many GPI-APs, which would usually be exported in the same vesicles as ceramide, are retained in the ER upon stress might contribute to this increase, since more ceramide-rich membrane domains remain in the ER. GPI-anchor remodeling proteins provide GPI-APs with ceramide-containing GPI-anchors. This allows them to associate with ceramide-rich domains and to engage with their export receptor, the p24 complex. The accumulation of GPI-APs together with p24 proteins, the subsequent binding of p24 to COPII and the concentration of the Dsl1 tethering complex eventually lead to the formation of ER clusters. Subsequently, Bro1p recruits ESCRT-III component Snf7p to these sites. ESCRT recruitment to the ER clusters is a prerequisite for the subsequent recruitment of ER-Golgi tether Tcb3p. Formation of ER clusters also triggers the recruitment of Nvj2p, another ER-Golgi tether. ER clusters are located in proximity to Cop1p-positive Golgi structures and possibly constitute an ER-Golgi contact site. This could serve the non-vesicular transport of ceramide mediated by both ER-Golgi tethers Nvj2p and Tcb3p under conditions that impair vesicular ceramide transport together with GPI-APs. In this way, ceramide is shunted towards the Golgi as rising concentrations in the ER would endanger the membrane environment and counteract the restoration of ER homeostasis.

8.1 ER contact sites

The ER forms contact sites with many organelles of the cell. Mitochondria, endosomes, peroxisomes, lipid droplets, and Golgi were all shown to form physical contacts with ER (Phillips & Voeltz, 2016). What all ER contact sites with other organelles have in common is the absence of ribosomes from these sites, as they are displaced by proteins involved in the structure of the membrane contact site (MCS; Phillips & Voeltz, 2016). We collaborated with the lab of Friedrich Förster at Utrecht university and Leanne de Jager performed cryo-electron tomography combined with correlative light microscopy with fluorescently tagged Snf7 at ER clusters. Her preliminary data suggested that ER clusters are highly tubular and that most sites of Snf7 localization are depleted for ribosomes (unpublished, not shown). This could be due to the MCS formation between ER clusters and the Golgi. However, her experiment did not show obvious Golgi structures in proximity of ER clusters. It is possible that early Golgi compartments are hard to distinguish from the ER in electron tomograms.

Why would the ER and Golgi form direct contacts during ER stress? Contacts between two organelles typically serve various purposes. ER-endosome contacts are increased in the process of endosome maturation, suggesting that ER contact contributes to maturation and/or the localization of endosomes (Friedman *et al*, 2013). Moreover, MCSs are sites of lipid transfer. The precursors of the mitochondrial lipid cardiolipin are synthesized in the ER and it was shown that contact between the ER and mitochondria is required for adequate cardiolipin levels in mitochondria (Voss *et al*, 2012).

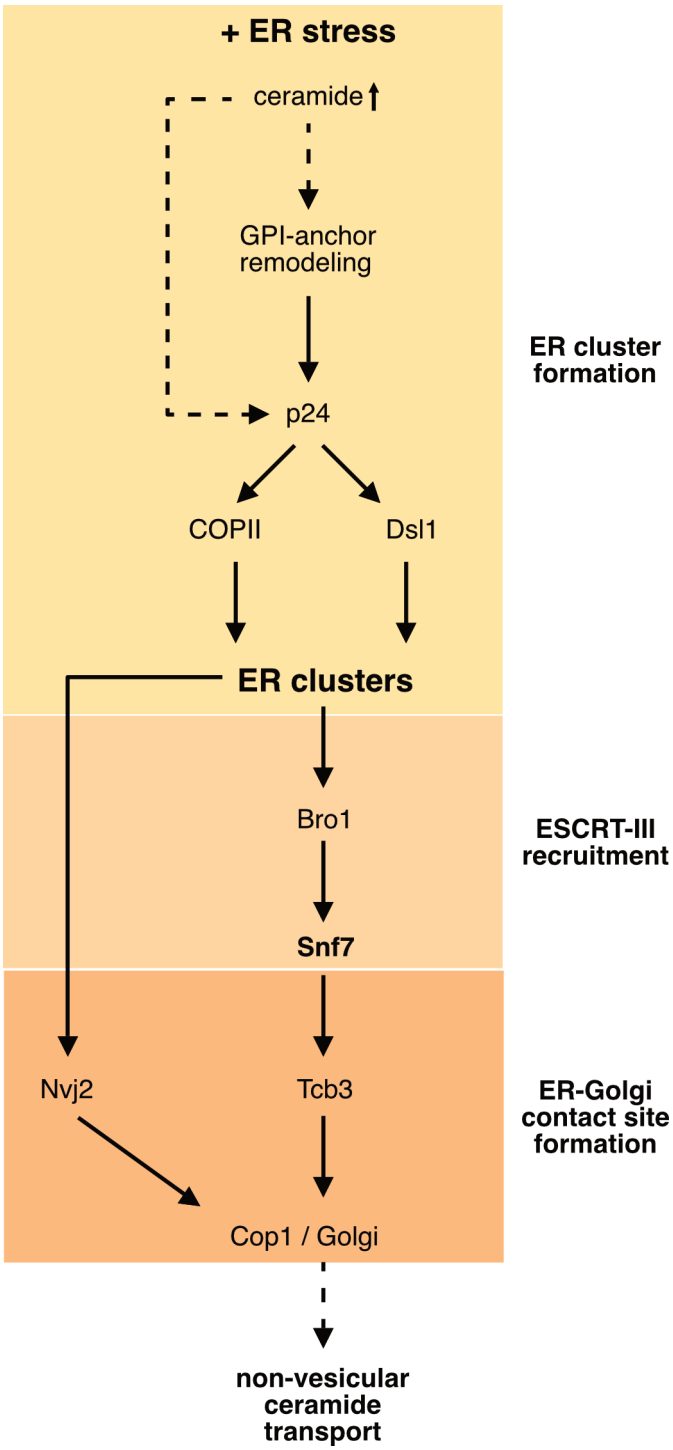

Figure 17. Speculative model of the ESCRT-assisted ER-Golgi contact site formation for the non-vesicular transport of ceramide in yeast.

Importantly, MCSs can maintain important transport processes when cellular conditions restrict vesicular traffic. One example is the non-vesicular trafficking of ceramide in yeast. Whereas non-vesicular trafficking of ceramide only contributes to a small fraction of ceramide trafficking at steady state, it becomes indispensable during ER stress (Liu *et al*, 2017). This observation hints towards the fact that in this case ER stress burdens the vesicular transport of ceramide, as this would explain the higher demand for non-vesicular ceramide transport. Therefore, membrane contact sites promote cell survival under certain conditions.

8.2 ER export of proteins at ER clusters

ER clusters display an interface for a variety of ER export components. Not only the general COPII ER export machinery, but also the p24 complex as the specific ER export receptor of GPI-anchored proteins localize to structures surrounding ER clusters or directly co-localize with them. This raised the question if ER clusters are preferred sites of protein export. I addressed this question, focusing on GPI-anchored proteins, as the specific requirement of the p24 proteins hinted towards a role in GPI-AP export. It is possible that ER export of GPI-APs occurs at a low level at ER clusters. This would allow a small subset of GPI-APs to leave the ER and continue maturation in the Golgi, even though general ER export of GPI-anchored proteins may be reduced (Anna Platzek, unpublished). I overexpressed the GPI-anchored protein Gas1p from the strong inducible *GAL* promoter to test if this condition triggered ER cluster formation and Snf7 recruitment to these sites. This appeared to be the case, albeit at a low frequency (data not shown). The analysis of this experiment remained difficult as ER morphology was altered (cells were grown in alternate sugar medium to allow the induction with galactose). Also, I did not address whether the strong expression and accumulation of Gas1p in the ER might have triggered ER stress. If so, Snf7 puncta formation might have been a consequence of ER stress, rather than an indication towards a role of Snf7 in Gas1p export. To have a more direct readout of the effect of ESCRT recruitment to ER clusters on the export of Gas1p, I inducibly expressed Gas1-sfGFP ectopically at the onset of ER stress treatment in wt and *bro1Δ* cells. However, I observed no consistent defect of Gas1-sfGFP export in *bro1Δ* cells (data not shown). It cannot be ruled out that the timing of ER stress and the level of induction of Gas1-sfGFP was not ideal. Also, it is possible that mild effects on Gas1-sfGFP export could not be detected with this particular experimental setup. Taken together, it is unclear if GPI-anchored proteins or any other secretory proteins are exported at ER clusters and if the recruitment of ESCRT machinery to ER clusters affects protein export in general. Even if it might not be the primary role of ESCRT proteins at ER clusters to promote protein export, it is possible that protein export occurs at these sites once ER clusters are established.

The lab of Jennifer Lippincott-Schwartz proposed that tubular protein carriers mediating transport towards the Golgi exist in mammalian cells under certain circumstances. In their model, COPII components localize to the base of the tubules and act as a gate keeper for cargo proteins, whereas COPI components localize to the tubules like beads on a string, promoting the transport of proteins along the tubules towards the Golgi (Weigel *et al*, 2021). We have acquired a preliminary ultrastructure

of ER clusters after ER stress and even though ER clusters appear tubular, they do look distinct from the tubular carriers that were described in mammalian cells (Weigel *et al*, 2021). Further experiments will determine if any similarities between the tubular carriers and ER clusters exist. In general, ER export in mammalian cells can give rise to more complex transport carriers. This may be due to the even greater spectrum of cargo. Another example is the export of procollagen. Typical COPII vesicles can vary between 60 and 80 nm in diameter (Stagg *et al*, 2008). Procollagen, however, can form 300-400 nm fibers in the ER lumen and requires the additional factors TANGO1 and cTAGE5 to be packed into specialized, larger carriers for protein export (Saito *et al*, 2009; Saito *et al*, 2011). In yeast, COPII components were only found as COPII vesicles so far. Whether other export structures exist in yeast needs to be addressed in the future.

There are cases described in literature, where a COPII subunit was implicated in the process of autophagy, rather than in protein secretion. One example is Lst1p, which was not required for the formation of ER clusters (Figure 10), but formed regular assemblies at these sites (Figure 12B). The COPII cargo adaptor Lst1p-Sec23p was shown to be involved in the selective sorting of misfolded cargo and in the induction of ER-phagy at specific ER domains (Cui *et al*, 2019). Moreover, work in *Drosophila melanogaster* connected ESCRT function and COPII trafficking with ERGIC and autophagosome formation (Wang *et al*, 2022). Eventually, work by the lab of Jennifer Lippincott -Schwartz described a process where the ESCRT proteins, ALIX (the Bro1p homologue in mammalian cells), ALG-2 and COPII collectively control the lysosome-dependent uptake of ERES in mammalian cells (Liao *et al*, 2024). Even though all of these publications link functional players of ESCRT recruitment to ER clusters with autophagy, I could experimentally exclude that ER clusters function in autophagy. First, deletions of core autophagy genes or ER-phagy receptors did not impair recruitment of Snf7 to ER clusters (data not shown). Second, ER clusters showed no specific proximity to the vacuole or to fluorescently tagged Atg8, which is commonly used as a marker for autophagic structures (data not shown).

8.3 Physiological relevance of ESCRT recruitment to ER clusters

ESCRT recruitment to ER clusters is a novel stress-induced phenotype that connects ESCRT function with ER export in the context of ER stress. It is possible that ER stress poses a scenario that impairs ER export of multiple cargoes, including the sphingolipid ceramide. This could explain why non-vesicular transport of ceramide only plays a minor role at steady state but is of great importance upon ER stress (Liu *et al*, 2017). Ceramide is not only a cargo by itself, but also fulfils a role in the export of GPI-anchored proteins. The importance of ceramide in ER export of GPI-anchored proteins is twofold: the fully remodeled GPI-anchor usually contains ceramide and ceramide has the tendency to form microdomains within the ER membrane (Umemura *et al*, 2007; Silva *et al*, 2006). These ceramide clusters are required for the clustering of GPI-anchored proteins prior to ER export (Watanabe *et al*, 2002). Even though ceramide is an essential precursor for complex sphingolipids in yeast and enables export of GPI-APs, accumulation of ceramide is toxic for cells (Eisenberg & Büttner, 2014). A potential reason for this is the

pore-forming characteristic of ceramide at high concentrations that was described *in vitro* (Siskind & Colombini, 2000). Therefore, maintaining adequate levels of ceramide in the ER membrane is pivotal for the cell. In yeast, complex sphingolipid synthesis is carried out at the Golgi (Funato & Riezman, 2001). Transport of ceramide from the ER to the Golgi is therefore not only important to avoid ceramide toxicity in the ER, but also to maintain higher sphingolipid synthesis. The data presented in this study hints towards a role of ESCRT recruitment to ER clusters in formation or stabilization of ER-Golgi contacts, where non-vesicular trafficking of ceramide could be carried out by Nvj2p and Tcb3p. Structurally, Nvj2p contains three domains: a transmembrane domain, which resides in the ER membrane; a Pleckstrin Homology (PH) domain that could bind phosphoinositides in the Golgi membrane and a Synaptotagmin-like mitochondrial-lipid-binding (SMP) domain (Liu *et al*, 2017; (Jeyasimman & Saheki, 2020). The SMP domain of Nvj2p is proposed to bind lipids and is essential for the Nvj2p-dependent non-vesicular transport of ceramide during stress (Liu *et al*, 2017). This SMP domain is structurally related to the SMP domain of extended synaptotagmins, which localize to contact sites of the ER and plasma membrane and require their SMP domain to transfer glycerolipids at these sites (Saheki *et al*, 2016; Yu *et al*, 2016). Nvj2p was also reported to bind ceramide (Gallego *et al*, 2010). Tcb3p is a yeast tricalbin and contains a transmembrane domain residing in the ER membrane, an SMP domain and multiple C2 domains (Kopec *et al*, 2010; Manford *et al*, 2012; Toulmay & Prinz, 2012; Ikeda *et al*, 2020). It was shown that the C2 domains are required for the localization of Tcb3p to ER-Golgi contact sites and its function as ER-Golgi tether (Ikeda *et al*, 2020). C2 domains can interact with acidic phospholipids (Schulz & Creutz, 2004). It is not clear if the SMP domain of Tcb3p binds and transports ceramide directly (Ikeda *et al*, 2020).

It is plausible that Nvj2p and Tcb3p bind and actively transport ceramide at stress-induced ER clusters. However, Liu and colleagues could show that an artificial ER-Golgi tether can facilitate the non-vesicular transport of ceramide under stress (Liu *et al*, 2017). It is therefore conceivable that any structure that establishes more stable ER-Golgi contacts contributes to non-vesicular ceramide transport.

How could ESCRT function at ER clusters contribute to non-vesicular ceramide transport at these sites? I could show that Tcb3p recruitment to cytosolic puncta depends on prior ESCRT recruitment to ER clusters (Figure 15C), whereas Nvj2p is recruited to ER clusters in an ESCRT-independent manner (data not shown). Therefore, ESCRT recruitment results in the recruitment of additional tethering capacity from Tcb3p to potentially stabilize existing ER-Golgi contacts established by Nvj2p. It is possible that ESCRT proteins in this case do not assume conformations that result in vesicle budding as in MVB formation, but rather act as a scaffold to allow the assembly of e.g. tethering proteins. One example for a scaffolding function of ESCRT proteins, is the fungal Rim pathway for the sensing of pH, where the ESCRTs establish a platform for proteins involved in the Rim signaling cascade (Ost *et al*, 2015). It is possible that a similar scenario holds true for the recruitment of ESCRT proteins to ER clusters. It is worth mentioning that ER clusters appear less defined in *bro1Δ* cells, even at the level of light microscopy (Figure 3A). This suggests that the presence of the ESCRT machinery at these sites impacts the morphology of ER clusters. It is conceivable that the concerted action of two membrane shaping machineries, ESCRTs and COPII, at ER clusters enables the formation of membrane structures

that cannot be formed by either one alone. The effect of ESCRT proteins on the ER membrane at ER clusters could provide a membrane environment and/or shape that allows more efficient clustering of tethering proteins. How the ESCRTs exactly contribute to ceramide homeostasis upon ER stress and if ESCRT recruitment to ER clusters does contribute to stress relief needs to be addressed in the future.

8.4 Limitations of this study

Here, I focused on the ER stress-induced recruitment of ESCRT proteins to ER clusters. However, it is plausible that ESCRT proteins aid non-vesicular trafficking of ceramide also at a low level at steady state. Vesicular trafficking accounts for most of the ceramide transport to the Golgi at steady state and only a small percentage can be attributed to non-vesicular trafficking (Liu *et al*, 2017). It was also shown that Svf1p is mainly responsible for non-vesicular ceramide trafficking at steady state (Limar *et al*, 2023). This would reduce the dynamic range to observe an effect of ESCRT proteins in ceramide trafficking. Lis Albert could show that over-expression of endogenous *BRO1* can trigger ESCRT recruitment to ER clusters in non-stressed cells (Lis Albert, unpublished). It would be informative to determine whether these ER clusters are also capable of ceramide trafficking in the absence of the ER stress stimulus. However, this would require a direct quantitative readout for ceramide levels in cells. It is plausible that ER clusters are extreme phenotypes of this biological process that one can only visualize by light microscopy after ER stress treatment. This does not exclude that ESCRT proteins also transiently act at the ER membrane in untreated cells, which however cannot be easily appreciated by widefield light microscopy.

This study used the expression of tagged, non-functional Snf7 expressed at a low level alongside the endogenous version. While this is a common practice in the ESCRT biology field to track ESCRT function (Teis *et al*, 2008), we observed that this experimental setup is not neutral to the recruitment of Snf7 to ER clusters. While endogenous, functional Snf7p is essential for the recruitment of Snf7-neon to occur upon stress, the absence of tagged Snf7 results in drastic drop of frequency of Snf7 recruitment to ER clusters (in this case judged by co-localization of Bro1p-mNeonGreen with ER clusters upon ER stress). This discrepancy might hinder the identification of the biological role of ESCRT recruitment to the ER. Whereas it helped me to identify machinery involved in ESCRT recruitment to the ER, it could block the functional consequences of ESCRT recruitment to ER clusters. This issue can only be circumvented by testing hypotheses regarding the function of ESCRT recruitment in the absence of tagged Snf7. This would likely involve the use of Bro1 variant *bro1Y320D*, which is unable to recruit Snf7 to ER clusters, but is almost fully functional in MVB sorting (Lis Albert, unpublished).

Our leading hypothesis is that ESCRT recruitment to ER clusters assists the non-vesicular transport of ceramide during ER stress conditions. Typically, only one ER cluster per cell is observed. If these sites were indeed structures that show substantial ceramide trafficking one would expect accumulation of ceramide at these sites. This, however, cannot be addressed by imaging at the moment, as no ceramide sensor is available that binds to and visualize ceramide.

Another difficulty is the change of Golgi morphology upon ER stress. Whereas many Golgi marker proteins show a distinct and characteristic Golgi staining at steady state (few spherical and ellipsoid structures), the staining after ER stress appears drastically different, with many smaller structures and hardly any preservation of the larger structures observed at steady state (Lis Albert, unblished). This morphological change impedes the description of ER-Golgi contact sites. This altered Golgi morphology might reflect reduced functionality of the Golgi. In mammalian cells, ethanol treatment of cells results in a dysfunction of SAR1A which blocks the COPII-dependent transport of PDIA3 (Petrosyan *et al*, 2015). Lack of PDIA3 in the Golgi impairs giantin dimerization and leads to Golgi fragmentation (Petrosyan *et al*, 2015). In this case, disruption of ER trafficking has a direct consequence for Golgi morphology.

8.5 Conservation of ESCRT recruitment to ER clusters

The ESCRT machinery is an ancient multicomplex protein machinery that is conserved from Archaea to Human. Many genes involved in Snf7 recruitment to ER clusters are conserved in mammalian cells. ESCRT-III component CHMP4A/B takes over the roles of Snf7p in mammalian cells and can form polymers, as well as interact with ALIX, the mammalian homologue of Bro1p (Katoh *et al*, 2003).
Albeit more complex, the IRE1 branch of the human UPR shares great functional and structural overlap with the main ER stress response in yeast (Walter & Ron, 2011). It is plausible that other ER stress responses are conserved from yeast to human as well.
Moreover, HT008, the human homologue of Nvj2p, was shown to be able to compensate for deletion of *NVJ2* in non-vesicular ceramide transport in yeast (Liu *et al*, 2017). In mammalian cells, CERT is mediating the non-vesicular transport of ceramide (Hanada *et al*, 2003). As yeast has various types of non-vesicular trafficking in place, it is conceivable that alternative routes for non-vesicular trafficking of ceramide exist in human cells as well.

9 OUTLOOK

This study presented indications for a role of ESCRT recruitment to ER clusters in the formation or stabilization of ER-Golgi contacts through recruitment of the ER-Golgi tether Tcb3p. This recruitment possibly stimulates non-vesicular ER export of ceramide during ER stress and alleviates toxicity by accumulation of ceramide in the ER membrane. Nevertheless, a direct role of ESCRT recruitment to ER clusters on the ER export of ceramide needs to be shown. One possibility to test this hypothesis is quantitative lipidomics. Ceramide is made in the ER and upon arrival in the Golgi converted to IPC and other complex sphingolipids. The ratio of IPC and ceramide can therefore be used to detect defects of ceramide transport from the ER to the Golgi. A similar approach was taken by Limar and colleagues to assign a role in non-vesicular ceramide transport to Svf1p at steady state (Limar *et al*, 2023). In our case, a lipidomics experiment could compare IPC:ceramide ratios in wt and *bro1Y320D* cells, at steady state and after ER stress. A lower IPC:ceramide ratio in *bro1Y320D* compared to wt cells would suggest a ceramide transport defect in these cells. Moreover, this would clarify if the observed effect were ER stress specific. As quantification of higher yeast sphingolipids is difficult, due to lack of adequate standards, total ceramide levels would be the first indication of impaired ceramide trafficking upon ER stress in cells lacking ESCRT recruitment to ER clusters. An even more sensitive approach would be to follow a cohort of newly synthesized ceramide on its way to conversion to sphingomyelin in a radioactive pulse-chase experiment in wt and *bro1Y320D* cells in the presence of ER stress, similar to an experiment performed by Liu and colleagues (Liu *et al*, 2017).

Moreover, growth assays could be used as a general readout for the fitness of yeast cells. Liu and colleagues showed that deletion of NVJ2 in the context of a *dga1Δlro1Δ* strain resulted in a strong growth defect in spotting assays on tunicamycin plates (Liu *et al*, 2017). This can be explained by the fact that non-vesicular transport relies even more on Nvj2p when cells lack *DGA1* and *LRO1* and therefore cannot convert excess ceramide into acyl-ceramide to store in LDs. I have observed that Snf7 recruitment to ER clusters is increased in *dga1Δlro1Δ,* both in untreated and tunicamycin-treated cells, suggesting that cells compensate for the loss of one ceramide removal pathway with another one. Future experiments will test if *bro1Y320D dga1Δlro1Δ cells* grow substantially worse on tunicamycin plates than wt cells. This would indicate that ESCRT recruitment to ER clusters upon ER stress supports cell survival when other means of clearing excessive ceramide are defective.

I confirmed in early experiments that Snf7 recruitment to ER clusters is an UPR-independent ER stress response (Figure 3B). It remains to be shown if and to what degree Snf7 recruitment to ER clusters contributes to ER stress relief and if there is an interplay with the UPR. The degree of UPR activation can be measured by using the Hac1 splicing reporter. Ire1p activity leads to the splicing of the Hac1 splicing reporter, enabling the translation of GFP (Pincus *et al*, 2010), which can be measured by flow cytometry. Using this tool, one could determine the levels of UPR activation upon ER stress in wt and *bro1Y320D* cells. If Snf7 recruitment to ER clusters indeed contributed to ER stress relief, the activation of the UPR should be stronger in cells that cannot recruit Snf7. It would be crucial to determine the dynamic range of the Hac1 splicing reporter beforehand. If my ER stress conditions used in this thesis

triggered the Hac1 splicing reporter already to the full extend, no further increase could be observed even if Snf7 recruitment contributed to ER stress relief.
Eventually, it remains to be tested whether ER stress-induced ESCRT recruitment to ER clusters is conserved in mammalian cells.

Taken together, this study adds to our understanding of ER stress responses in yeast and describes a new aspect of ESCRT biology in the context of ER-Golgi trafficking and potentially membrane contact site formation.

10 REFERENCES

Alonso Y Adell M, Migliano SM & Teis D (2016) ESCRT-III and Vps4: a dynamic multipurpose tool for membrane budding and scission. *The FEBS Journal* 283: 3288–3302

Amodio G, Renna M, Paladino S, Venturi C, Tacchetti C, Moltedo O, Franceschelli S, Mallardo M, Bonatti S & Remondelli P (2009) Endoplasmic reticulum stress reduces the export from the ER and alters the architecture of post-ER compartments. *The International Journal of Biochemistry & Cell Biology* 41: 2511–2521

Aragón T, Van Anken E, Pincus D, Serafimova IM, Korennykh AV, Rubio CA & Walter P (2009) Messenger RNA targeting to endoplasmic reticulum stress signalling sites. *Nature* 457: 736–740

Barlowe C, d'Enfert C & Schekman R (1993) Purification and characterization of SAR1p, a small GTP-binding protein required for transport vesicle formation from the endoplasmic reticulum. *Journal of Biological Chemistry* 268: 873–879

Barlowe CK & Miller EA (2013) Secretory Protein Biogenesis and Traffic in the Early Secretory Pathway. *Genetics* 193: 383–410

Belden WJ & Barlowe C (2001) Role of Erv29p in Collecting Soluble Secretory Proteins into ER-Derived Transport Vesicles. *Science* 294: 1528–1531

Bertolotti A, Zhang Y, Hendershot LM, Harding HP & Ron D (2000) Dynamic interaction of BiP and ER stress transducers in the unfolded-protein response. *Nat Cell Biol* 2: 326–332

Boncompain G & Weigel AV (2018) Transport and sorting in the Golgi complex: multiple mechanisms sort diverse cargo. *Current Opinion in Cell Biology* 50: 94–101

Braakman I, Helenius J & Helenius A (1992) Manipulating disulfide bond formation and protein folding in the endoplasmic reticulum. *The EMBO Journal* 11: 1717–1722

Breitling J & Aebi M (2013) N-Linked Protein Glycosylation in the Endoplasmic Reticulum. *Cold Spring Harbor Perspectives in Biology* 5: a013359–a013359

Buchwalter A, Schulte R, Tsai H, Capitanio J & Hetzer M (2019) Selective clearance of the inner nuclear membrane protein emerin by vesicular transport during ER stress. *eLife* 8: e49796

Bulleid NJ, Bassel-Duby RS, Freedman RB, Sambrook JF & Gething MJH (1992) Cell-free synthesis of enzymically active tissue-type plasminogen activator. Protein folding determines the extent of *N*-linked glycosylation. *Biochemical Journal* 286: 275–280

Burda P & Aebi M (1999) The dolichol pathway of N-linked glycosylation. *Biochimica et Biophysica Acta (BBA) - General Subjects* 1426: 239–257

Castillon GA, Watanabe R, Taylor M, Schwabe TME & Riezman H (2009) Concentration of GPI-Anchored Proteins upon ER Exit in Yeast. *Traffic* 10: 186–200

Cheatham AM, Sharma NR & Satpute-Krishnan P (2023) Competition for calnexin binding regulates secretion and turnover of misfolded GPI-anchored proteins. *Journal of Cell Biology* 222: e202108160

Chen X, VanValkenburgh C, Liang H, Fang H & Green N (2001) Signal Peptidase and Oligosaccharyltransferase Interact in a Sequential and Dependent Manner within the Endoplasmic Reticulum. *Journal of Biological Chemistry* 276: 2411–2416

Connerly PL, Esaki M, Montegna EA, Strongin DE, Levi S, Soderholm J & Glick BS (2005) Sec16 is a Determinant of Transitional ER Organization. *Current Biology* 15: 1439–1447

Čopič A, Latham CF, Horlbeck MA, D'Arcangelo JG & Miller EA (2012) ER Cargo Properties Specify a Requirement for COPII Coat Rigidity Mediated by Sec13p. *Science* 335: 1359–1362

Covino R, Hummer G & Ernst R (2018) Integrated Functions of Membrane Property Sensors and a Hidden Side of the Unfolded Protein Response. *Molecular Cell* 71: 458–467

Cox JS, Shamu CE & Walter P (1993) Transcriptional induction of genes encoding endoplasmic reticulum resident proteins requires a transmembrane protein kinase. *Cell* 73: 1197–1206

Cox JS & Walter P (1996) A Novel Mechanism for Regulating Activity of a Transcription Factor That Controls the Unfolded Protein Response.

Cui Y, Parashar S, Zahoor M, Needham PG, Mari M, Zhu M, Chen S, Ho H-C, Reggiori F, Farhan H, *et al* (2019) A COPII subunit acts with an autophagy receptor to target endoplasmic reticulum for degradation. *Science* 365: 53–60

D'Arcangelo JG, Crissman J, Pagant S, Čopič A, Latham CF, Snapp EL & Miller EA (2015) Traffic of p24 Proteins and COPII Coat Composition Mutually Influence Membrane Scaffolding. *Current Biology* 25: 1296–1305

D'Arcangelo JG, Stahmer KR & Miller EA (2013) Vesicle-mediated export from the ER: COPII coat function and regulation. *Biochimica et Biophysica Acta (BBA) - Molecular Cell Research* 1833: 2464–2472

Eisenberg T & Büttner S (2014) Lipids and cell death in yeast. *FEMS Yeast Research* 14: 179–197

Elrod-Erickson MJ & Kaiser CA (1996) Genes that control the fidelity of endoplasmic reticulum to Golgi transport identified as suppressors of vesicle budding mutations. *MBoC* 7: 1043–1058

d'Enfert C, Wuestehube LJ, Lila T, Schekman R. Sec12p-dependent membrane binding of the small GTP-binding protein Sar1p promotes formation of transport vesicles from the ER. J Cell Biol. 1991 Aug;114(4):663-70. doi: 10.1083/jcb.114.4.663. PMID: 1907973; PMCID: PMC2289894.

Espenshade P, Gimeno RE, Holzmacher E, Teung P & Kaiser CA (1995) Yeast SEC16 gene encodes a multidomain vesicle coat protein that interacts with Sec23p. *The Journal of cell biology* 131: 311–324

Fath S, Mancias JD, Bi X & Goldberg J (2007) Structure and Organization of Coat Proteins in the COPII Cage. *Cell* 129: 1325–1336

Friedman JR, DiBenedetto JR, West M, Rowland AA & Voeltz GK (2013) Endoplasmic reticulum–endosome contact increases as endosomes traffic and mature. *MBoC* 24: 1030–1040

Funato K & Riezman H (2001) Vesicular and nonvesicular transport of ceramide from ER to the Golgi apparatus in yeast. *The Journal of Cell Biology* 155: 949–960

Gable K, Slife H, Bacikova D, Monaghan E & Dunn TM (2000) Tsc3p Is an 80-Amino Acid Protein Associated with Serine Palmitoyltransferase and Required for Optimal Enzyme Activity. *Journal of Biological Chemistry* 275: 7597–7603

Gallego O, Betts MJ, Gvozdenovic-Jeremic J, Maeda K, Matetzki C, Aguilar-Gurrieri C, Beltran-Alvarez P, Bonn S, Fernández-Tornero C, Jensen LJ, *et al* (2010) A systematic screen for protein–lipid interactions in *Saccharomyces cerevisiae*. *Molecular Systems Biology* 6: 430

Gaut JR & Hendershot LM (1993) The modification and assembly of proteins in the endoplasmic reticulum. *Current Opinion in Cell Biology* 5: 589–595

Hanada K (2003) Serine palmitoyltransferase, a key enzyme of sphingolipid metabolism. *Biochimica et Biophysica Acta (BBA) - Molecular and Cell Biology of Lipids* 1632: 16–30

Hanada K, Kumagai K, Yasuda S, Miura Y, Kawano M, Fukasawa M & Nishijima M (2003) Molecular machinery for non-vesicular trafficking of ceramide. *Nature* 426: 803–809
Hannun YA & Obeid LM (2018) Sphingolipids and their metabolism in physiology and disease. *Nat Rev Mol Cell Biol* 19: 175–191

Henne WM, Buchkovich NJ & Emr SD (2011) The ESCRT Pathway. *Developmental Cell* 21: 77–91

Hirata R, Nihei C & Nakano A (2013) Isoform-selective Oligomer Formation of Saccharomyces cerevisiae p24 Family Proteins. *Journal of Biological Chemistry* 288: 37057–37070

Ho N, Yap WS, Xu J, Wu H, Koh JH, Goh WWB, George B, Chong SC, Taubert S & Thibault G (2020) Stress sensor Ire1 deploys a divergent transcriptional program in response to lipid bilayer stress. *Journal of Cell Biology* 219: e201909165

Hugenroth M & Bohnert M (2020) Come a little bit closer! Lipid droplet-ER contact sites are getting crowded. *Biochimica et Biophysica Acta (BBA) - Molecular Cell Research* 1867: 118603

Hurley JH (2015) ESCRT s are everywhere. *The EMBO Journal* 34: 2398–2407

Ikeda A, Schlarmann P, Kurokawa K, Nakano A, Riezman H & Funato K (2020) Tricalbins Are Required for Non-vesicular Ceramide Transport at ER-Golgi Contacts and Modulate Lipid Droplet Biogenesis. *iScience* 23: 101603

Ito H, Fukuda Y, Murata K, Kimura A. Transformation of intact yeast cells treated with alkali cations. J Bacteriol. 1983 Jan;153(1):163-8. doi: 10.1128/jb.153.1.163-168.1983. PMID: 6336730; PMCID: PMC217353.

Janke C, Magiera MM, Rathfelder N, Taxis C, Reber S, Maekawa H, Moreno-Borchart A, Doenges G, Schwob E, Schiebel E, Knop M. A versatile toolbox for PCR-based tagging of yeast genes: new fluorescent proteins, more markers and promoter substitution cassettes. Yeast. 2004 Aug;21(11):947-62. doi: 10.1002/yea.1142. PMID: 15334558.

Jeong H, Park J & Lee C (2016) Crystal structure of Mdm12 reveals the architecture and dynamic organization of the ERMES complex. *EMBO Reports* 17: 1857–1871

Jeyasimman D & Saheki Y (2020) SMP domain proteins in membrane lipid dynamics. *Biochimica et Biophysica Acta (BBA) - Molecular and Cell Biology of Lipids* 1865: 158447

Jimenez AJ, Maiuri P, Lafaurie-Janvore J, Divoux S, Piel M & Perez F (2014) ESCRT Machinery Is Required for Plasma Membrane Repair. *Science* 343: 1247136

Katoh K, Shibata H, Suzuki H, Nara A, Ishidoh K, Kominami E, Yoshimori T & Maki M (2003) The ALG-2-interacting Protein Alix Associates with CHMP4b, a Human Homologue of Yeast Snf7 That Is Involved in Multivesicular Body Sorting. *Journal of Biological Chemistry* 278: 39104–39113

Katzmann DJ, Babst M & Emr SD (2001) Ubiquitin-Dependent Sorting into the Multivesicular Body Pathway Requires the Function of a Conserved Endosomal Protein Sorting Complex, ESCRT-I. *Cell* 106: 145–155

Kim J, Sitaraman S, Hierro A, Beach BM, Odorizzi G & Hurley JH (2005) Structural Basis for Endosomal Targeting by the Bro1 Domain. *Developmental Cell* 8: 937–947

Kopec KO, Alva V & Lupas AN (2010) Homology of SMP domains to the TULIP superfamily of lipid-binding proteins provides a structural basis for lipid exchange between ER and mitochondria. *Bioinformatics* 26: 1927–1931

Kratochvílová K, Moráň L, Paďourová S, Stejskal S, Tesařová L, Šimara P, Hampl A, Koutná I & Vaňhara P (2016) The role of the endoplasmic reticulum stress in stemness, pluripotency and development. *European Journal of Cell Biology* 95: 115–123

Kukuruzinska MA & Lennon K (1995) Diminished activity of the first N-glycosylation enzyme, dolichol-P-dependent N-acetylglucosamine-l-P transferase (GPT), gives rise to mutant phenotypes in yeast. *Biochimica et Biophysica Acta*

Lee MCS, Hamamoto S & Schekman R (2002) Ceramide Biosynthesis Is Required for the Formation of the Oligomeric H+-ATPase Pma1p in the Yeast Endoplasmic Reticulum. *Journal of Biological Chemistry* 277: 22395–22401

Lee MCS, Orci L, Hamamoto S, Futai E, Ravazzola M & Schekman R (2005) Sar1p N-Terminal Helix Initiates Membrane Curvature and Completes the Fission of a COPII Vesicle. *Cell* 122: 605–617

Li Z, Vizeacoumar FJ, Bahr S, Li J, Warringer J, Vizeacoumar FS, Min R, VanderSluis B, Bellay J, DeVit M, *et al* (2011) Systematic exploration of essential yeast gene function with temperature-sensitive mutants. *Nat Biotechnol* 29: 361–367

Liao Y-C, Pang S, Li W-P, Shtengel G, Choi H, Schaefer K, Xu CS & Lippincott-Schwartz J (2024) COPII with ALG2 and ESCRTs control lysosome-dependent microautophagy of ER exit sites. *Developmental Cell* 59: 1410-1424.e4

Limar S, Körner C, Martínez-Montañés F, Stancheva VG, Wolf VN, Walter S, Miller EA, Ejsing CS, Galassi VV & Fröhlich F (2023) Yeast Svf1 binds ceramides and contributes to sphingolipid metabolism at the ER cis-Golgi interface. *Journal of Cell Biology* 222: e202109162

Liu L-K, Choudhary V, Toulmay A & Prinz WA (2017) An inducible ER–Golgi tether facilitates ceramide transport to alleviate lipotoxicity. *Journal of Cell Biology* 216: 131–147

Longtine, M.S., Mckenzie III, A., Demarini, D.J., Shah, N.G., Wach, A., Brachat, A., Philippsen, P. and Pringle, J.R. (1998), Additional modules for versatile and economical PCR-based gene deletion and modification in *Saccharomyces cerevisiae*. Yeast, 14: 953-961.

Lopez S, Rodriguez-Gallardo S, Sabido-Bozo S & Muñiz M (2019) Endoplasmic Reticulum Export of GPI-Anchored Proteins. *IJMS* 20: 3506

Lowther J, Naismith JH, Dunn TM & Campopiano DJ (2012) Structural, mechanistic and regulatory studies of serine palmitoyltransferase. *Biochemical Society Transactions* 40: 547–554

Malis Y, Hirschberg K & Kaether C (2022) Hanging the coat on a collar: Same function but different localization and mechanism for COPII. *BioEssays* 44: 2200064

Manford AG, Stefan CJ, Yuan HL, MacGurn JA & Emr SD (2012) ER-to-Plasma Membrane Tethering Proteins Regulate Cell Signaling and ER Morphology. *Developmental Cell* 23: 1129–1140

Matlack KES, Misselwitz B, Plath K & Rapoport TA BiP Acts as a Molecular Ratchet during Posttranslational Transport of Prepro-_, Factor across the ER Membrane.

Matsuoka K, Morimitsu Y, Uchida K & Schekman R (1998) Coat Assembly Directs v-SNARE Concentration into Synthetic COPII Vesicles. *Molecular Cell* 2: 703–708

McCullough J, Frost A & Sundquist WI (2018) Structures, Functions, and Dynamics of ESCRT-III/Vps4 Membrane Remodeling and Fission Complexes. *Annu Rev Cell Dev Biol* 34: 85–109

Miller EA, Beilharz TH, Malkus PN, Lee MCS, Hamamoto S, Orci L & Schekman R (2003) Multiple Cargo Binding Sites on the COPII Subunit Sec24p Ensure Capture of Diverse Membrane Proteins into Transport Vesicles. *Cell* 114: 497–509

Miller EA & Schekman R (2013) COPII — a flexible vesicle formation system. *Current Opinion in Cell Biology* 25: 420–427

Milstein, C., Brownlee, G., Harrison, T. *et al.* A Possible Precursor of Immunoglobulin Light Chains. *Nature New Biology* **239**, 117–120 (1972).

Mingarro I, Nilsson I, Whitley P & Von Heijne G (2000) Different conformations of nascent polypeptides during translocation across the ER membrane. *BMC Cell Biol* 1: 3

Mori K, Ma W, Gething M-J & Sambrook J (1993) A transmembrane protein with a cdc2+CDC28-related kinase activity is required for signaling from the ER to the nucleus. *Cell* 74: 743–756

Muñiz M, Morsomme P & Riezman H (2001) Protein Sorting upon Exit from the Endoplasmic Reticulum. *Cell* 104: 313–320

Muñiz M, Nuoffer C, Hauri H-P & Riezman H (2000) The Emp24 Complex Recruits a Specific Cargo Molecule into Endoplasmic Reticulum–Derived Vesicles. *The Journal of Cell Biology* 148: 925–930
Muñiz M & Riezman H (2016) Trafficking of glycosylphosphatidylinositol anchored proteins from the endoplasmic reticulum to the cell surface. *Journal of Lipid Research* 57: 352–360

Nagiec MM, Baltisberger JA, Wells GB, Lester RL & Dickson RC (1994) The LCB2 gene of Saccharomyces and the related LCB1 gene encode subunits of serine palmitoyltransferase, the initial enzyme in sphingolipid synthesis. *Proc Natl Acad Sci USA* 91: 7899–7902

Nakano A & Brada D (1988) A Membrane Glycoprotein, Secl2p, Required for Protein Transport from the Endoplasmic Reticulum to the Golgi Apparatus in Yeast.

Nakano A & Muramatsu M (1989) A Novel GTP-binding Protein, Sarlp, Is Involved in Transport from the Endoplasmic Reticulum to the Golgi Apparatus. *The Journal of Cell Biology* 109: 15

Nikawa J & Yamashita S (1992) *IRE1* encodes a putative protein kinase containing a membrane-spanning domain and is required for inositol phototrophy in *Saccharomyces cerevisiae*. *Molecular Microbiology* 6: 1441–1446

Novick P, Field C & Schekman R (1980) Identification of 23 complementation groups required for post-translational events in the yeast secretory pathway. *Cell* 21: 205–215

Okamoto M, Kurokawa K, Matsuura-Tokita K, Saito C, Hirata R & Nakano A (2012) High-curvature domains of the ER are important for the organization of ER exit sites in *Saccharomyces cerevisiae*. *Journal of Cell Science*: jcs.100065

Okamura K, Kimata Y, Higashio H, Tsuru A & Kohno K (2000) Dissociation of Kar2p/BiP from an ER Sensory Molecule, Ire1p, Triggers the Unfolded Protein Response in Yeast. *Biochemical and Biophysical Research Communications* 279: 445–450

Ost KS, O'Meara TR, Huda N, Esher SK & Alspaugh JA (2015) The Cryptococcus neoformans Alkaline Response Pathway: Identification of a Novel Rim Pathway Activator. *PLoS Genet* 11: e1005159

Pan X, Roberts P, Chen Y, Kvam E, Shulga N, Huang K, Lemmon S & Goldfarb DS (2000) Nucleus–Vacuole Junctions in *Saccharomyces cerevisiae* Are Formed Through the Direct Interaction of Vac8p with Nvj1p. *MBoC* 11: 2445–2457

Papagiannidis D, Bircham PW, Lüchtenborg C, Pajonk O, Ruffini G, Brügger B & Schuck S (2021) Ice2 promotes ER membrane biogenesis in yeast by inhibiting the conserved lipin phosphatase complex. *The EMBO Journal* 40: e107958

Papanikou E, Day KJ, Austin J & Glick BS (2015) COPI selectively drives maturation of the early Golgi. *eLife* 4: e13232

Petrosyan A, Cheng P-W, Clemens DL & Casey CA (2015) Downregulation of the small GTPase SAR1A: a key event underlying alcohol-induced Golgi fragmentation in hepatocytes. *Sci Rep* 5: 17127

Phillips BP, Gomez-Navarro N & Miller EA (2020) Protein quality control in the endoplasmic reticulum. *Current Opinion in Cell Biology* 65: 96–102

Phillips MJ & Voeltz GK (2016) Structure and function of ER membrane contact sites with other organelles. *Nat Rev Mol Cell Biol* 17: 69–82

Pincus D, Chevalier MW, Aragón T, Van Anken E, Vidal SE, El-Samad H & Walter P (2010) BiP Binding to the ER-Stress Sensor Ire1 Tunes the Homeostatic Behavior of the Unfolded Protein Response. *PLoS Biol* 8: e1000415

Pineau L, Colas J, Dupont S, Beney L, Fleurat-Lessard P, Berjeaud J, Bergès T & Ferreira T (2009) Lipid-Induced ER Stress: Synergistic Effects of Sterols and Saturated Fatty Acids. *Traffic* 10: 673–690
Promlek T, Ishiwata-Kimata Y, Shido M, Sakuramoto M, Kohno K & Kimata Y (2011) Membrane aberrancy and unfolded proteins activate the endoplasmic reticulum stress sensor Ire1 in different ways. *MBoC* 22: 3520–3532

Radanović T & Ernst R (2021) The Unfolded Protein Response as a Guardian of the Secretory Pathway. *Cells* 10: 2965

Rapoport TA, Li L & Park E (2017) Structural and Mechanistic Insights into Protein Translocation. *Annu Rev Cell Dev Biol* 33: 369–390

Roberg KJ, Crotwell M, Espenshade P, Gimeno R & Kaiser CA (1999) *LST1* Is a *SEC24* Homologue Used for Selective Export of the Plasma Membrane ATPase from the Endoplasmic Reticulum. *The Journal of Cell Biology* 145: 659–672

Saheki Y, Bian X, Schauder CM, Sawaki Y, Surma MA, Klose C, Pincet F, Reinisch KM & De Camilli P (2016) Control of plasma membrane lipid homeostasis by the extended synaptotagmins. *Nat Cell Biol* 18: 504–515

Saito K, Chen M, Bard F, Chen S, Zhou H, Woodley D, Polischuk R, Schekman R & Malhotra V (2009) TANGO1 Facilitates Cargo Loading at Endoplasmic Reticulum Exit Sites. *Cell* 136: 891–902

Saito K, Yamashiro K, Ichikawa Y, Erlmann P, Kontani K, Malhotra V & Katada T (2011) cTAGE5 mediates collagen secretion through interaction with TANGO1 at endoplasmic reticulum exit sites. *MBoC* 22: 2301–2308

Satpute-Krishnan P, Ajinkya M, Bhat S, Itakura E, Hegde RS & Lippincott-Schwartz J (2014) ER Stress-Induced Clearance of Misfolded GPI-Anchored Proteins via the Secretory Pathway. *Cell* 158: 522–533

Schuck S, Prinz WA, Thorn KS, Voss C & Walter P (2009) Membrane expansion alleviates endoplasmic reticulum stress independently of the unfolded protein response. *Journal of Cell Biology* 187: 525–536

Schulz TA & Creutz CE (2004) The Tricalbin C2 Domains: Lipid-Binding Properties of a Novel, Synaptotagmin-Like Yeast Protein Family. *Biochemistry* 43: 3987–3995

Shamu CE & Walter P (1996) Oligomerization and phosphorylation of the Ire1p kinase during intracellular signaling from the endoplasmic reticulum to the nucleus. *The EMBO Journal* 15: 3028–3039

Shindiapina P & Barlowe C (2010) Requirements for Transitional Endoplasmic Reticulum Site Structure and Function in Saccharomyces cerevisiae. *MBoC* 21: 1530–1545

Sidrauski C, Cox JS & Walter P (1996) tRNA Ligase Is Required for Regulated mRNA Splicing in the Unfolded Protein Response. *Cell* 87: 405–413

Sidrauski C & Walter P (1997) The Transmembrane Kinase Ire1p Is a Site-Specific Endonuclease That Initiates mRNA Splicing in the Unfolded Protein Response. *Cell* 90: 1031–1039

Sikorski RS, Hieter P. A system of shuttle vectors and yeast host strains designed for efficient manipulation of DNA in Saccharomyces cerevisiae. Genetics. 1989 May;122(1):19-27. doi: 10.1093/genetics/122.1.19. PMID: 2659436; PMCID: PMC1203683.

Silva L, De Almeida RFM, Fedorov A, Matos APA & Prieto M (2006) Ceramide-platform formation and -induced biophysical changes in a fluid phospholipid membrane. *Molecular Membrane Biology* 23: 137–148

Silva LC, De Almeida RFM, Castro BM, Fedorov A & Prieto M (2007) Ceramide-Domain Formation and Collapse in Lipid Rafts: Membrane Reorganization by an Apoptotic Lipid. *Biophysical Journal* 92: 502–516

Siskind LJ & Colombini M (2000) The Lipids C2- and C16-Ceramide Form Large Stable Channels. *Journal of Biological Chemistry* 275: 38640–38644

Sohn K, Orci L, Ravazzola M, Amherdt M, Bremser M, Lottspeich F, Fiedler K, Helms IB & Wieland T (1996) A Major Transmembrane Protein of Golgi-derived COPI-coated Vesicles Involved in Coatorner Binding. *The Journal of Cell Biology* 135

Stagg SM, LaPointe P, Razvi A, Gürkan C, Potter CS, Carragher B & Balch WE (2008) Structural Basis for Cargo Regulation of COPII Coat Assembly. *Cell* 134: 474–484

Teis D, Saksena S & Emr SD (2008) Ordered Assembly of the ESCRT-III Complex on Endosomes Is Required to Sequester Cargo during MVB Formation. *Developmental Cell* 15: 578–589

Thaller DJ, Allegretti M, Borah S, Ronchi P, Beck M & Lusk CP (2019) An ESCRT-LEM protein surveillance system is poised to directly monitor the nuclear envelope and nuclear transport system. *eLife* 8: e45284

Tojima T, Suda Y, Jin N, Kurokawa K & Nakano A (2024) Spatiotemporal dissection of the Golgi apparatus and the ER-Golgi intermediate compartment in budding yeast. *eLife* 13: e92900

Tong AH, Boone C. Synthetic genetic array analysis in Saccharomyces cerevisiae. Methods Mol Biol. 2006;313:171-92. doi: 10.1385/1-59259-958-3:171. PMID: 16118434.

Toulmay A & Prinz WA (2012) A conserved membrane-binding domain targets proteins to organelle contact sites. *Journal of Cell Science* 125: 49–58

Travers KJ, Patil CK, Wodicka L, Lockhart DJ, Weissman JS & Walter P (2000) Functional and Genomic Analyses Reveal an Essential Coordination between the Unfolded Protein Response and ER-Associated Degradation. *Cell* 101: 249–258

Umemura M, Fujita M, Yoko-o T, Fukamizu A & Jigami Y (2007) Saccharomyces cerevisiae CWH43 Is Involved in the Remodeling of the Lipid Moiety of GPI Anchors to Ceramides□D. *Molecular Biology of the Cell* 18

Voss C, Lahiri S, Young BP, Loewen CJ & Prinz WA (2012) ER-shaping proteins facilitate lipid exchange between the ER and mitochondria in *S. cerevisiae*. *Journal of Cell Science*: jcs.105635

Walter P & Ron D (2011) The Unfolded Protein Response: From Stress Pathway to Homeostatic Regulation. *Science* 334: 1081–1086

Wang R, Miao G, Shen JL, Fortier TM & Baehrecke EH (2022) ESCRT dysfunction compromises endoplasmic reticulum maturation and autophagosome biogenesis in Drosophila. *Current Biology* 32: 1262-1274.e4

Watanabe R, Funato K, Venkataraman K, Futerman AH & Riezman H (2002) Sphingolipids Are Required for the Stable Membrane Association of Glycosylphosphatidylinositol-anchored Proteins in Yeast. *Journal of Biological Chemistry* 277: 49538–49544

Weigel AV, Chang C-L, Shtengel G, Xu CS, Hoffman DP, Freeman M, Iyer N, Aaron J, Khuon S, Bogovic J, *et al* (2021) ER-to-Golgi protein delivery through an interwoven, tubular network extending from ER. *Cell* 184: 2412-2429.e16

Welihinda AA & Kaufman RJ (1996) The Unfolded Protein Response Pathway in. *Journal of Biological Chemistry* 271: 18181–18187

Wen C & Greenwald I (1999) p24 Proteins and Quality Control of LIN-12 and GLP-1 Trafficking in *Caenorhabditis elegans*. *The Journal of Cell Biology* 145: 1165–1175

Yoo J, Mashalidis EH, Kuk ACY, Yamamoto K, Kaeser B, Ichikawa S & Lee S-Y (2018) GlcNAc-1-P-transferase–tunicamycin complex structure reveals basis for inhibition of N-glycosylation. *Nat Struct Mol Biol* 25: 217–224

Yu H, Liu Y, Gulbranson DR, Paine A, Rathore SS & Shen J (2016) Extended synaptotagmins are Ca^{2+}-dependent lipid transfer proteins at membrane contact sites. *Proc Natl Acad Sci USA* 113: 4362–4367

Zarges C & Riemer J (2024) Oxidative protein folding in the intermembrane space of human mitochondria. *FEBS Open Bio* 14: 1610–1626

11 ACKNOWLEDGEMENTS

First, I would like to thank Sebastian for his input throughout my PhD but also for his support, professionally and personally at times when the PhD became second priority. I started off with a lab rotation in your lab, continued with my Master thesis and ended up starting a PhD. Even though I worked on three different projects during these times, I always felt that you valued my ideas and promoted me to become an independent scientist. Thank you for the opportunities to present my science at two international conferences. I would also like to thank my first examiner Axel Mogk and my chair of TAC Karin Schumacher. Thank you for all your valuable input at my TAC meetings. Thank you, Karin, for providing the Schuck lab with an intermediate home after our old institute broke down. I would also like to thank Joachim Moser von Filseck for joining me as a fourth examiner on short notice. I would also like to thank Liz Miller and Friedrich Förster for the opportunity to join their labs for a few days and learn techniques relevant for this project. I would like to thank all staff from ZMBH and BZH that enabled me to do my work every day. This includes the scullery and media kitchen (Melanie, Linda, Selen), the cleaning service at ZMBH and BZH and both administrations. I would like to particularly thank Anke Sander for always being there for me when I was fighting with forms and bureaucracy. Thanks to Monika Langlotz for your help with flow cytometry and thanks to Holger Lorenz for helping me dive into the subject of image deconvolution. I would also like to thank Arne Giebeler from Nikon for all support with our microscope. I would like to thank Matthias Meurer and Daniel Kirrmaier from the lab of Michael Knop for all your help regarding yeast techniques. Without you, the screens would not have been possible.
I would like to thank all rotation and Master students that worked on this project: Carlos, Natalie and Fay. Thank you for the wonderful time and your scientific contributions to this project. Also, thanks to my high school biology teacher Silke Reinhardt for getting my excited about biology.
A PhD is a wild journey with many ups and many downs, and then many more downs. I started off in science because I was curious, and I really liked to see how things come together the more we understand about a biological process. But in the end, it is the people that I met along the way that I value the most and that helped me to get through all downs. Thank you, Imogen, for your supervision and the amazing time in Cambridge. Thank you, Leanne, for your work, your supervision and for being such a fun human being. I cannot wait for the next joint long run. Thank you, Celine and Julia from the Kaessmann lab, for the fun time, even though our dark, small lab space in 345 was everything but fun.
Thanks to all old Schookees that made up the Schuck lab when I joined. Thank you, Dimitris, for supervising me in my lab rotation and getting me hyped about yeast, imaging, the ER and this lab. Thank you for teaching me how to boulder and for having a great taste of music. I enjoyed all our discussions, be it on walks or elsewhere. Thank you, Jasmin, for supervising me at the start of my PhD and for showing me the wonderful world of ESCRT recruitment to ER clusters. You started this project, and I can only hope that you like where it went. Thank you, Peter, for your bioinformatical skills. Both screens would have not been possible without you. Thank you for lighting the spark for beer brewing in this lab. Thank you, Tamas, for the jam sessions we had. Thank you, Carlos, for your work and for the positive atmosphere you always spread. There is no better roommate I could imagine for lab retreats. Thank

you, Aye, for your stories and entertainment. There were so many moments when you cheered me up and had my crying from laughter. I will never recover from this. Thanks to all current Schookees! Thank you, Inge, for your warm welcome when we joined the BZH. Thank you, Anna, for the chats about coffee and fun times at Monday bouldering. Thanks to all the newbies, Natalie, Sneha and Klára! You are great additions to the group, and I am confident that the Schookee spirit will live on with you. Thank you, Petra, for being a wonderful desk neighbor and for the creativity you brought into our group. Thank you for keeping up general things that we PhD students are using every day. Thank you, S(chn)ibi, for being another wonderful desk neighbor. I really enjoyed the start of your PhD when I handed the SHRED project over to you and all of our conversations. Thank you, (Sch)Niklas, for the shared passion for cake and sweets. The ICC would be nothing without you. Thank you for the brewing evenings and Monday Bouldering. Thank you, Rolf, for making me join the jam sessions you had with Tamas. This made me fall in love with the guitar again. You introduced me to my favourite activity to detach from work in my spare time. Thanks for all weekly music sessions that will hopefully happen more regularly now that I hand in this work. Thank you, Giulia, for all our conversations about food and life, all music sessions and all your support in difficult times. I am not exaggerating when I say that you were my older sister in this lab.

I would like to thank all my friends from the Master studies that accompanied me over the last years of PhD. Thank you, Andi, for being my best man and a wonderful friend. For all the laughters, runs and so much more. Thank you Bassi and Jan, for all evenings of the Thursday Bars, HOTD and whatever trash TV show we could come up with. These (almost) weekly evenings with you and Andi were always something I looked forward to. Thank you, Andrea, for all bouldering evenings and all events circling around food.

Thank you, Lis. For all your work on this shared project but even more for all memories we collected along the way. Thank you for the great experiences at conferences and workations. I will never forget all of these impessions. Thank you for being there for me in difficult times, be it personal or work-related. Thank you for all project meetings, chats, coffee breaks, millions of Rosinis, all music sessions, runs, and bouldering sessions. Thank you for believing in me. I would have not finished this PhD without you. I never thought that a stranger would join my PhD project and end up being my best friend.

I would like to thank my family, especially my mum and dad, my brother Stefan, Michèle and of course Jonah. Also, thanks to my extended family in Bonn. Your support enabled this work.

Dad, I wish you were here to witness this. But I know that you would ask me this, so: Yes. My yeast is doing fine and growing well.

Last but not least, I would like to thank Lena. We have been through a lot over the last couple of years. Thank you for your endless support and chats. Thank you for enduring me in stressful times. Thank you that you kept me going and cheered my up whenever I was down. Thank you for the feeling of being at home. I am sure that I would have not managed this work without you.